MAGAININ 2a - INDUCED PERMEABILIZATION OF PHOSPHOLIPID VESICLES

1991

GRANT

UNIFORMED SERVICES UNIVERSITY OF THE HEALTH SCIENCES
F. EDWARD HEBERT SCHOOL OF MEDICINE
4301 JONES BRIDGE ROAD
BETHESDA, MARYLAND 20889-4799

GRADUATE AND
ITINUING EDUCATION

TEACHING HOSPITALS
WALTER REED ARMY MEDICAL CENTER
NAVAL HOSPITAL, BETHESDA
MALCOLM, GROW AIR FORCE MEDICAL CENTER
WILFORD HALL AIR FORCE MEDICAL CENTER

APPROVAL SHEET

Title of Dissertation: **"Magainin 2a - Induced Permeabilization of Phospholipid Vesicles"**

Name of Candidate: Earl Grant, Jr.
Doctor of Philosophy Degree
January 2, 1991

Dissertation and Abstract Approved:

Committee Chairperson	Jan 2, 1991 Date
Committee Member	Jan 2, 1991 Date
Committee Member	Jan 2, 1991 Date
Committee Member	Jan 2, 1991 Date
Committee Member	April 16, 1991 Date

The author hereby certifies that the use of any copyrighted material in the dissertation manuscript entitled:

"Magainin 2a-Induced Permeabilization of Phospholipid Vesicles"

beyond brief excerpts is with the permission of the copyright owner, and will save and hold harmless the Uniformed Services University of the Health Sciences from any damage which may arise from such copyright violations.

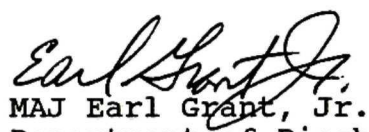

MAJ Earl Grant, Jr., MS, USA
Department of Biochemistry
Uniformed Services University
of the Health Sciences

ABSTRACT

Title of Thesis: Magainin 2a-Induced Permeabilization of Phospholipid Vesicles.

Earl Grant, Jr., Doctor of Philosophy, 1991

Thesis directed by: Mark A. Roseman, Ph.D.

Department of Biochemistry

The magainins, a class of antimicrobial peptides secreted by the frog Xenopus laevis, appear to kill cells by permeabilizing the plasma membrane. To gain some insight into the mechanism of action, we have studied the magainin 2a-induced release of entrapped 6-carboxyfluorescein (6CF) from small unilamellar vesicles (SUVs) of phosphatidylserine (PS).

Addition of peptide to the SUVs causes an initial rapid release of dye, lasting about 100 sec, followed by a much slower release of the remaining dye. The following experiments rule out the possibility that the biphasic kinetics are due to, (a) metastability of the starting vesicles, (b) interaction of vesicles with aggregates of peptide arising from the concentrated stock solution, (c) irreversible inactivation of the peptide upon interaction with the vesicles, or (d) peptide-induced fusion of the vesicles:

1. Sequential addition of peptide at 100 sec intervals produces biphasic kinetics with each addition.

2. Biphasic kinetics are still observed with pre-incubated dilute solutions of peptide.

3. Biphasic kinetics are still observed after pre-incubation of peptide with unloaded vesicles.

4. Light scattering of the SUVs does not significantly increase upon addition of peptide.

A binding isotherm, determined by the "indirect method" (Thron, C. D. (1964) J. Pharmacol. Exp. Ther. 145, 194-201) showed that r, the ratio of bound peptide per lipid, varies linearly with free peptide and that the fractional rate of dye release increases linearly with r. These results indicate that the peptide does not significantly aggregate on the vesicle surface, and that leakage does not arise from multimeric peptide aggregates. This tends to rule out the possibility that channels are responsible for the leakage.

Fluorescence quenching studies showed that dye is released in an "all-or-none" manner. Although this suggests that channels are causing the leakage, all-or-none release was also observed under certain conditions with Triton X-100.

We conclude that the fast release is caused by transient destabilization of the bilayer upon initial interaction of the SUVs with peptide. The mechanism of slow release remains to be determined.

MAGAININ 2a-INDUCED PERMEABILIZATION OF PHOSPHOLIPID VESICLES

by

Earl Grant, Jr.

Thesis submitted to the Faculty of the Department of Biochemistry Graduate Program of the Uniformed Services University of the Health Sciences in partial fulfillment of the requirements for the degree of Doctor of Philosophy, 1991

DEDICATION

To Ivory, Earl, and Joseph in recognition and appreciation of your sacrifice, strength, and support. I love you and thank God that we are family.

Praise God from whom all blessings flow through Jesus Christ by the Holy Spirit. Thank you Lord for this good and perfect gift.

ACKNOWLEDGEMENT

I would like to acknowledge the following individuals who served on my committee:

Dr. Mark A. Roseman ---	for his guidance, advice, positive approach to research, and detailed review of this thesis
Dr. Troy J. Beeler ---	for his suggestions, scientific insight, and careful review of this thesis
Dr. Hao-Chia Chen ---	for his wise insight and careful review of this thesis
Dr. Robert W. Williams ---	for his help and careful review of this thesis
Dr. Noreen Williams ---	for her helpful and encouraging discussions and careful review of this thesis

TABLE OF CONTENTS

LIST OF FIGURES

LIST OF FIGURES (continued)

LIST OF FIGURES (continued)

LIST OF TABLES

ABBREVIATIONS

PS, phosphatidylserine; 6CF, 6-carboxyfluorescein; OG, octylglucoside; MGN2a, Magainin 2a; LUVs, large unilamellar vesicles; SUVs, small unilamellar vesicles; SDS, sodium dodecyl sulfate; EDTA, ethylenediaminetetraacetic acid; MGN1, Magainin 1; MGN2, Magainin 2; PGLa, Peptide beginning with Glycine and ending with amidated Lysine; Pipes, piperazine-N,N'-bis(2-ethanesulfonic acid); CD, circular dichroism; NMR, nuclear magnetic resonance spectroscopy; TFE, 2,2,2,-trifluoroethanol; and PC, phosphatidylcholine.

INTRODUCTION

Magainin was originally isolated as "PGS", which stands for "Peptide beginning with Glycine and ending with Serine" (Giovannini et al., 1987). Earlier studies had shown that the dermal glands of many species of amphibia could produce secretions containing polypeptides of varied physiological activities (Erspamer and Melchiorri, 1980; Nakajima, T., 1981). Giovannini et al. (1987) induced glandular secretions from the South African frog, Xenopus laevis, by noradrenaline injections; analysis of the skin secretions by fast atom bombardment mass spectrometry and high performance liquid chromatography (HPLC) showed that a relatively large number of peptides in the secretory vesicles have molecular masses between 2400 - 2700 Da. Although no physiological activities for these peptides were identified at that time, this group of isolated peptides containing PGS and (Gly-10, Lys-22) PGS would later become known as the antimicrobial peptides, magainins.

The antimicrobial activity of magainins was first characterized by Zasloff (1987). It is interesting to note that the observant eye plus the inquiring mind of the scientist will lead to significant findings. This combination of observation and inquisitiveness led Dr. Zasloff to the isolation of a family of peptides with broad - spectrum

antimicrobial activity. The laboratory of Dr. Zasloff was studying RNA expression in eukaryotes by utilizing the Xenopus laevis oocyte system. The studies required the removal of the ovaries surgically, and the surgical procedure was completed by suturing the muscle wall and skin separately. Zasloff was intrigued by the fact that these animals rarely developed infection even though the surgical procedure was nonsterile and the water-filled tanks were microbially contaminated. This absence of infection suggested that there may be some factor in the skin of the frog aiding this type of remarkable wound healing.

To isolate the antimicrobial factor(s), the skin from the ventral surface of one adult female Xenopus laevis was used to make a crude extract, which was subsequently fractionated by ion exchange chromatography and gel filtration (Zasloff, 1987). The active fractions were identified as those that inhibited growth of E. coli colonies on agarose plates. SDS gel electrophoresis of these active fractions revealed peptides with molecular weights between 2000 and 3000 Da. Two closely related peptides with the highest specific activity were called "magainins" (derived from "magain", the Hebrew word for shield (Zasloff, 1987)). These two peptides, MGN1 and MGN2, were the same as (Gly-10, Lys-22)-PGS and PGS respectively that had been isolated earlier by Giovannini et al. (1987). The 21 residue peptide PGLa isolated from the skin of Xenopus laevis also displays

antimicrobial activity similar to that of MGN1 and MGN2 although it shares no significant sequence homology (Soravia et al., 1988).

The magainins appear to function as a host antimicrobial defense system for Xenopus laevis, protecting the frog from wound infection and exhibiting broad-spectrum antibacterial, antifungal, and antiparasitic activity (Zasloff, 1987; Zasloff et al., 1988). It was also demonstrated that synthetic magainin peptides are indistinguishable from the natural products with respect to chromatographic properties and biological activity (Zasloff et al., 1988). Therefore, it is suggested that magainins may function as the vertebrate counterpart of the cecropins, a family of 37-residue amphiphilic, nonhemolytic peptides, which represent a major, inducible, antibacterial defense system of insects (Zasloff, 1987).

The magainins are packaged in secretory vesicles in the dermal glands of the Xenopus laevis, and disruption of these glands causes the release of secretory products. It is suggested that the regeneration of these secretory products in the dermal glands takes between 2-6 days. The large hydrophobic prepro-magainins are processed within 15-120 minutes after secretion, then undergo rapid proteolysis. The magainin precursors are processed through post-translational proteolysis inside the secretory vesicle by basic-residue-specific endopeptidases to yield the active ma-

gainins. (Giovannini et al., 1987)

A full length cDNA encoding for prepro-magainin has been isolated and characterized (Terry et al., 1988), and contains one copy of MGN1 and five copies of MGN2. Each magainin unit is flanked at the carboxyl terminus by an adjacent Lys-Arg pair. Although in other systems cleavage can occur between the two residues or on the carboxyl side of the pair (Loh et al., 1985), the specificity of the protease in Xenopus laevis skin that removes these basic residues is not yet known. The final major processing step would involve cleavage between Arg-Gly, a cleavage site that has been implicated in the processing of additional peptides from the Xenopsin, Caerulein, and PGLa precursors (Terry et al., 1988; Gibson et al., 1986).

The magainin peptides have displayed a very broad range of cytotoxic specificity toward species of bacteria, fungi, and parasites (Zasloff, 1987; Zasloff et al., 1988). The activity is dose dependent and unaffected by pH within the range of 5.8 to 8.0 (Juretic et al., 1989a and 1989b).

The effective and selective specificity of magainin action revolves around a paradoxical property; the peptides, in order to prevent infection, must be toxic to foreign cells yet harmless to the host cells. Westerhoff et al. (1989a) suggest a number of ways that this selectivity could be achieved.

First, proteolytic degradation of magainin could

significantly reduce the circulating concentration that would be available to interact with host cells. This possibility is supported by the observation that Xenopus laevis secretes proteases that are active on magainin peptides and the magainins appear very susceptible to proteolysis (Juretic et al., 1989b; Terry et al., 1988).

Second, in the absence of some external stimulus (i.e. noradrenaline or bacterial infection) the concentration of circulating magainin is negligible; tight regulation of magainin secretion could therefore control magainin-host cell interaction (Giovannini et al., 1987).

Third, although magainins have been shown to behave as uncouplers and dissipators of the electrochemical potential of isolated mitochondria, the plasma membrane of the host cell may prevent the peptides from entering the cell (Westerhoff et al., 1989a).

Fourth, the lipid composition of the target membrane may alter the magainin activity. It has been shown that magainins readily permeabilize PS liposomes, which resemble the lipid composition of E. coli, but do not permeabilize PC liposomes, which resemble the lipid composition of mammalian plasma membranes (Matsuzaki et al., 1989a). Rana and Blazyk (1989) postulate that the lipopolysaccharide in the outer membrane of Salmonella typhimurium may act as a molecular sponge for the cationic peptide, inhibiting its lethal attack on the plasma membrane. In addition, the high cho-

lesterol content of the plasma membrane of eukaryotic cells may contribute to the reduced activity of magainin.

Fifth, the magainins display a synergistic activity when combined with PGLa in the presence of liposomes (Williams et al., 1990). This synergistic activity could serve to reduce the effective concentration of each magainin required to provide antimicrobial protection. All of these or combinations of these factors may play an integral role in regulating the selective lethality of the magainins.

There are at present two 23-residue antimicrobial peptides that are classified as magainins: MGN1 and MGN2. The sequences of these peptides are as follows:

MGN1: Gly-Ile-Gly-Lys-Phe-Leu-His-Ser-Ala-Gly-Lys-Phe-Gly-Lys-Ala-Phe-Val-Gly-Glu-Ile-Met-Lys-Ser

MGN2: Gly-Ile-Gly-Lys-Phe-Leu-His-Ser-Ala-Lys-Lys-Phe-Gly-Lys-Ala-Phe-Val-Gly-Glu-Ile-Met-Asn-Ser

These peptides have a net positive charge of +3 to +5 at pH 7.0. Their sequence suggests that they can form amphiphilic helices about 30 angstroms in length (Williams et al., 1990), which is long enough to span a lipid bilayer. The ability of the magainins to form amphipathic alpha-helices and their net positive charge suggest that they can bind to and effect the permeability barrier of certain lipid bilay-

ers (Green et al., 1987).

The secondary structures of the magainins have been assessed by Raman spectroscopy, NMR, CD, and analogue comparison studies. Raman spectroscopic measurements suggest that MGN2a, when bound to dipalmitoylphosphatidylglycerol (DPPG) liposomes, is 58% alpha-helix (which corresponds to an alpha-helix 20 Å in length (Williams et al., 1990)). However, the upper limit for the average helix content of MGN2a may be set at 70% in order to account for end effects of helical segments. This upper limit was established by using the difference in helix content for melittin, a 26-residue peptide from bee venom, determined by Raman spectroscopy and X-ray diffraction. The Raman estimate of the helix content of melittin crystals (84%) is 12% below the helix content determined by X-ray diffraction (Williams et al., 1990). Thus, these end effects could lead to at least a 12% under-estimation of the average helix content of molecules of approximately 20-30 residues in length that possess end helical residues. Two-dimensional NMR studies of MGN2a in 25% TFE indicate that some alpha-helix is formed although no quantitative amount was reported (Marion et al., 1988). CD of the peptides in 40% TFE indicates 24% and 26% alpha-helix content for MGN1 and MGN2 respectively (Chen et al., 1988). CD measurements made in the presence and absence of liposomes indicate that MGN1 has an unordered structure in aqueous solution and in the presence of phos-

phatidylcholine vesicles; in contrast, it forms 57% alpha-helix upon binding to phosphatidylserine vesicles (Matsuzaki et al., 1989a).

Collectively, these data show that whereas magainins form unordered or random coil structures in aqueous solution, they form alpha-helix structures in membrane mimetic solvents or when bound to liposomes. However, quantitative differences between Raman spectra of MGN2a in TFE and MGN2a mixed with lipid vesicles suggest that TFE may not be an adequate model solvent to evaluate the secondary structure of magainins in a membrane environment (Williams et al., 1990). This is further illustrated by the difference in alpha-helix content of MGN1 in 40% TFE (24%) and of MGN1 bound to PS vesicles (57%). Thus, although the membrane mimetic solvent TFE may underestimate the amount of alpha-helix content of the magainins in a membrane environment, the qualitative environmental effect on the secondary structure is clear.

The contribution of secondary structure to the antimicrobial activity of the magainins has been assessed by structural-analogue studies. Using synthesized magainin analogues with modifications designed to promote or inhibit alpha-helix formation, Chen et al. (1988) found that both an alpha-helical structure and a free alpha-amino terminus are required for maximal antimicrobial activity. The analogue that displayed maximal antimicrobial activity was one having

Gly-13 and Gly-18 replaced by the helix promoting residue, L-alanine. This suggests a positive correlation between propensity to form helix and increased antimicrobial activity. This positive correlation was also shown by Raman measurements of these analogues bound to liposomes (Williams et al., 1990). Cuervo et al. (1988) measured the antimicrobial activity of 50 omission analogues of the magainins and found that the N-terminal region of the peptides is crucial for antimicrobial activity. In contrast, the C-terminal analogues showed a greater tendency to maintain antimicrobial activity following amino acid omission coupled with some species selectivity and variable hemolytic action against human erythrocytes. MGN2a with glycine-18 omitted had equal antimicrobial activity, but significantly increased hemolytic activity. These data suggest that the N-terminal region and amino acids Gly-13 and Gly-18 are significant contributors to the magainins antimicrobial activity and the lack of hemolytic activity is controlled by the C-terminal region.

Zasloff (1987) showed that magainins are active against protozoa; within minutes of exposure to the magainins these organisms swell and subsequently burst, suggesting that the major site of action of the magainins is the plasma membrane. The proposed site of action and the availability of synthetic magainins serve as a launching pad to begin unravelling the details of the peptide-lipid interaction of the magainins.

If the magainins' broad spectrum activity is due to permeabilization of plasma membranes the peptides may disrupt the energy metabolism of the bacteria by dissipating the electrochemical gradient. Indeed, the magainins do disrupt energy metabolism of E. coli, and of its functional analogue, the mitochondrion, by dissipating the electric potential across the membrane and uncoupling respiration from other energy-requiring processes (Westerhoff et al., 1989b). It was also shown that MGN2a causes membrane depolarization of E. coli cells and of liposomes containing cytochrome oxidase (Juretic et al., 1989a). From the non-linear dose-response curve, these data further suggested that activity involves a cooperative interaction of peptide molecules. Indeed, Juretic et al. (1989a) suggest that the concentration dependence is indicative of a multimeric active complex consisting of 3-5 molecules. Westerhoff et al. (1989b) showed that the respiratory rate of isolated mitochondria and cytochrome oxidase liposomes varied sigmoidally with magainin concentration, indicating a cooperative effect. It has also been suggested that MGN2 and PGLa, when added to lipid bilayers together, interact cooperatively and synergistically to reduce the membranes permeability barrier (Juretic et al., 1989b and Williams et al., 1990). However, I would suggest that cooperativity may not be directly concluded from sigmoidal dose-response curves because Thron (1964) showed that detergent-induced hemolysis

of erythrocytes also display sigmoidal dose-response curves.

There are currently few reported studies in which liposomes are used to investigate the interaction of magainin with the lipid bilayer. Dose response studies with cytochrome oxidase unilamellar liposomes suggest that magainin dissipates the membrane potential by forming aggregates of 4-5 molecules and that these concentrations of MGN2a that uncouple respiration of cytochrome oxidase liposomes is comparable to the concentration that shows antimicrobial action against E. coli (Juretic et al., 1989b). Matsuzaki et al. (1989a) who investigated the effect of MGN1 on the release of trapped calcein from liposomes, observed that MGN1 induces leakage of calcein from negatively charged vesicles (i.e. phosphatidylserine) but not from neutral vesicles (i.e. phosphatidylcholine). They also determined that MGN1 binds to bovine brain PS vesicles with a binding constant of 3.8×10^5 M^{-1}, a binding number of one magainin per 10 lipids and a critical binding number, (the minimum number of peptide molecules per lipid molecule required to initiate leakage,) of approximately 0.03 per lipid molecule. They suggest that the MGN1 interaction with acidic lipids begins with an electrostatic interaction, followed by hydrophobic interactions which causes alpha-helix formation and subsequent leakage of vesicle contents. These studies with liposomes suggest that the magainin's mechanism of action may be explained by two different models. On the one hand,

it may require formation of a multimeric complex (i.e. channel/pore) through electrostatic and hydrophobic interactions (Juretic et al., 1989b and Westerhoff et al., 1989b). Alternatively, the magainin molecules may cause localized destabilization of the membrane permeability barrier by acting as a detergent that interacts with the membrane by electrostatic and hydrophobic interactions (Matsuzaki et al., 1989a). However, further liposome work with vesicles made of phospholipids found in bacterial and mitochondrial membranes is needed in order to more fully evaluate the lipid interaction of magainins in the different membrane systems.

The mechanism by which the magainins permeabilize cell membranes has not been elucidated. As indicated above, the magainins may destabilize the membrane by acting as detergents or by forming membrane channels/pores (Zasloff, 1987; Guy & Raghunathan, 1988). It is conceivable that magainins may interact with specific receptors on the bacterial cell membrane, although liposome studies suggest that in the absence of membrane proteins magainins do interact with the lipid bilayer and increases its permeability. Whether or not magainins require receptors in vivo is not yet known. Most of the studies on the magainins suggest that they function by forming channels. Investigation of the interaction of MGN2 with membranes utilizing a patch-clamp apparatus suggest that voltage-dependent channels form

in artificial phospholipid bilayers (Cruciani et al., 1988). Planar lipid bilayer studies have also suggested that the magainins may form channels; Duclohier et al. (1989) found a weakly voltage-dependent macroscopic conductance that appears anion-selective. However, I would like to point out that large aqueous peptide and salt (1M KCl) concentrations and high voltages (-120mV to -280mV) were required to see this activity. These extreme conditions may not be relevant to the in vivo peptide-lipid interaction. They suggest further, based on single channel experiments, that at rest the magainins exist as pre-aggregates on the membrane surface and when voltage is applied the peptide becomes inserted into the bilayer to form a channel. Accordingly, aggregation of magainin on the membrane may be a critical step promoting antimicrobial activity. Indeed, the ability of magainin to aggregate has been demonstrated in aqueous solution. MGN2 spontaneously polymerizes into 13nm diameter filaments having a 30nm periodic helical substructure that is optimized at low pH and high ionic strength (Urrutia, et al., 1989). Although low pH and high ionic strength may not be physiologically relevant, they do demonstrate that conditions of increased hydrophobicity enhances MGN2's ability to polymerize; this may be related to its ability to aggregate in cell membranes and form pores. However, it could be argued that the aggregation of magainin on the membrane surface could cause localized destabilization of the mem-

brane, thereby altering the membrane permeability barrier. If, as Williams et al. (1990) suggest, the average length of the MGN2a helix is less than 20 angstroms when bound to liposomes, the peptide would not be long enough to span the membrane as a channel. However, the data of Williams et al. (1990) can not rule out the possibility that a small fraction of the magainin forms longer helices which can form channels. Collectively the present data can be explained either by postulating that magainin forms channels or that magainin acts as a surface active detergent. Since further mechanisms may yet be elucidated, continued investigation is warranted.

To gain some insights about the mechanism of magainin activity it may be fruitful to look at the mechanisms of toxin action as a comparison. The magainins and toxins are members of a class of proteins and polypeptides called cytolysins, which possess a common cytolytic region containing a cationic site flanked by a hydrophobic surface. This structure enables them to disrupt the permeability barrier of target cells, albeit by different mechanisms (Kini and Evans, 1989). The offensive (relative to eukaryotic cells) members of this class, the toxins, initiate their cytolytic effect by a number of mechanisms that include membrane destabilization, membrane digestion, channel formation, receptor binding, and protein denaturation. Many of these toxin mechanisms are well characterized and could serve as

the catalyst for deeper insight into the mechanism of the defensive members of this class, the magainins.

One of the best characterized examples of a toxin channel former is Staphylococcus aureus alpha-toxin. It is a single polypeptide chain with a molecular weight of 34000 (Fussle, et al., 1981). The hemolytic and solute releasing activity of alpha-toxin suggested that the primary site of action was the lipid bilayer (Freer, et al., 1968). Alpha-toxin was shown to have broad reactivity toward both nucleated cells and erythrocytes and it caused release of low molecular weight markers from liposomes (Bernheimer, et al., 1972 and Cassidy et al., 1974).

Native alpha-toxin exhibits a sedimentation coefficient of 3S, but upon binding to the membrane forms a 12S complex, which suggests oligomerization of the monomer in the membrane (Arbuthnott et al., 1967). Freeze-etch electron microscopy revealed ring-shaped formations on toxin-treated membranes that were believed to be the 12S membrane bound toxin complex (Freer et al., 1973). Yet these data did not provide a mechanism that explains how alpha-toxin damages membranes.

The mechanism of alpha-toxin's membrane perturbing activity was elucidated by Fussle et al. (1981). This group sought to isolate membrane bound alpha-toxin, characterize its biochemical and ultrastructural properties, and its ability to form function membrane lesions. Alpha-toxin was

isolated from a detergent extract of toxin-treated rabbit or human erythrocytes by three purification steps: 1) Gel chromatography, 2) Sucrose density gradient ultracentrifugation, and 3) Reconstitution of alpha-toxin into artificial lipid vesicles. The nonelutability of the toxin from biological and artificial membranes treated with various salt solutions analyzed by SDS gel electrophoresis and rocket immunoelectrophoresis demonstrated the toxin's amphiphilicity. The isolated protein was identified as alpha-toxin on the basis of immunoprecipitation, amino acid analysis, and electron microscopic negative staining. Current data suggests that alpha-toxin molecules initially bind to a target membrane, then self-associate to form a pore of a discrete size that is embedded within the lipid bilayer. Further studies to evaluate the function of alpha-toxin using erythrocytes as targets indicate that the toxin generates pores approximately 2nm in diameter, and that penetrate into the hydrophobic domain of the bilayer (Thelestam et al., 1983). Toxin-induced release of defined molecular markers entrapped in resealed erythrocyte ghosts was measured to determined the effective pore size; the results indicated the presence of a membrane lesion that permitted selective release of marker molecules whose effective diameter did not exceed 30 angstroms. Based on these data the following mechanism of action was proposed: 1) Alpha-toxin is a hydrophilic molecule which, upon contact with a target lipid bilayer, spon-

taneously self-associates on and in the membrane to form an amphiphilic oligomeric complex; 2) The membrane associated complex has the structure of a thick-walled cylinder which contains a central pore; 3) The cylinder orients perpendicular to the membrane plane and penetrates at least partially in the lipid bilayer, thus forming an aqueous channel that would account for the primary toxin-dependent membrane permeability defect. (Fussle et al., 1981)

Melittin, the main component of bee venom, serves as a second example of a toxin whose mechanism of action has been extensively investigated. It is generally believed that melittin interacts with membranes as a surface-active peptide (Terwilliger et al., 1982). Melittin has been shown to cause direct lysis of all cells tested and of intracellular organelles including lysosomes and mitochondria (Haberman, 1972; Olson et al., 1974; Weissmann et al., 1969). It also lyses phospholipid vesicles of various phospholipid compositions (Sessa et al., 1969). The lytic action of melittin on vesicle membranes suggests that melittin does not require interaction with membrane proteins in order for it to affect the permeability barrier of membranes.

Melittin is capable of penetrating monolayers at air-water interfaces, and of forming monolayers by itself (Haberman, 1972; DeGrado et al., 1981). It is believed that melittin's lytic action is due to a detergent-like surface activity although the lack of parallelism between surface

activity and hemolytic activity suggests that it does not function as a simple detergent (Haberman, 1972).

Spectroscopic studies that include infrared, Raman, circular dichroism, and tryptophan fluorescence all indicate that melittin is alpha-helical when associated with the lipid bilayer. Whether melittin exists in the membrane as a monomer or some form of oligomer is not yet clear (Dawson et al., 1978; Lavialle et al., 1982; Drake, et al., 1979). The studies on the fluorescence of tryptophan 19 suggest that the tryptophan penetrates only slightly into the membrane and the positively charged carboxy end of melittin is exposed to aqueous solution (Debony et al., 1979; Georghiou et al., 1982). Studies with planar lipid bilayers suggest two different views. Kempf et al. (1982) observed that melittin produces a broad range (10^{-9} - 10^{-10}S) of conductance increases rather than discrete channel-type openings. In contrast, Tosteson et al. (1985a) observed single channel openings in melittin-doped bilayers that appeared to be discrete voltage-dependent anion-selective channels. The mechanism of melittin action has been further studied by detailed kinetic measurements of melittin-induced red blood cell lysis. DeGrado et al. (1982) suggest that melittin-induced lysis of human erythrocytes is a biphasic process which is the result of rapid binding of melittin to the erythrocyte outer membrane, formation of transient openings, translocation of melittin across the bilayer into the cyto-

plasm, and steady state transient membrane openings produced by dimers of internalized melittin.

In contrast, Tosteson et al. (1985b) report that the observed kinetic characteristics of lysis and cation movement suggest that melittin modifies the permeability of the red blood cell membrane for only the first few minutes after membrane interaction. This finding, along with direct observation of cell crenation, (by Nomarsky optics), with swelling and cell lysis within 10-30 seconds after the change in morphology suggests that melittin produces lysis of human erythrocytes by a colloid osmotic mechanism.

Although melittin has been extensively studied, there is yet disagreement about the molecular mechanism of melittin action. There appear to be two basic models. First, melittin can form an aqueous channel/pore that produces ionic imbalance resulting in colloid osmotic lysis. Second, melittin's lytic action results from disruption of the phospholipid structure of the membrane. Thus, a consensus mechanism of action of melittin has yet to be elucidated.

In addition to these two toxins, another peptide, hypelcin A, warrants discussion. This hydrophobic peptide, which contains α-aminoisobutyric acid (Aib) residues was isolated from Hypocrea peltata (Fujita et al., 1984a) and demonstrates antimicrobial activity against various fungi and bacteria (Fujita et al., 1984b). It also uncouples

oxidative phosphorylation in rat liver mitochondria (Takaishi et al., 1980).

In order to gain some basic insight about the peptide's mechanism of action, Matsuzaki et al. (1989b) investigated the hypelcin A-induced permeabilization of and interaction with PC vesicles. They evaluated the hypelcin A-induced leakage of the entrapped dye, calcein, from lipid vesicles in both the gel state and liquid-crystalline state. The calcein leakage rate was dependent on both the peptide and lipid concentrations. A more systematic analysis of this dependency suggested that the binding of hypelcin A to egg PC vesicles could be explained by partition based on the linear binding isotherm. From these results and the concentration-independent CD spectra of the peptide in buffer, the leakage is best explained by interaction of the monomeric peptide with the lipid bilayer. Thus Matsuzaki et al. (1989b) conclude that the monomeric peptide with an increased helical content, complexed with the lipids, perturbs the lipid organization and induces the increased permeability. Although the detailed mechanism of hypelcin A is still not fully elucidated and no data suggesting biphasic release kinetics were presented, this study provides a model starting point to begin understanding the overall features of peptide-lipid interactions at the molecular level.

Thus, these two examples of toxins and hypelcin A reveal the involved process and integration of various

studies and techniques required to adequately unravel the mechanism of action of a cytolytic agent. However, in the case of melittin it also shows that even after extensive investigation the complete mechanism can still remain veiled awaiting different experimental approaches, new technology, or a more encompassing model to explain the current findings. On the other hand in the case of hypelcin A, it provides a straight forward starting point for unveiling the mechanism of action of a given cytolysin. Thus, the complete elucidation of the mechanism of action of a cytolytic agent proves to be an extensive experimental endeavor.

The overall mechanism of magainin action remains to be elucidated. There is no clear model to explain the structure of the magainin complex on membranes. Very little is known about how magainin interacts with and affects the permeability properties of membranes. Most of the suggested mechanisms of action are based on patch-clamp (Cruciani et al., 1988), planar lipid bilayer (Duclohier et al., 1989), or cytochrome oxidase liposome (Juretic et al., 1989b) studies. Despite the suggestions of these studies a consistent model is still not known.

The primary objective of this project is to investigate the membrane interaction properties of MGN2a in a model membrane system. The interaction of magainin with model membranes was investigated using SUVs. In comparison to the natural target, such as bacteria or parasites, SUVs

provide several advantages for studying membrane-protein interactions. For example, membrane-magainin interactions can be studied without the possible interference from intrinsic membrane proteins and the properties and composition of the lipid bilayer can be easily varied. With respect to other model systems, such as multilamellar vesicles, SUVs have the advantage of having only one bilayer for the magainin peptide to interact with. LUVs are more difficult to size and characterize and it is not possible to obtain a homogeneous population. Thus as a membrane model, SUVs offer the advantages of a single, protein-free bilayer of consistent size and stability to study the interaction of magainin peptides with membranes.

An assay which measures the release of the fluorescent dye, 6CF from 6CF-loaded SUVs was employed to determine the functional activity of MGN2a on the vesicles. Vesicles loaded with entrapped dyes have frequently been used to investigate membrane-protein interactions. Specifically, the release of 6CF from vesicles treated with cytolytic agents has been used as evidence of channel formation or membrane perturbation (Blumenthal et al., 1984). The 6CF release assay provides a convenient method to test conditions for optimal peptide-vesicle interaction as well as the characterization of the channel or membrane destabilizing properties of the magainin on vesicles.

The goal of this research is to propose a model for

the interaction of magainin with membranes by performing detailed kinetic measurements using fluorescence spectroscopy and a model membrane system. I hope these model studies will provide a more basic knowledge about the peptide-lipid interaction. In addition, these studies would be valuable to those interested in the design and synthesis of analogues of magainin as potential therapeutic agents especially in the area of wound healing. Thus, these studies will better elucidate the relationship of the cytolytic agent with its target cell.

EXPERIMENTAL PROCEDURES

A. Materials

Phosphatidylserine, isolated from bovine brain, was purchased from Avanti Polar lipids; 6-Carboxyfluorescein (Figure 1) from Eastman Kodak; Sephadex G-25 and Sepharose-2BCL from Pharmacia; Econo-Pac 10-DG desalting columns from Bio-Rad; melittin (bee venom) and n-Octyl-β-D-Glucopyranoside (Octylglucoside) from Sigma Chemical Company; Triton X-100, specially purified for membrane research, from Boehringer Mannheim. Magainin 2a was a generous gift from Dr. Michael Zasloff.

B. Buffers

1. Buffer A: 150mM NaCl, 10mM Pipes, 1mM EDTA, 100mM sucrose (pH 7.0).
2. Buffer B: 150mM NaCl, 10mM Pipes, 1mM EDTA (pH 7.0).
3. Dye solution: 150mM NaCl, 10mM Pipes, 1mM EDTA, 100mM 6CF (pH 7.0).

Figure 1

The structure of 6-Carboxyfluorescein (6CF).

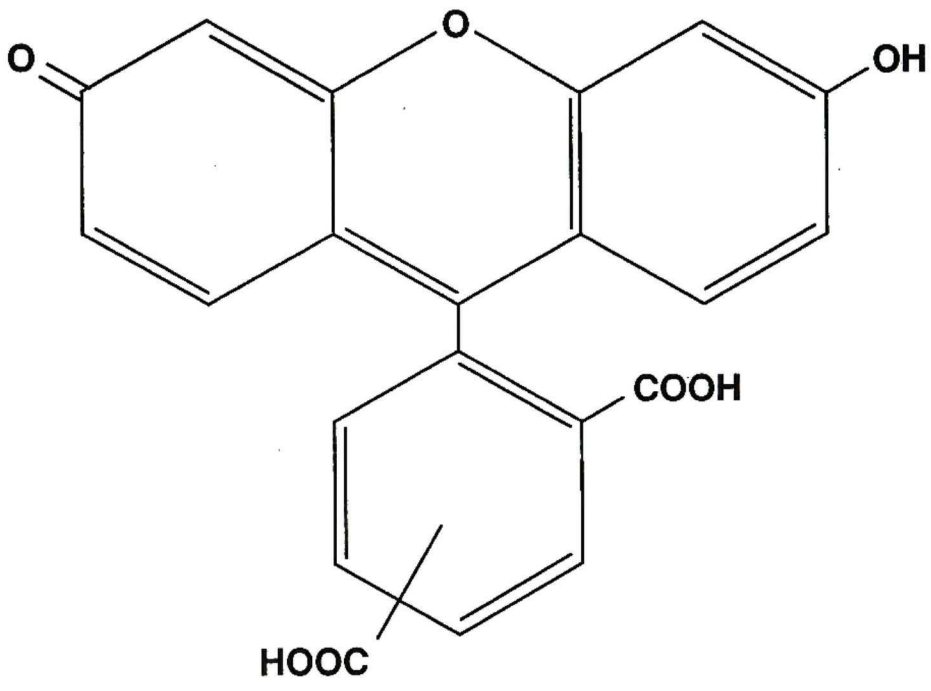
O
O
OH
COOH
HOOC

C. Methods

Preparation of LUVs by Reverse Phase Evaporation

LUVs of PS containing entrapped 6CF were prepared by the reverse phase ether evaporation method (Duzgunes et al., 1983) as follows. The lipid was dried to a film by rotary evaporation under reduced pressure in a 25 ml round bottom flask, then placed under high vacuum overnight to remove residual solvent. Three milliliters of ether was added to the lipid film, then vortexed. One ml of 100mM 6CF in buffer B was added to the lipid-ether mixture and the solution was briefly sonicated with a micro-tip until an emulsion was formed. The ether was removed under reduced pressure at 25°C by rotary evaporation. (During evaporation, the solution forms a gel which subsequently collapses into an aqueous suspension.) An additional 2 ml of 6CF solution was then added and the remaining ether was removed under higher vacuum. After all the ether was evaporated, the vesicles were passed successively through 0.4, 0.2, 0.1, and 0.08 micron Nuclepore filters held in a Swinlock apparatus. The vesicles were passed sequentially over an Econo-Pac 10-DG column (10ml) and Sepharose-2BCL Column (30ml) in order to remove extravesicular 6CF and contaminating small unilamellar vesicles, respectively. It was assumed that the vesicles formed in 100mM 6CF contained the same concentra-

tion of entrapped 6CF. At this concentration of 6CF, the fluorescence is minimal due to self quenching of the dye. The typical final lipid concentration was 8mM.

Preparation of SUVs by Sonication

SUVs of PS, containing entrapped 6CF, were prepared as follows. The lipid (20 mg) was first dried to a film by rotary evaporation in a 25 ml round bottom flask, then dissolved in 5ml of benzene and frozen by continuous turning on a bed of crushed dry ice. The benzene/lipid mixture was then lyophilized overnight under high vacuum to remove the solvent. Two milliliters of 6CF in buffer B was added, the dispersion was vortexed, followed by sonication in a cup horn using a Heat Systems-ultrasonic sonicator (W-375). Unentrapped 6CF was removed by gel filtration (Econo-pac 10-DG desalting column, buffer A used as an eluent). The separated vesicular fraction was subjected to ultracentrifugation in a 50 Ti rotor at 45K rpm for 15 min (Beckman, ultracentrifuge) to produce a homogeneous population of vesicles (Barenholz et al., 1977). The lipid concentration was determined by phosphate analysis (Bartlett, 1959) and the typical final lipid concentration was 10mM.

Assay of the Functional Activity of MGN2a

The functional activity of MGN2a on SUVs was determined by monitoring the release of entrapped 6CF from SUVs after the addition of MGN2a to these vesicles. For most experiments, 6CF was entrapped in SUVs at a self-quenching concentration of 100mM. Upon dye release and dilution in the extravesicular medium, the self-quenching is relieved and the fluorescence of the dye immediately increases. The dequenching of dye thereby permits continuous monitoring of 6CF release from vesicles. An Aminco SPF-500C spectrofluorometer was used to monitor fluorescence, with excitation at 490nm and emission measured at 520nm. The bandpass slit widths were adjusted to 4nm.

MGN2a-mediated release was initiated by the addition of 5 to 20 ul of 0.37mM MGN2a (in buffer B) to 2 ml of 25-30uM PS SUV in buffer A. In some experiments, the order of addition was reversed. Release was initiated by the addition of 5 to 7 ul of an 8-12mM stock solution of PS SUVs to 2 ml of 0.925-3.7uM MGN2a in buffer A. The assay temperature for all experiments was held constant at 25°C by a VWR water circulator. The release of 6CF was monitored for 500 sec at each MGN2a concentration. The total releasable fluorescence was determined by the addition of 20ul of 10% Triton X-100 to the vesicle samples. Magainin activity on vesicles was assessed by determining:

$$\text{Percent 6CF Release} = (F-F_i)/F_t-F_i) \times 100$$

where F = relative fluorescence at a time point

after addition of MGN2a

F_i = initial fluorescence of PS SUVs containing 6CF

F_t = total fluorescence after Triton X-100 addition

Percent Quenching, $\%Q = (1 - F_o/F_{max}) \times 100$

where $F_o = F - F_i$

$F_{max} = F_t - F_i$

A schematic representation of the 6CF release assay is shown in Figure 2.

Determination of the Mode of 6CF Release from SUVs

The mode of 6CF release from vesicles interacting with MGN2a was assessed to determine whether vesicles released dye in a so-called "all-or-none" or "graded" fashion. All-or-none release is self-explanatory; graded release refers to a uniform leakage of vesicle contents (Figure 3). The assessment was possible because the fluorescent entrapped dye was highly quenched at 100mM 6CF. Partial (graded) release of dye from SUVs results in the dilution of dye within vesicles; quenching is partially relieved and the intrinsic fluorescence within SUVs increases. Graded release could be differentiated from all-or-none release by determining the residual fluorescence of SUVs in the absence and presence of Triton X-100. F_o/F_t ratios were measured

Figure 2

Assay for MGN2a functional activity. MGN2a was added to both SUVs and LUVs loaded with 100mM 6CF. The release of 6CF after MGN2a addition was followed to endpoint fluorometrically. Total releasable dye was determined by the addition of 10% Triton X-100 to the vesicles. Percent quenching (%Q), the amount of 6CF remaining in the vesicles, was calculated using the following formula:

$$\% Q = (1 - F_o/F_{max})100$$

where, $F_o = F - F_i$

$F_{max} = F_t - F_i$

(F_t = total fluorescence after Triton X-100 addition)

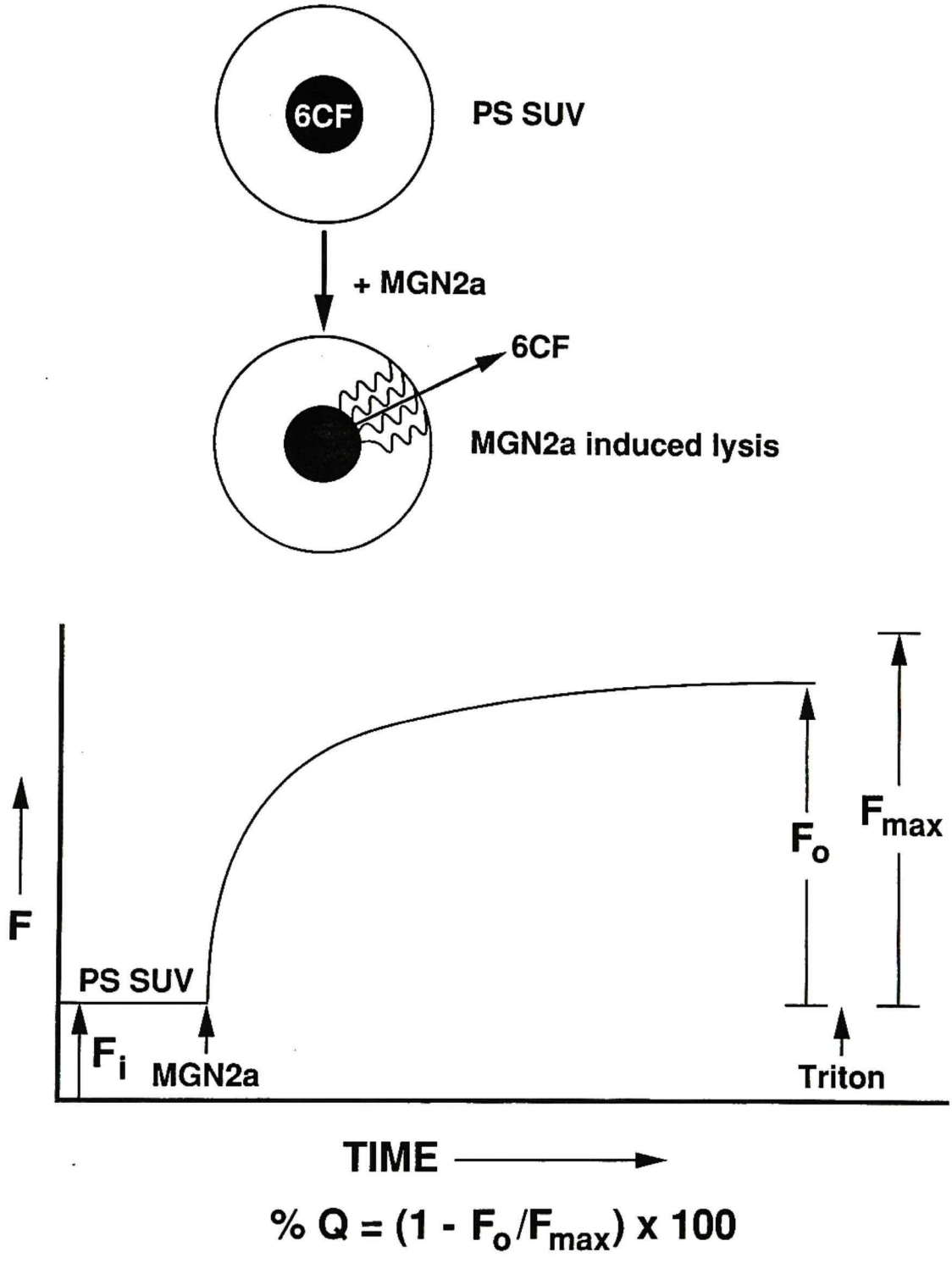

$$\% Q = (1 - F_o/F_{max}) \times 100$$

Figure 3

Depiction of All-or-None versus Graded release mechanisms. In this example, addition of MGN2a to PS SUVs causes the vesicles to lose 50% of their contents. This could be due to:

1. All the vesicles losing half their contents (Graded Release).
2. Half the vesicles losing all their contents (All-or-None Release).

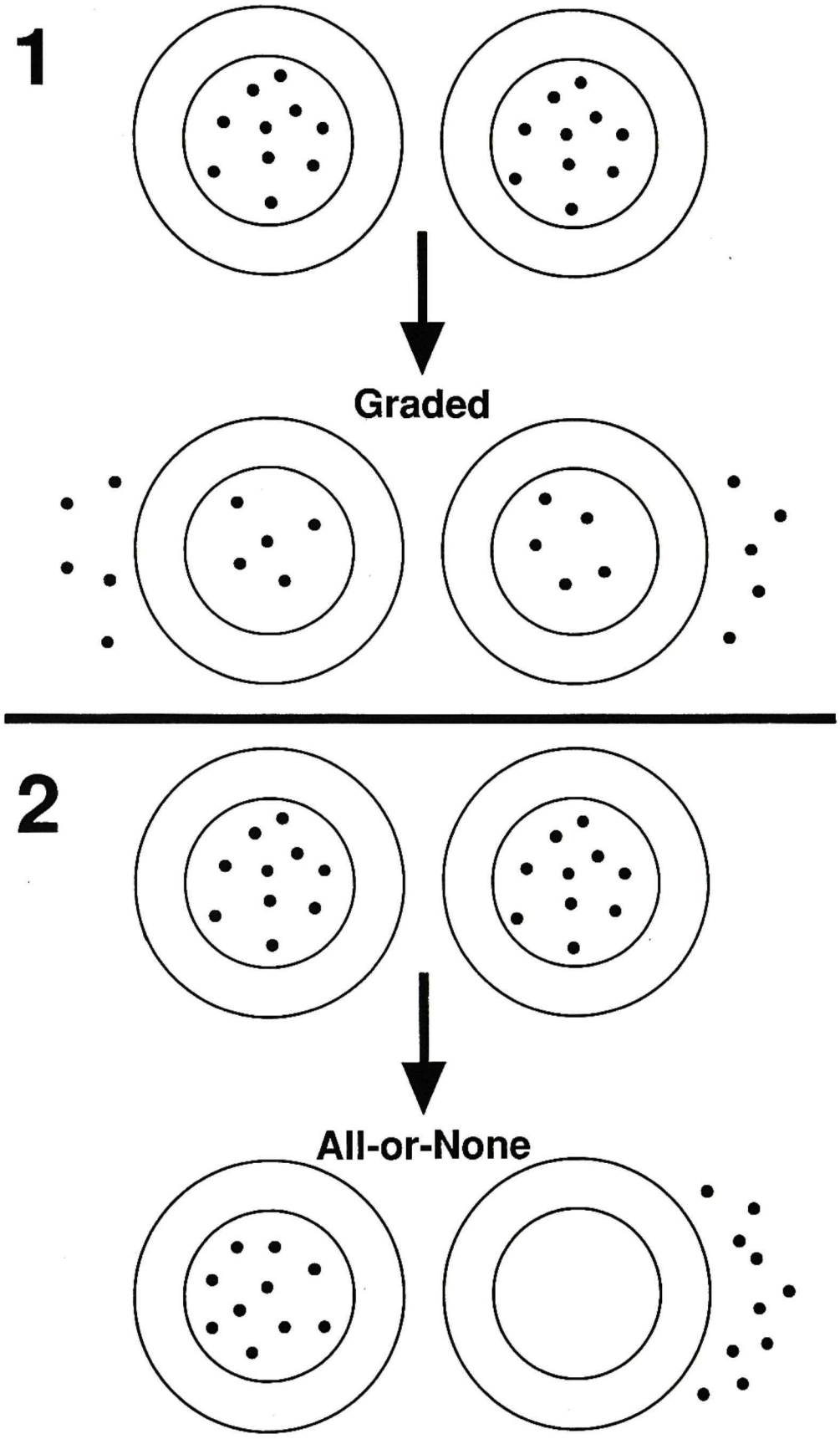
1
Graded
2
All-or-None

and compared for the amount of MGN2a that caused release of 6CF from the SUVs.

F_o/F_t: F_o = residual SUV fluorescence after removal of released dye by Sephadex G-25 chromatography.

F_t = total fluorescence after treatment of vesicles with Triton X-100.

If a fraction of MGN2a-treated SUVs leaked all of their dye (all-or-none), then the F_o/F_t ratio of the remaining unlysed vesicles would be the same as the F_o/F_t ratio of the control SUVs. However, if all MGN2a-treated vesicles leaked some of their dye, the F_o/F_t ratio would be greater than the control. The increase in F_o/F_t ratios of MGN2a-treated SUVs were compared to a quenching curve (constructed as described below) for standard vesicle preparations containing different concentrations of entrapped dye. The standard curve allowed the prediction of F_o/F_t values for graded release based on the percent of 6CF release.

The assay was performed as follows: MGN2a and SUVs (25-30uM PS) were mixed in 2 ml of Buffer A at 25°C, and release of 6CF was followed for 500 seconds fluorometrically. Further release of 6CF was arrested by addition of an equivilent amount of unloaded SUVs. The arresting of 6CF release by unloaded PS SUVs is probably due to a shift in the binding equilibrium of MGN2a after addition of these vesicles, which reduces the number of MGN2a bound to loaded vesicles.

1-ml aliquots of the MGN2a/SUVs mixture were rapidly passed over 5ml-Sephadex G25 columns (by centrifugation at maximum speed for 15 seconds at room temperature in a clinical centrifuge) to separate free 6CF from the vesicles. Vesicle fractions of 0.5ml were then added to 1.5ml of buffer A and analyzed for residual 6CF in the absence and presence of Triton X-100 (20ul of 10% Triton X-100) in order to determine F_o and F_t.

To establish a standard quenching curve, vesicles containing various concentrations (1-100mM) of entrapped 6CF were prepared by sonicating the lipid in buffer containing the appropriate concentration of dye. The F_o/F_t ratios of these vesicles were determined immediately after preparation and used to determined the percent quenching. The standard curve, shown in Figure 4 was used to predict F_o/F_t ratios for any given percentage of 6CF release by the graded release mechanism (Weinstein et al., 1984). For example, according to the curve, a vesicle starting with 30mM 6CF that loses half its dye will show a change (drop) in %Q from a value of 81 to a value of 63.

Light Scattering

The intensity of light scattered at 90° by vesicles in the presence and absence of MGN2a was measured in an Aminco (SPF 500C) spectrofluorometer, using incident light

Figure 4

Standard quenching curve for 6CF entrapped within PS SUVs. SUVs containing different concentrations of entrapped 6CF were prepared by cup horn sonication. Immediately after vesicle preparation, the initial quenched fluorescence (F_o) and the total fluorescence (F_t), measured after the addition of Triton X-100 to SUVs, were determined for each sample. A quenching curve was made by plotting the percent quenching (%Q), $((1 - F_o/F_t) \times 100)$, versus the log of the concentration of 6CF trapped within the vesicles.

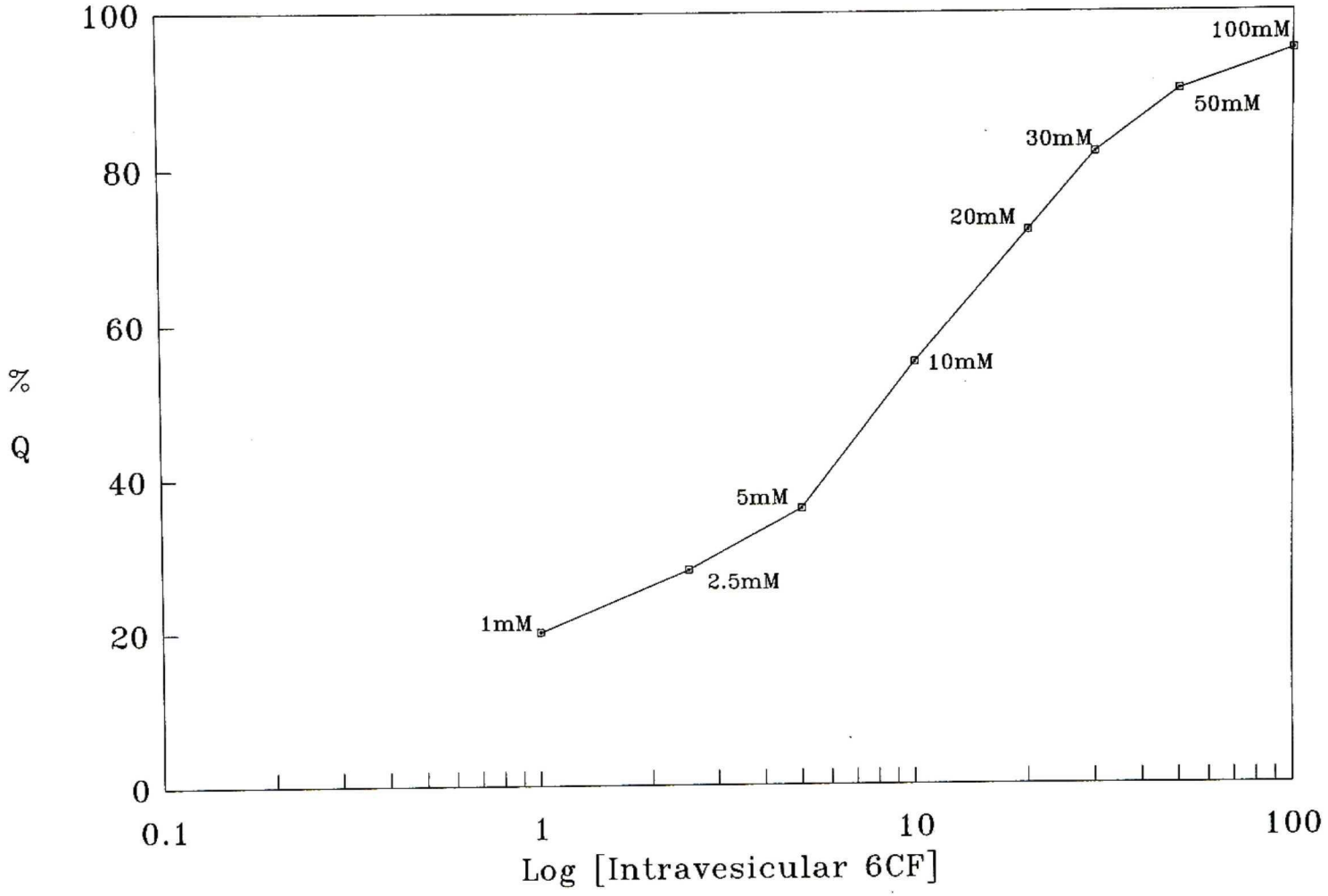

$\%Q = (1-(F/Fmax)) \times 100$

of 400nm and measuring the scattered light at the same wavelength; the band-pass slits were set at 4nm. Samples contained SUVs (25-30uM PS) and various amounts of subsequently added MGN2a.

Osmolarity Measurements

Buffers were prepared with 10mM Pipes, 1mM EDTA, 150mM NaCl (pH 7.0) and either no sucrose, 0.1M sucrose, 0.15M sucrose, 0.2M sucrose, 0.4M sucrose, or 0.1M 6CF. The osmolarity of the buffer solutions was measured with an Osmette Precision Osmometer, model 2007 (Precision Systems, Inc.). Two milliliters of each buffer solution was measured in the Osmette, which was calibrated with precise salt standards in order to obtain a direct digital readout in milliosmoles.

Effect of MGN2a on the Permeability of PS Vesicles

Addition of MGN2a to PS SUVs caused the release of 6CF, as shown in Figure 5. (6CF shows no significant leakage from PS vesicles in the absence of peptide (Figure 5)). A rapid initial burst of 6CF release, followed by a slower phase, suggests that the kinetics of 6CF release from PS vesicles is not a simple first order process. Indeed, a semilog plot of the kinetic data indicates that the process is at least bi-exponential (Figure 6).

Before investigating the kinetics of release in detail, we felt it necessary to establish three things about the interaction of the peptide with the vesicles. First, we wanted to know whether osmolarity is a critical factor determining the susceptibility of the vesicles to peptide-induced dye release. Second, we wanted to know whether addition of peptide causes wholesale changes in vesicle morphology, in particular aggregation and/or fusion to larger structures. Third, we wanted to determine a binding isotherm for the peptide-vesicle interaction.

Effect of Extravesicular Osmotic Pressure on 6CF Release from SUVs Induced by MGN2a

Figure 5

MGN2a-induced release of 6CF from PS suvs. The amount of dye release was monitored after addition of the indicated amounts of MGN2a to loaded vesicles (PS concentration = 30uM).

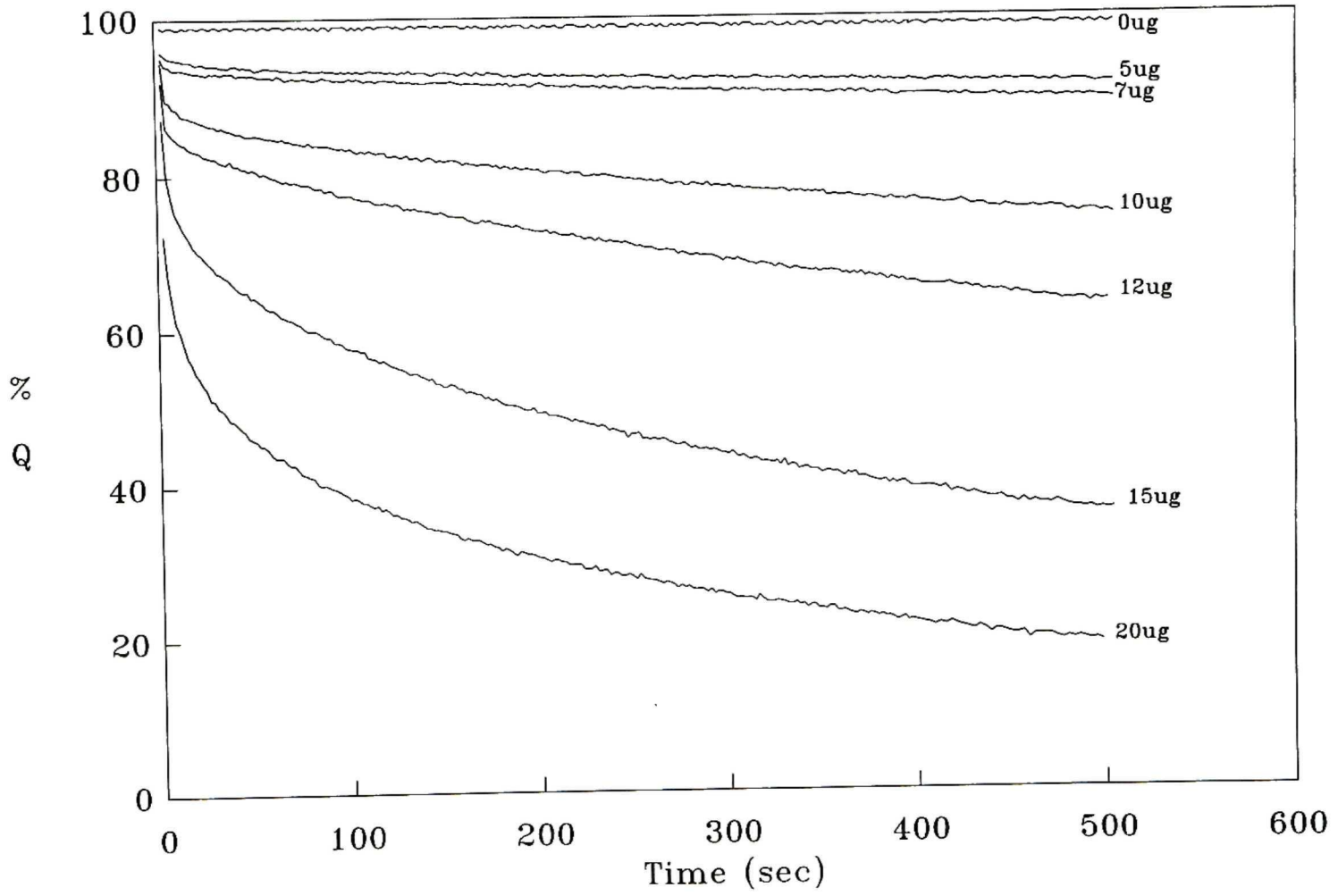

% Q = (1 - (F/Fmax)) x 100

Figure 6

Semilog plot of MGN2a-induced release of 6CF from PS SUVs. These curves are replots of the results shown in Figure 5.

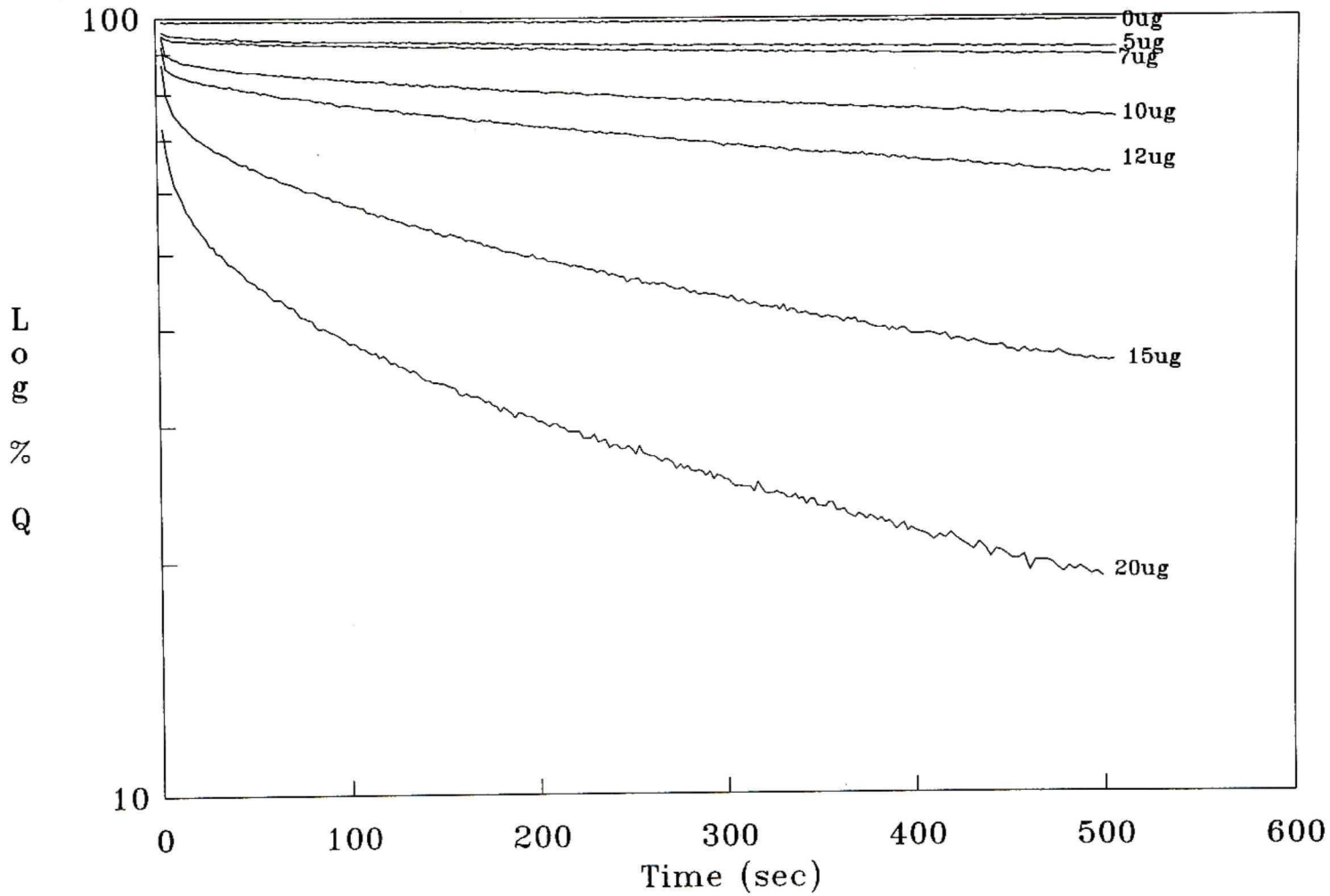

% Q = (1 − (F/Fmax)) x 100

It has been reported that substantial initial 6CF release can occur when an osmotic gradient exists across the lipid bilayer in which the osmotic pressure of the vesicle interior is higher than the osmotic pressure of the external media (Lelkes, 1984). Figures 7 and 8 demonstrate that the initial release of 6CF is slightly enhanced when MGN2a is added to vesicles suspended in buffer in which an osmotic gradient exists compared with MGN2a added to vesicles in buffer that contains sucrose to adjust the osmolarity near iso-osmotic conditions. However, it was of interest to determine whether dye release was sensitive to osmotic gradients in which the osmotic pressure of the external medium was higher than the osmotic pressure of the vesicle interior. The osmolarity of the solutions used in these experiments was determined as described in Materials and Methods. Table I shows the osmolarity of the solutions used. It was found that initial dye release after 1 min induced by MGN2a is not significantly sensitive to osmotic gradients in which the osmolarity of the external medium is higher than the vesicle interior (Figure 9). Therefore, we conducted all experiments using buffer that contained 100mM sucrose in order to eliminate the osmotic gradient which might cause anomalous results.

Light - Scattering Studies

Figure 7

MGN2a-induced release of 6CF from PS SUVs in buffer containing no sucrose. Loaded vesicles (PS concentration = 29uM) were placed in buffer B for 100 sec prior to addition of the indicated amounts of MGN2a.

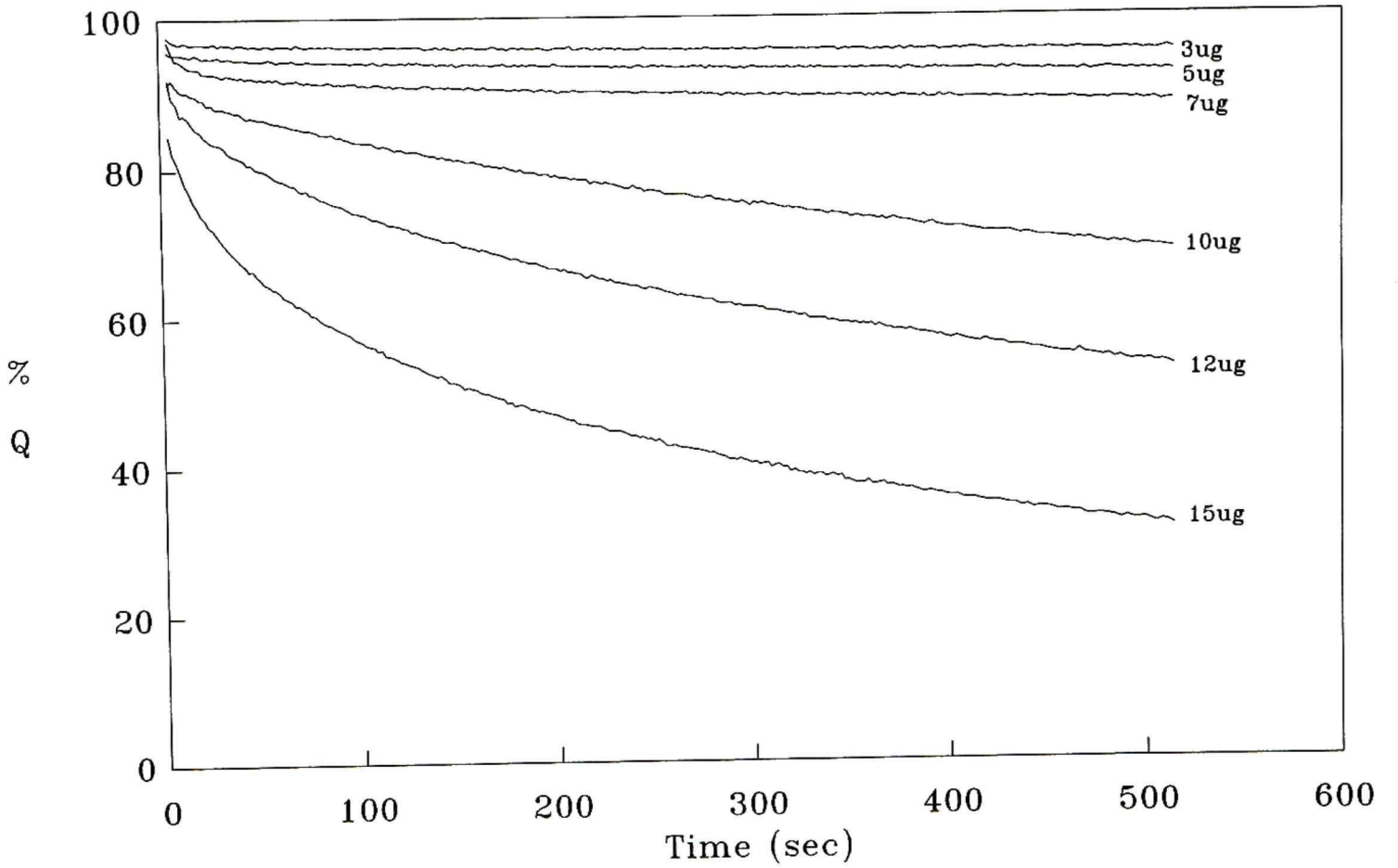

%Q = (1 - F/Fmax) x 100

Figure 8

MGN2a-induced release of 6CF from PS SUVs in buffer containing sucrose. Loaded vesicles (PS concentration = 29uM) were placed in buffer A for 100 sec prior to addition of the indicated amounts of MGN2a.

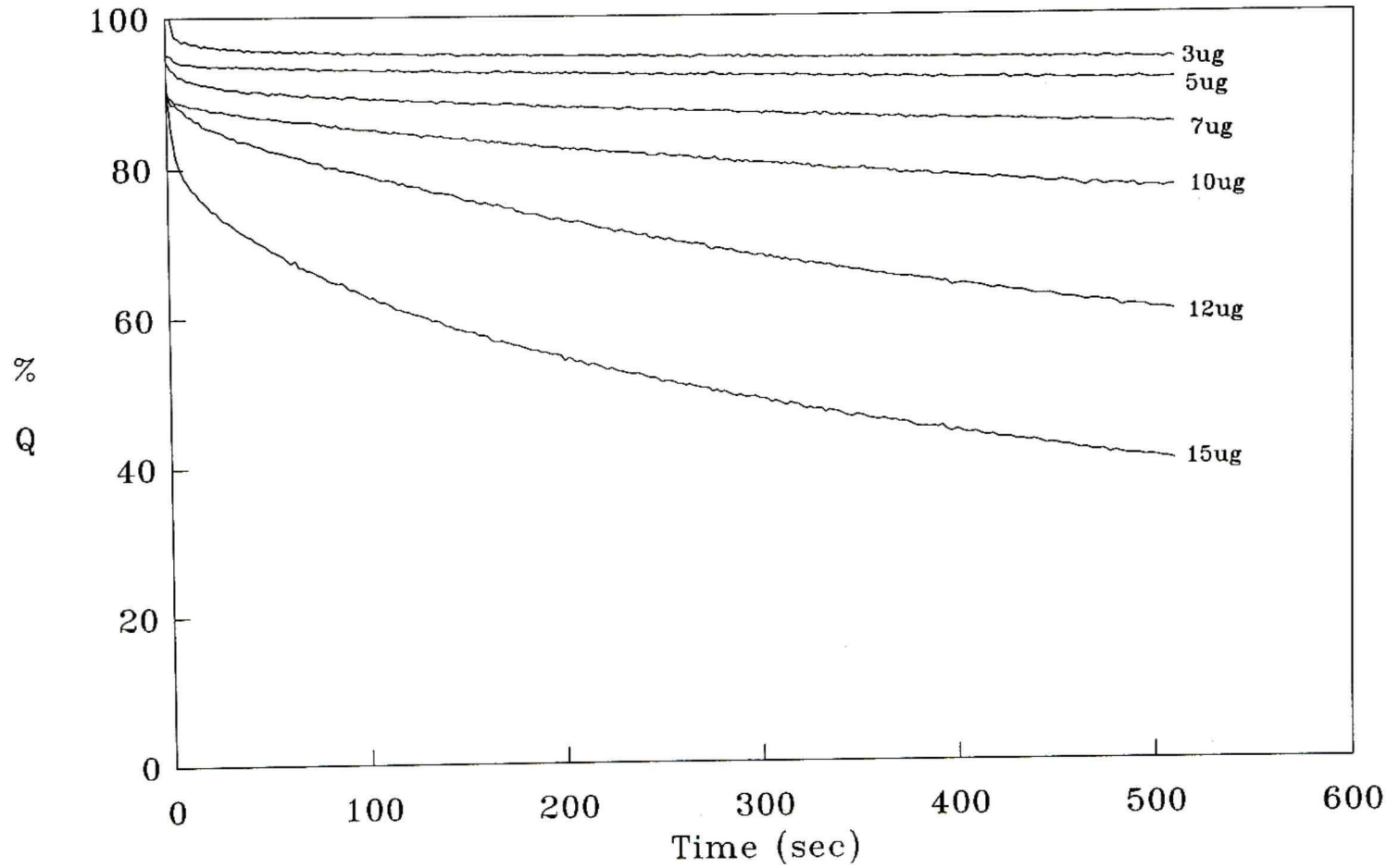

%Q = (1 - F/Fmax) x 100

Table I. Osmolarity of Buffer B Containing Various Concentrations of Sucrose or 6CF

Sample	Osmolarity
Buffer B only	331mOsm
100mM 6CF	436mOsm
100mM Sucrose	415mOsm
150mM Sucrose	462mOsm
200mM Sucrose	535mOsm
400mM Sucrose	804mOsm

Figure 9

Osmotic dependence of peptide-induced release of 6CF from PS SUVs. Small aliquots of MGN2a were added to 6CF loaded SUVs. The SUVs were pre-equilibrated in 2ml of buffer B containing from 0.15M - 0.4M Sucrose. The 6CF leakage rate, defined as percent leakage for the initial minute, is plotted as a function of ug of MGN2a at different concentrations of sucrose.

Concentration of Sucrose: + , 0.15M Sucrose

Δ , 0.2M Sucrose

✦ , 0.4M Sucrose

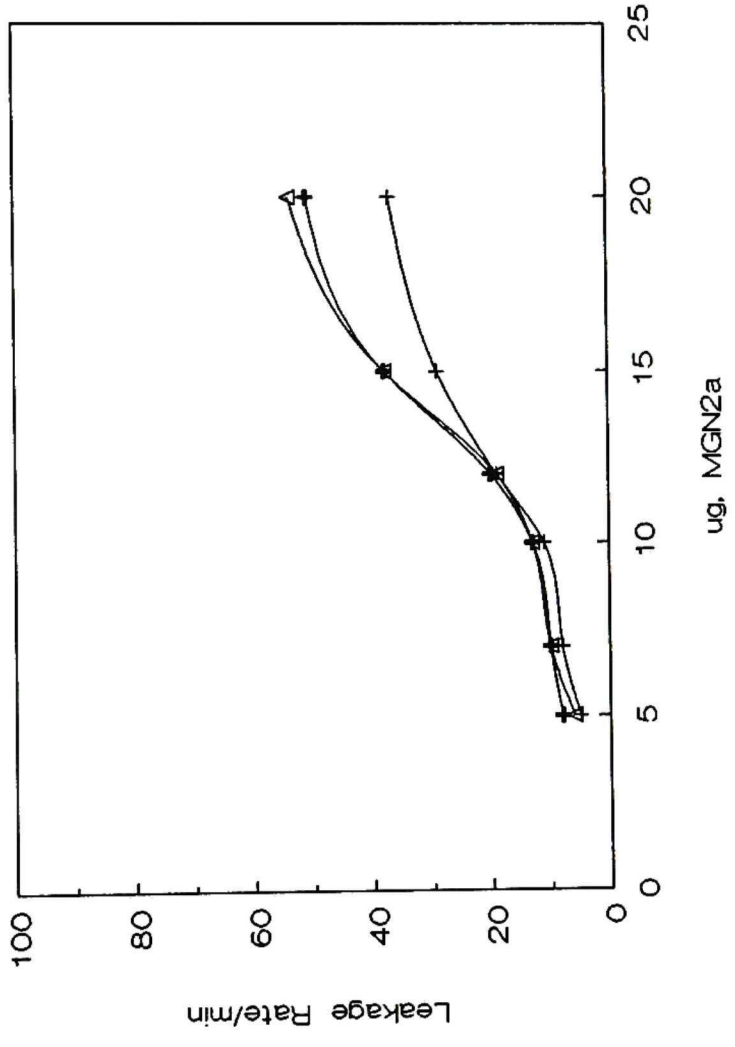
Leakage Rate/min
100
80
60
40
20
0
0
5
10
15
20
25
ug. MGN2a

In order to determine whether MGN2a was causing aggregation or fusion of vesicles, light-scattering measurements were performed as described in Materials and Methods. Since SUVs have been shown to be Rayleigh scatterers, the following equation applies for a dilute solution of particles measured at a fixed wavelength and scattering angle:

$$i/I_o = K(\delta\tilde{n}/\delta c)^2 \, M \, c$$

where i is the intensity of scattered light, I_o is the intensity of incident light, $\delta\tilde{n}/\delta c$ is the refractive index increment, M is the molecular weight, c is the concentration of the particles in gm/ml, and K is a constant.

Even in the absence of fusion or aggregation, the light scattering of the SUVs is expected to increase upon binding because the peptide increases M, c, and perhaps $\delta\tilde{n}/\delta c$. Since we are interested only in the relative increase in the scattering upon the addition of peptide, the following equation can be used:

$$i_c/i_v = [(\delta\tilde{n}/\delta c)_c^2 \, M_c \, c_c]/[(\delta\tilde{n}/\delta c)_v^2 \, M_v \, c_v]$$

where the subscripts v and c refer to the vesicles and peptide-vesicle complexes, respectively. The amount of MGN2a bound per lipid molecule under each set of experimental conditions was calculated on the basis of a binding

constant of 1.12×10^5 M^{-1} (see following section). From this, the ratios M_c/M_v and c_c/c_v could be calculated.

Although the refractive index increments were not measured, one can reasonably estimate the limits of this factor, as discussed by Roseman et al. (1977). The value of $\delta\tilde{n}/\delta c$ for a complex is given by the equation:

$$(\delta\tilde{n}/\delta c)_c = W_l \times (\delta\tilde{n}/\delta c)_l + W_p \times (\delta\tilde{n}/\delta c)_p$$

where $(\delta\tilde{n}/\delta c)_c$ is the refractive index increment for a complex, W_l and W_p are the weight fractions of lipid and protein, respectively, and $(\delta\tilde{n}/\delta c)_l$ and $(\delta\tilde{n}/\delta c)_p$ are the refractive index increments for pure lipid and protein, respectively. Using a value of 0.1478 ml/g for the refractive index increment of lipid and a range of 0.15 to 0.2 ml/g for the refractive index increment of proteins, one can calculate the range of refractive index increments for the complexes. With these values it is then possible to calculate the predicted ratio of i_c/i_v in the absence of fusion or aggregation.

If the entire population of complexes undergoes fusion or aggregation, the predicted intensity ratio is obtained by multiplying i_c/i_v by the number of vesicles participating in the fusion event or in the aggregate. Clearly, the smallest number of vesicles that can fuse or aggregate is two. In practice, it has never been reported

that such limited fusion or aggregation takes place; agents that promote aggregation or fusion usually lead to the formation of particles having almost twenty times the mass of the starting SUVs.

As shown in Table II, the modest increases in light scattering that occur upon addition of MGN2a to the SUVs can be attributed to increases in the mass of the particles. We conclude from these results that negligible fusion or aggregation is taking place.

Determination of the MGN2a-Lipid Binding Constant

To determine the affinity of MGN2a for the PS vesicles we utilized the so-called "indirect method", which has been used to determine the affinity of permeabilizing agents for liposomes or cells (Thron, 1964 and Matsuzaki et al., 1989a). The theoretical basis of this method is as follows. If one measures the fractional leakage rate over a large range of peptide and lipid concentrations, the results can be represented as a surface on a three dimensional orthoginal plot where z, y, x axes are activity (fractional leakage rate), total peptide concentration, and total lipid concentration respectively. The set of planes parallel to the y-x axis and cutting through the surface constructed from the experimental data gives a set of "iso-activity" curves in which the total peptide concentration is plotted

Table II. MGN2a-Induced Increases in Light-Scattering (LS) of PS SUVs[a]

Sample[b]	Measured (i_c/i_v)[c]	Theoretical LS Lower Limit of (i_c/i_v)[d]	Theoretical LS Upper Limit of (i_c/i_v)[e]	Theoretical Lower Limit for Aggregation or Fusion[f]
5ug MGN	1.31	1.17	1.23	2.34
7ug MGN	1.23	1.25	1.34	2.50
10ug MGN	1.54	1.34	1.47	2.68
12ug MGN	1.91	1.44	1.61	2.88
15ug MGN	1.92	1.56	1.78	3.12
20ug MGN	2.38	1.77	2.09	3.54

a. This table describes the observed LS increase and the theoretical increases in LS based solely on increases in molecular weight and mass of particles upon peptide binding in the absence of fusion or aggregation.

b. 5 to 20ul of 0.37mM MGN2a was added to SUVs (PS concentration = 25-30uM) loaded with 100mM 6CF and LS was measured using a spectrofluorometer as described in Materials and Methods.

c. (i_c/i_v) is the relative increase in light scattering (see text).

d. Assumes the ratio of the squares of the refractive index increments is unity.

e. Assumes that the ratio of the squares of the refractive index increments will increase in proportion to the percent increase in mass and molecular weight of the vesicle upon MGN2a binding, as described in the text.

f. 2 x (Theoretical LS Lower Limit for Complex).

against total lipid concentration at various levels of constant activity.

If one makes the reasonable assumption that the fractional leakage rate is dependent only on the ratio of bound peptide per lipid molecule, each iso-activity curve must be linear according the following conservation equation:

$$[P]_o = [P]_f + r[L]$$

where $[P]_o$ is total concentration of peptide, $[P]_f$ is the concentration of unbound peptide, [L] is the total concentration of lipid, and r is the ratio of bound peptide to lipid. Consequently, a series of $[P]_o$ versus [L] plots generates a family of straight lines with slopes of r and intercepts of $[P]_f$.

Figure 10 shows dose - response curves for the fractional leakage rate after 1 min at four different lipid concentrations. Figure 11 shows that plots of $[P]_o$ versus [L] do in fact yield a linear relation, with a least squares correlation coefficient of greater than 0.990. The r and the $[P]_f$ values were obtained from the slopes and the intercepts, respectively. (Similar plots were obtained for the fractional leakage rate and $[P]_o$ versus [L] after 10-90 sec and the results were not significantly different.) Figure 12 shows the binding isotherm for MGN2a interacting with PS SUVs according to the estimated values of r and $[P]_f$. Since the binding isotherm is linear, the interaction of MGN2a

Figure 10

Dependence of 6CF leakage rate on peptide and lipid concentrations. Small aliquots of MGN2a were added to 6CF loaded SUVs. The 6CF leakage rate, defined as percent leakage for the initial minute, is plotted as a function of $[P]_o$ at different [L].

[L]: + , 25uM

Δ , 50uM

O , 75uM

+ , 100uM

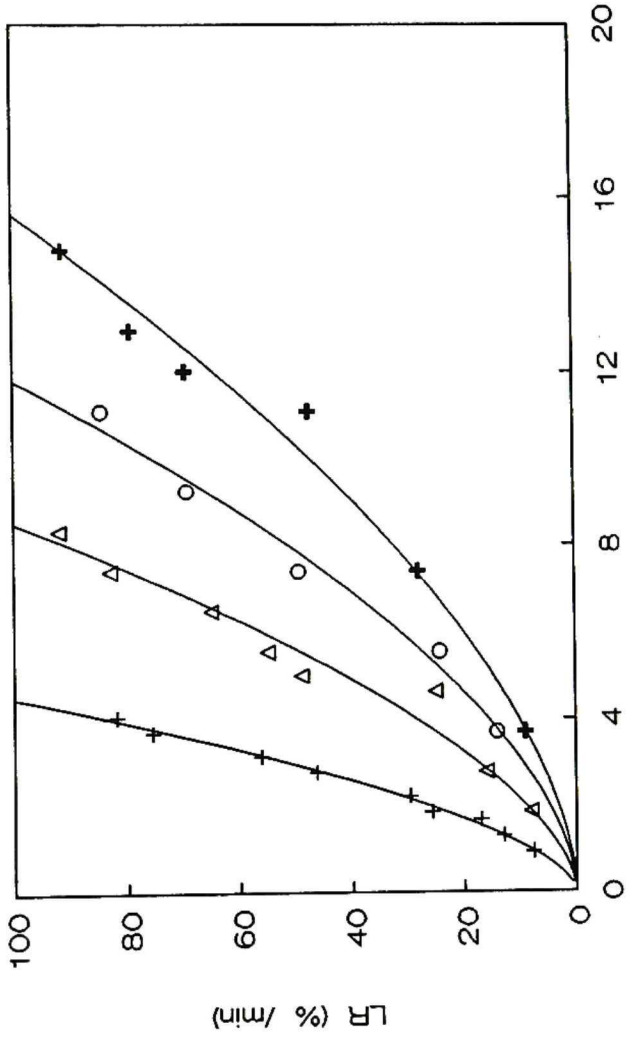
LR (% /min)
100
80
60
40
20
0
0
4
8
12
16
20
[P]o (uM)

Figure 11

Estimation of free and membrane-bound peptide concentrations. Four pairs of $[P]_o$ and [L] values at a given leakage rate were obtained from Figure 10. $[P]_o$ is plotted against [L] according to the equation, $[P]_o = [P]_f + r[L]$. The free peptide concentration, $[P]_f$, and the amount of the membrane-bound peptide per lipid molecule, r, were evaluated from the intercept and slope, respectively. Leakage rate (% min^{-1}):

+ , 20; ▲ , 30; △ , 40; ● , 50; ○ , 60; ▽ , 70;

✦ , 80; ◇ , 90. The lines are least-square fits.

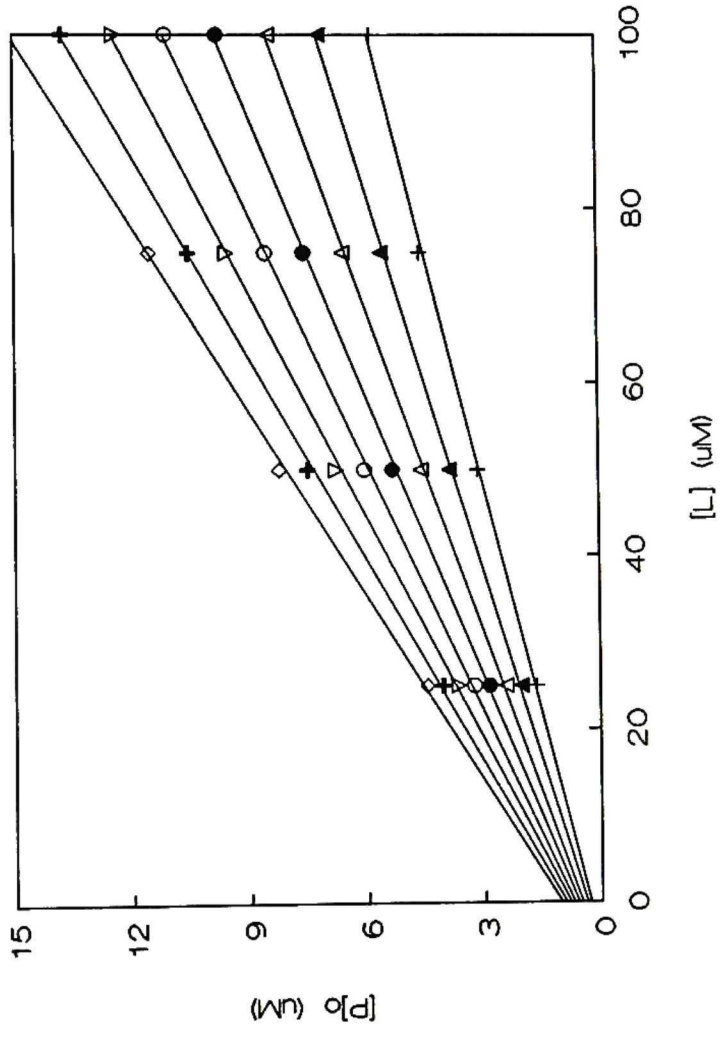
[P]o (uM)
15
12
9
6
3
0
0
20
40
60
80
100
[L] (uM)

Figure 12

Binding isotherm for the interaction of MGN2a with 6CF loaded PS SUVs. The relationship between r and $[P]_f$ obtained from Figure 11 is shown.

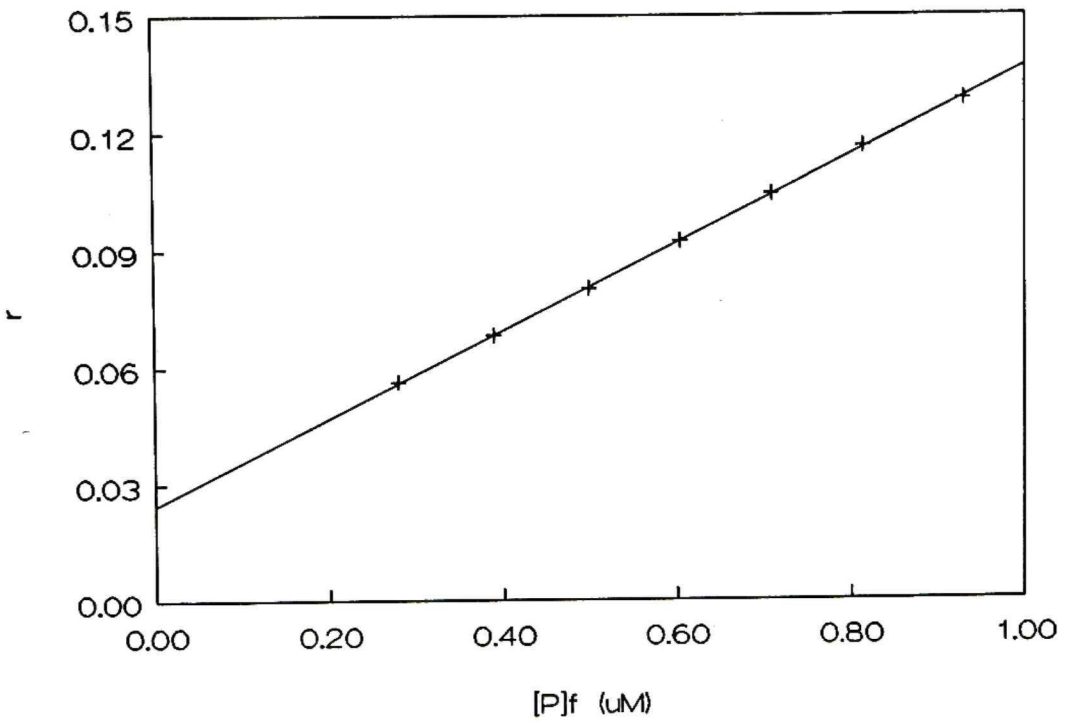
0.15
0.12
0.09
0.06
0.03
0.00
r
0.00
0.20
0.40
0.60
0.80
1.00
[P]f (uM)

with SUVs over the experimental range of lipid and protein concentrations can be accounted for by simple partitioning, with a binding constant (obtained from the slope) of 1.12 x 10^5 M^{-1}. This linearity argues against there being a significant change in the aggregation number of MGN2a upon interaction with vesicles. If in fact the peptide exists mainly as monomers in the aqueous phase, then it exists primarily as monomers on the vesicle.

A plot of leakage rate versus r (Figure 13) is linear, and extrapolates to a so-called "critical" r value of 0.03, which is in agreement with the r value determined for MGN1 (Matsuzaki et al., 1989a). A critical value of 0.03 means that the peptide does not begin to cause leakage until the bound peptide/lipid ratio reaches this value. The necessity to accumulate a critical amount of peptide on the vesicle in order to induce leakage is also reflected in the dose response curves of Figure 10.

It is likely that if we were able to extend the dose-response curves to higher peptide concentrations, the complete dose-response curves would appear sigmoidal. A sigmoidal dose -response curve has been interpreted to mean that a peptide forms multimeric channels in the membrane through cooperative interaction of the monomers (Juretic et al., 1989a and Westerhoff et al., 1989b). However, sigmoidal dose response curves have also been observed with detergents (Thron, 1964). In addition, the fact that leak-

Figure 13

Quantitative analysis of MGN2a-induced leakage of 6CF from PS SUVs. Relationship between the leakage rate and the amount of PS-bound MGN2a.

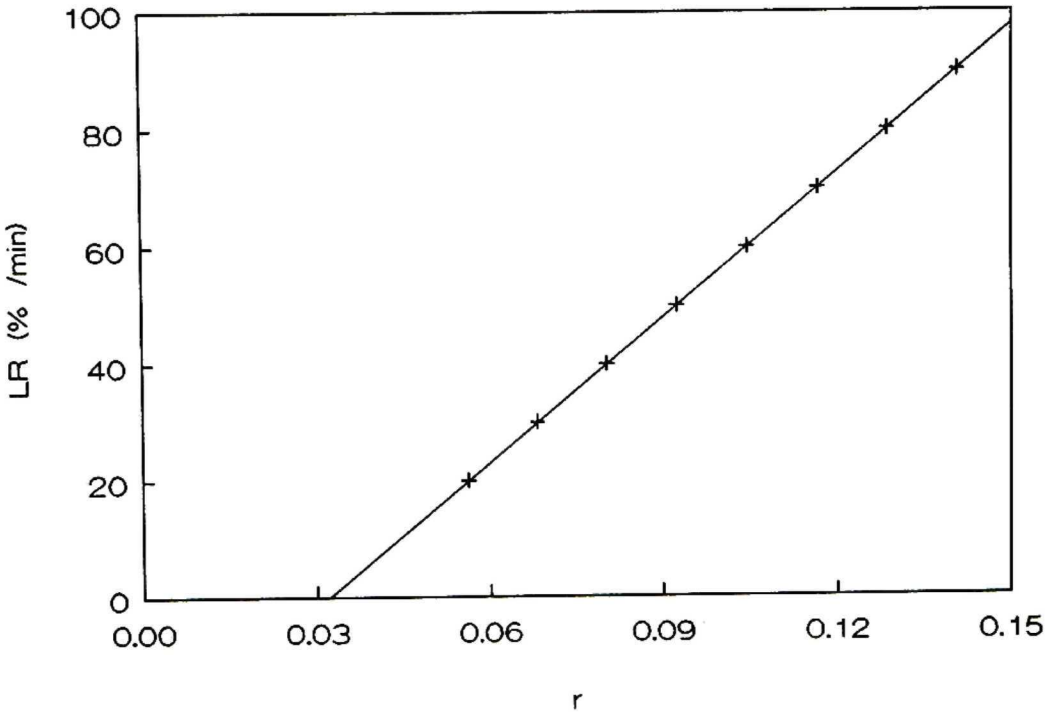
100
80
60
40
20
0
LR (% /min)
0.00
0.03
0.06
0.09
0.12
0.15
r

age is linearly dependent on r (Figure 13) also argues against a leakage mechanism based on aggregation of peptide monomers to form multimeric channels.

Studies on the Biphasic Release of 6CF:

a. Possibility of MGN2a-induced Global Destabilization of SUVs

This biphasic leakage rate depended on both the peptide and the lipid concentration. As shown in Figure 14, an increase in the peptide concentration or a decrease in the lipid concentration resulted in an enhanced fractional leakage rate. As shown in the previous section, the observed leakage phenomenon involves a reversible binding process.

One possible explanation for the biphasic release is based on the assumption that the packing of the lipids in SUVs is not in the lowest energy configuration for vesicles of this size. Conceivably, sonication could trap the lipids in a metastable state. If this were the case, addition of MGN2a could catalyze an initial rapid global relaxation of the structure to a state that is compatible with the geometric constraints of the vesicle.

If so, one would predict that a single addition of MGN2a would cause a rapid release of dye concomitant with

Figure 14

Leakage of 6CF as a function of peptide and lipid concentration. MGN2a-induced leakage of 6CF was obtained by adding small aliquots of MGN2a to 6CF-loaded SUVs. Experimental conditions, where $[P]_o$ is the peptide concentration in uM and [L] is the lipid concentration in uM are as follows: Line 1, $[P]_o$=0 and [L]=25-30; Line 2, $[P]_o$=1.85 and [L]=25-30; Line 3, $[P]_o$=3.7 and [L]=50-60; Line 4, $[P]_o$=3.7 and [L]=25-30.

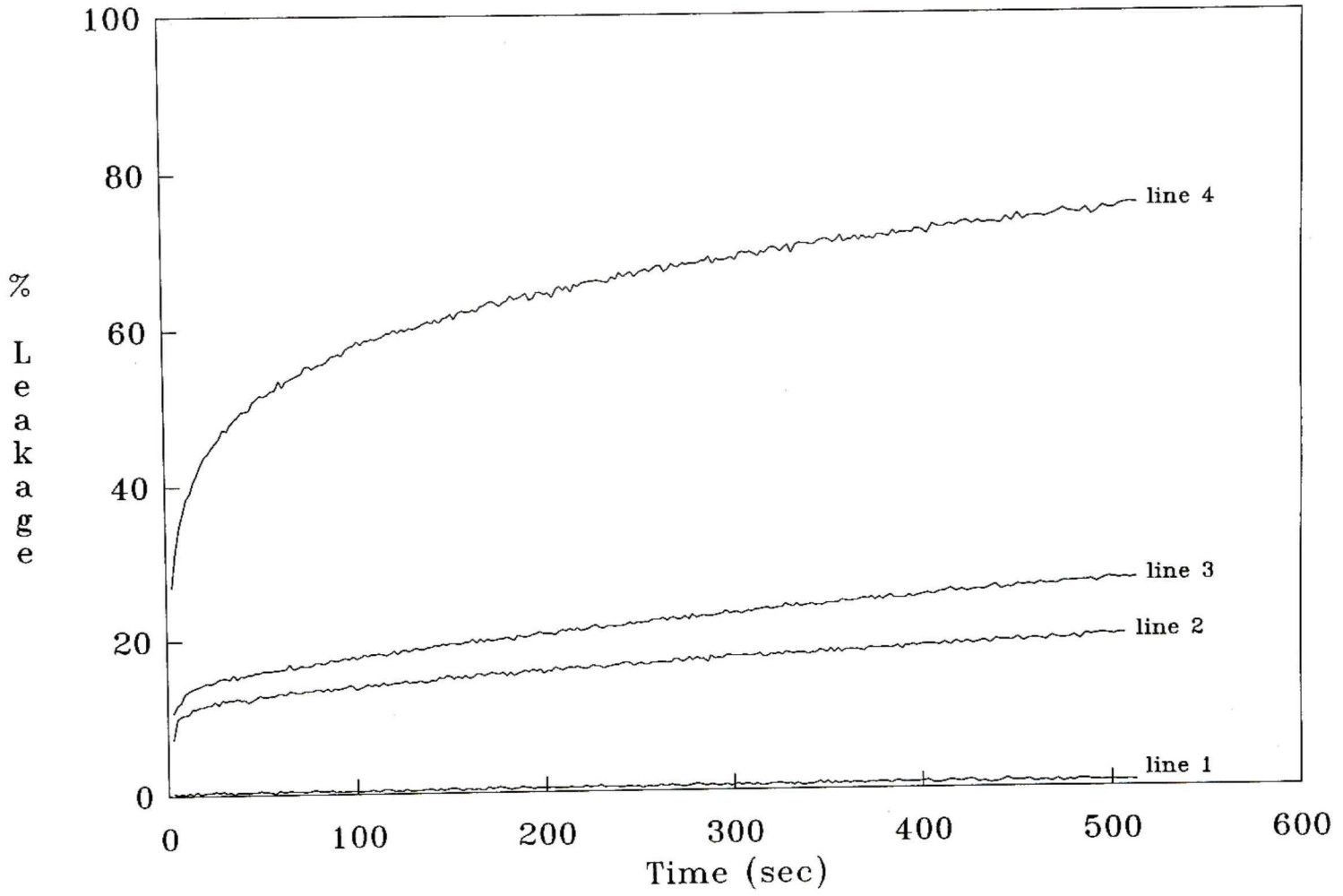
100
80
60
40
20
0
% Leakage
line 4
line 3
line 2
line 1
0
100
200
300
400
500
600
Time (sec)

inducing a relaxation of the vesicle, whereas subsequent additions of MGN2a to the vesicle would have much less effect on dye release. One would also predict that addition of MGN2a to LUVs would not show biphasic release kinetics.

Figure 15 shows the effect of adding successive additions of MGN2a to SUVs. Clearly, each subsequent addition causes an additional biphasic release of dye. Furthermore, as shown in Figures 16 and 17 biphasic release kinetics are also observed with LUVs. Therefore, it does not appear as if the biphasic release is due to an initial global reorganization of the lipids in the SUVs, or to some peculiar properties of the small vesicles.

b. Possibility of SUVs Interacting with Water Soluble Aggregates of MGN2a

Another explanation for the biphasic kinetics is that MGN2a, which may exist as aggregates in the concentrated stock solution, may initially bind to the vesicles in an aggregated form. Interaction of MGN2a aggregates with the lipid bilayer could cause disruption of the permeability barrier resulting in rapid release of 6CF. After the initial interaction of MGN2a aggregates with the vesicle, the aggregates could disperse through lateral diffusion in conjunction with phospholipid repacking to form a moderately destabilized structure that permits slow leakage of 6CF. If

Figure 15

Successive addition of MGN2a to 6CF loaded vesicles. Small aliquots of MGN2a, in the amounts indicated, followed by subsequent addition of equal aliquots of MGN2a were allowed to interact with 6CF loaded SUVs.

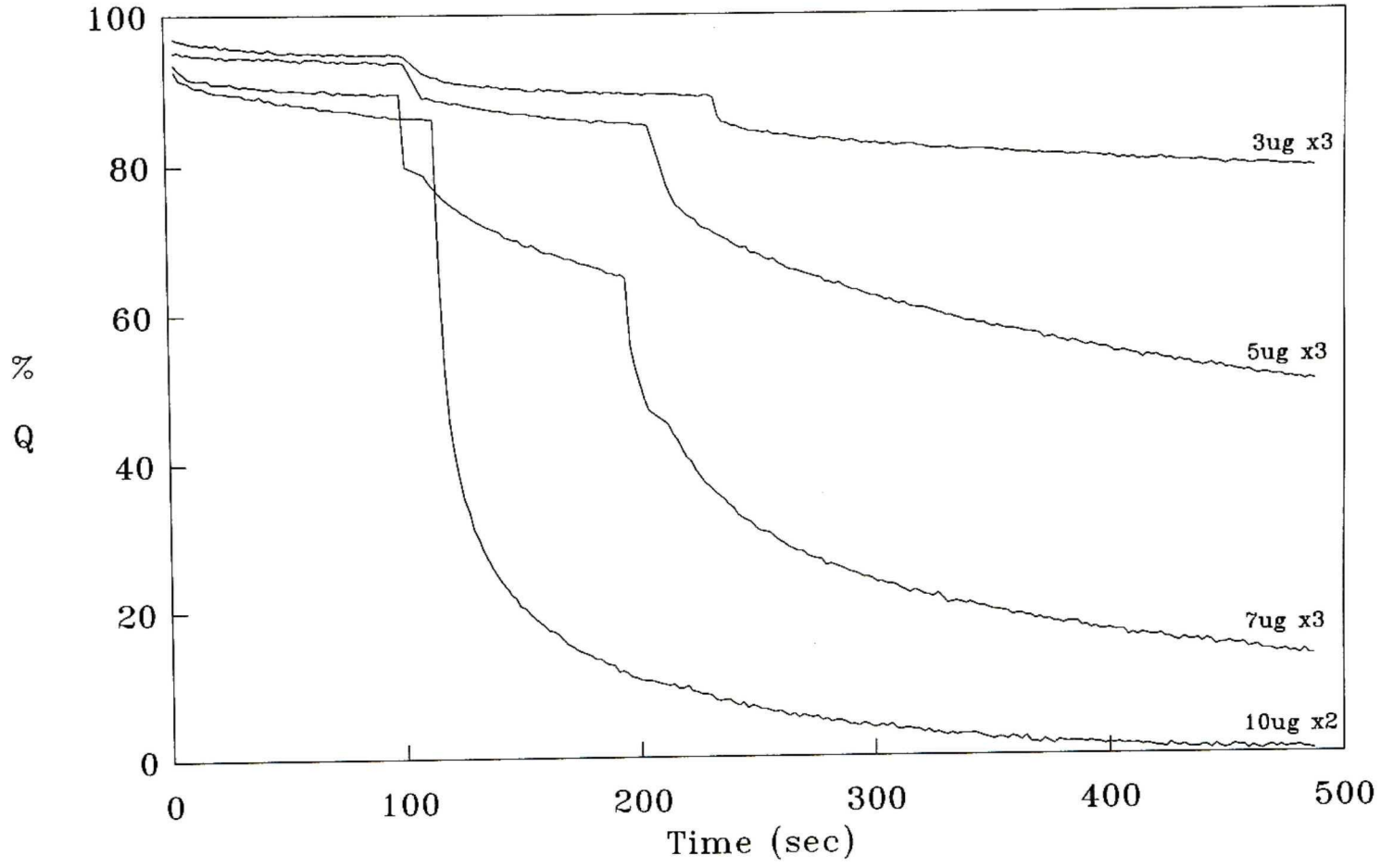

% Q = (1 - (F/Fmax)) x 100

Figure 16

MGN2a-induced release of 6CF from PS LUVs. Small aliquots of MGN2a were added to PS LUVs loaded with 100mM 6CF prepared as described in Materials and Methods. PS concentration was 25uM, in buffer A.

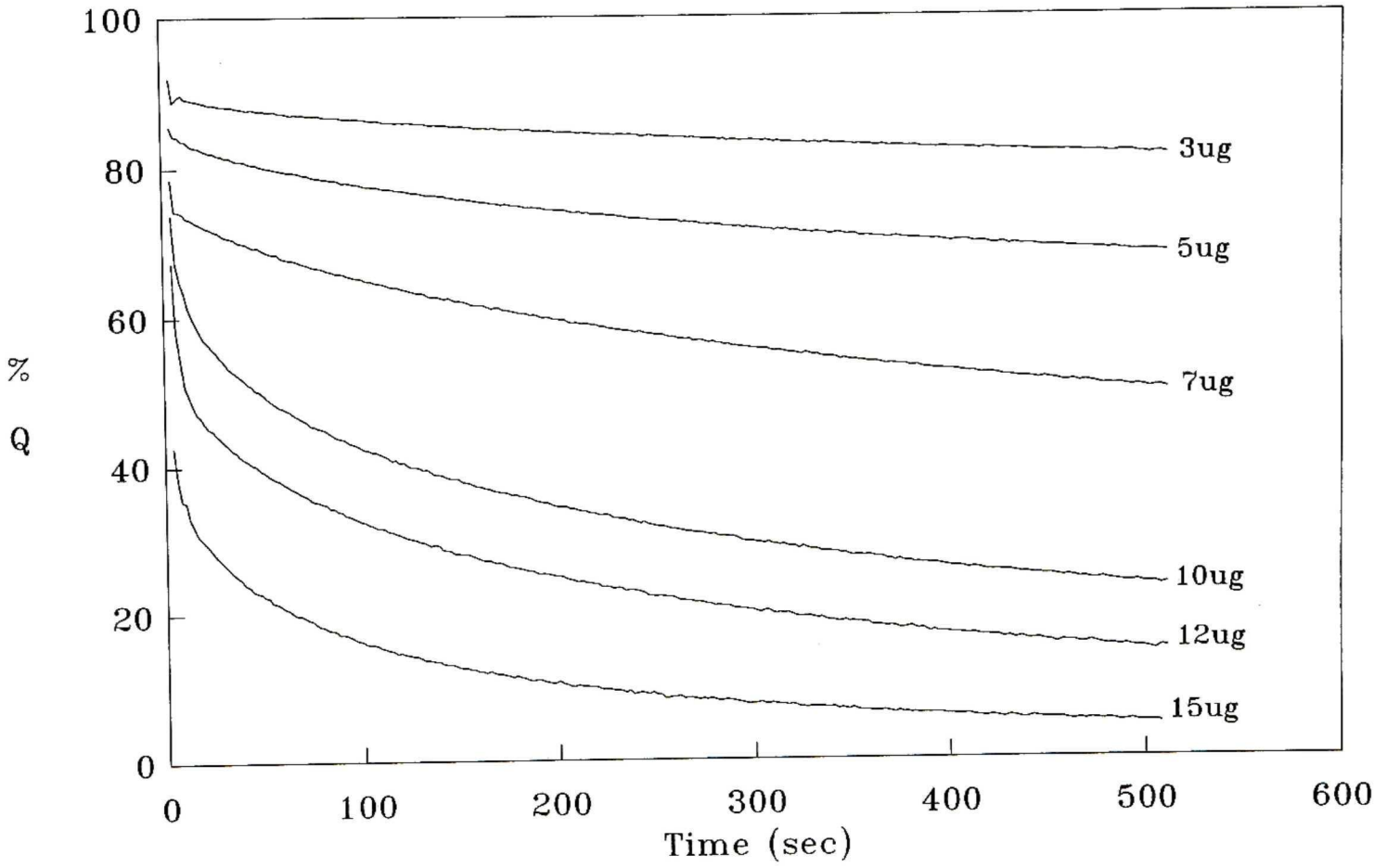

%Q = (1−F/Fmax) x 100

Figure 17

Semilog Plot of MGN2a-induced release of 6CF from PS LUVs. These curves are replots of the results shown in Figure 16.

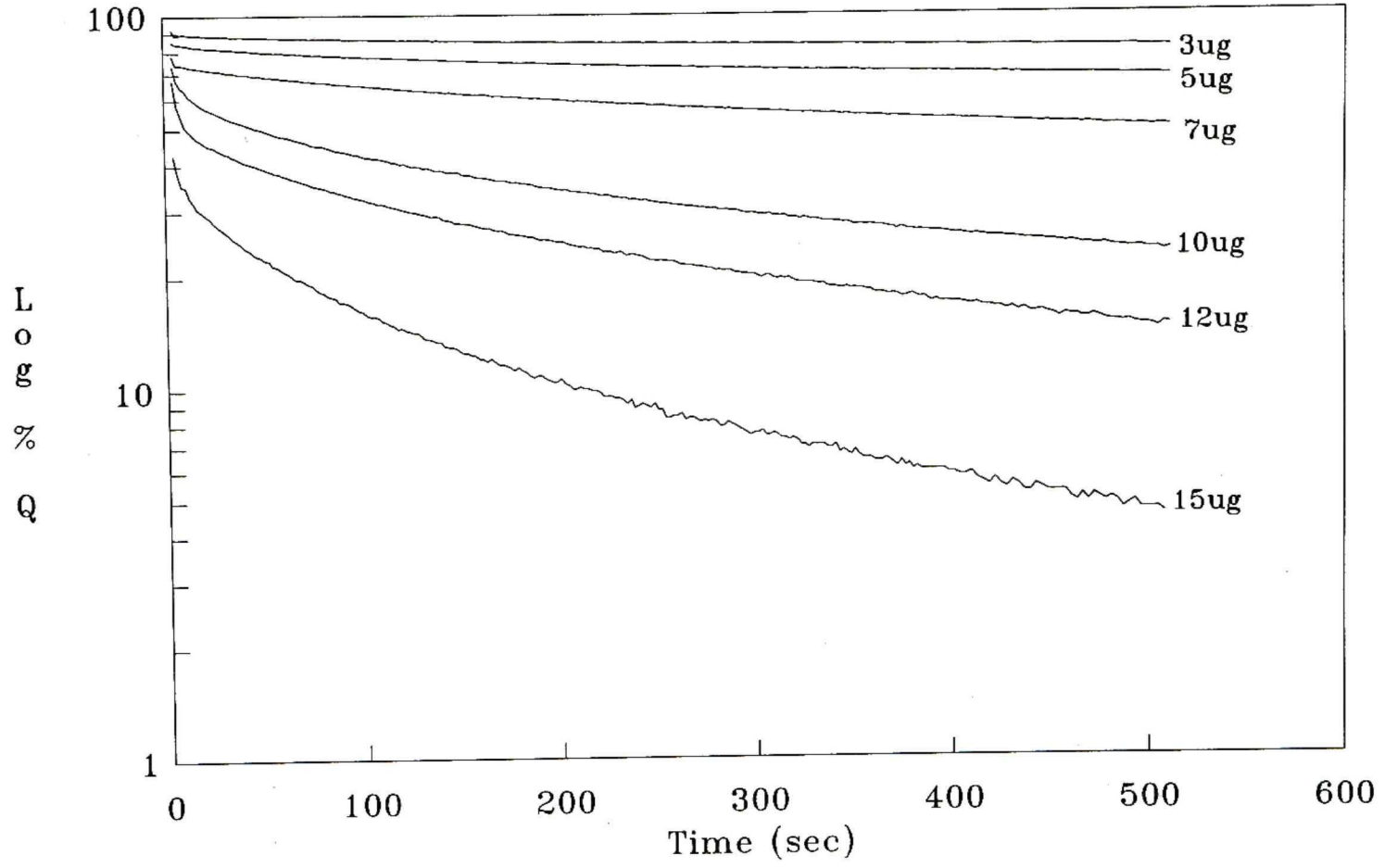

%Q = (1−F/Fmax) x 100

this is true, then preincubation of MGN2a in buffer A before adding PS SUVs should allow for the dissociation of aggregates to form more monomers, and addition of vesicles to this MGN2a solution should display a much smaller fast release phase.

Initial preincubation of 20ug MGN2a (3.7uM) in buffer A for 5 to 60 minutes prior to vesicle addition showed only a modest reduction in MGN2a-induced biphasic leakage of 6CF (Figure 18). Preincubation of MGN2a for 24 hours prior to vesicle addition showed a marked reduction in the initial fast release of 6CF (Figure 19). However, as described below, it was determined that this observation was due to MGN2a binding to the walls of the tubes as has been demonstrated for melittin (Tosteson et al., 1985b). When 3.7uM MGN2a was mixed with buffer A in a cuvette and allowed to stand for different times prior to vesicle addition, there was a small reduction in the overall leakage of 6CF (Figure 18). In contrast, when 3.7uM MGN2a was subjected to continuous stirring in buffer A in the cuvette for 5-60 minutes prior to vesicle addition, there was significant reduction in 6CF leakage with almost complete removal of the fast phase after 60 minutes of stirring (Figure 20). This significant reduction in MGN2a-induced leakage could be eliminated by the following procedure. First, MGN2a was stirred in a cuvette for 1 hr to saturate the binding sites of the glass walls. This solution was then removed without

Figure 18

Effect on functional activity of pre-equilibrating MGN2a in buffer A. MGN2a (3.7uM) was added to 2ml of buffer A and allowed to stand for 5-60 minutes prior to addition of 6CF loaded vesicles (PS concentration = 28uM).

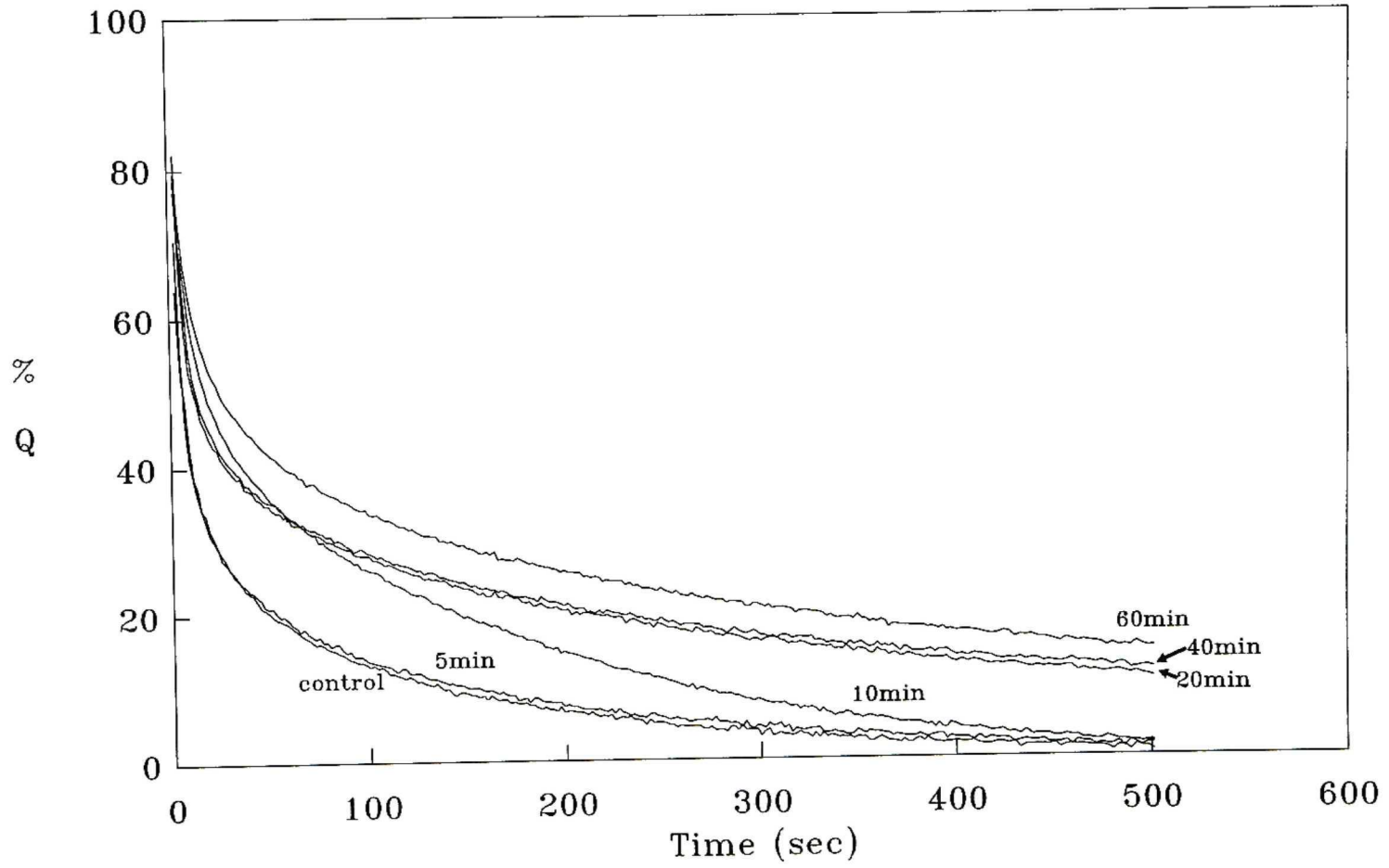

% Q = (1 – (F/Fmax)) x 100

Figure 19

Effect on functional activity of pre-equilibrating MGN2a for 24 hours in buffer A. The indicated amounts of MGN2A were added to 2ml of buffer A in test tubes that were allowed to stand at room temperature for 24 hours. Dye release was initiated by the addition of 6CF loaded PS SUVs (PS concentration = 26uM) to the MGN2a/ Buffer A mixture.

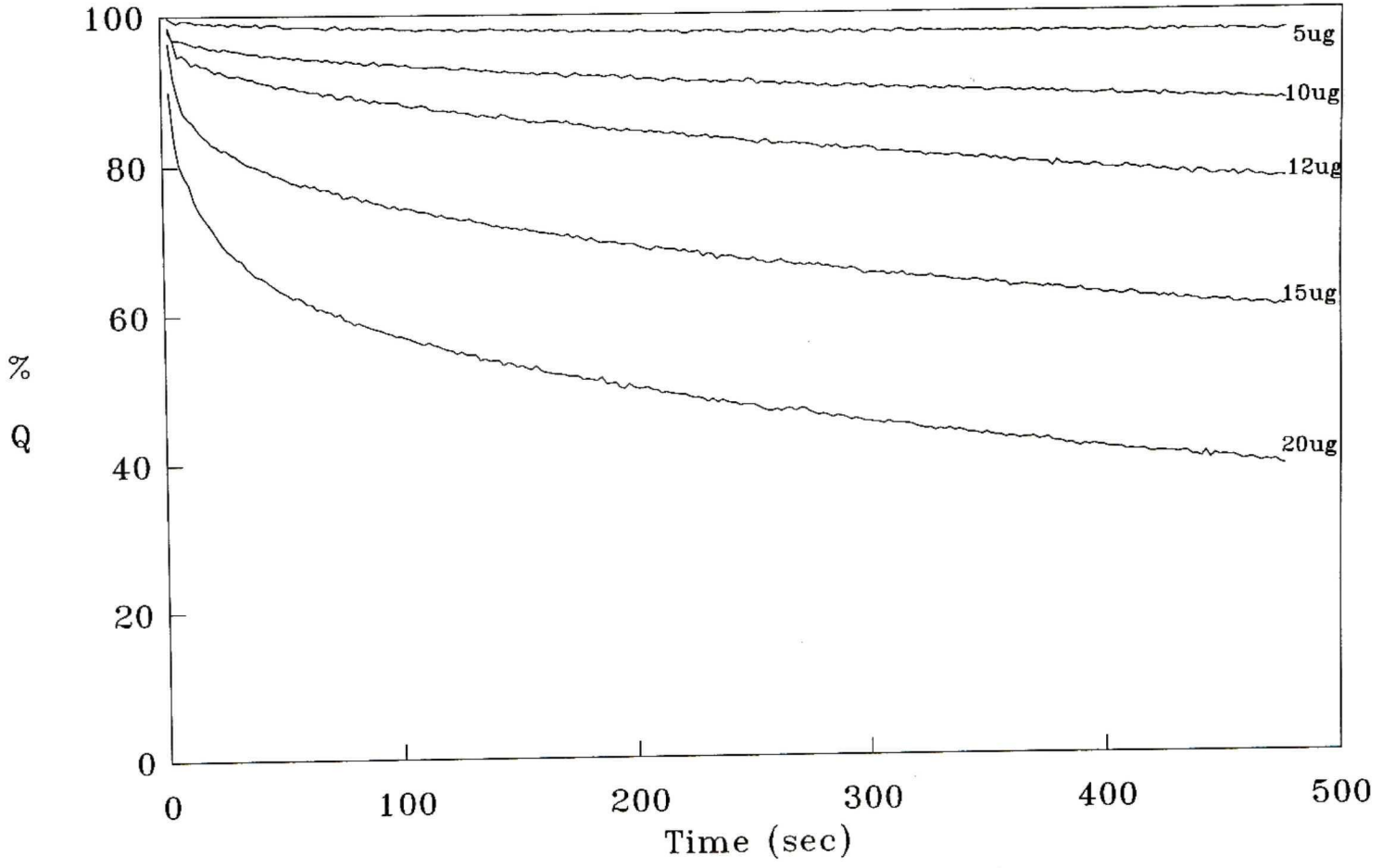

% Q = (1 – (F/Fmax)) x 100

Figure 20

The effect on functional activity of allowing MGN2a to pre-equilibrate in buffer A with continued stirring. MGN2a (3.7uM) was mixed with 2 ml of buffer A and stirred in a cuvette for 5-60 minutes prior to addition of 6CF (100mM) loaded vesicles. The PS concentration was 28uM.

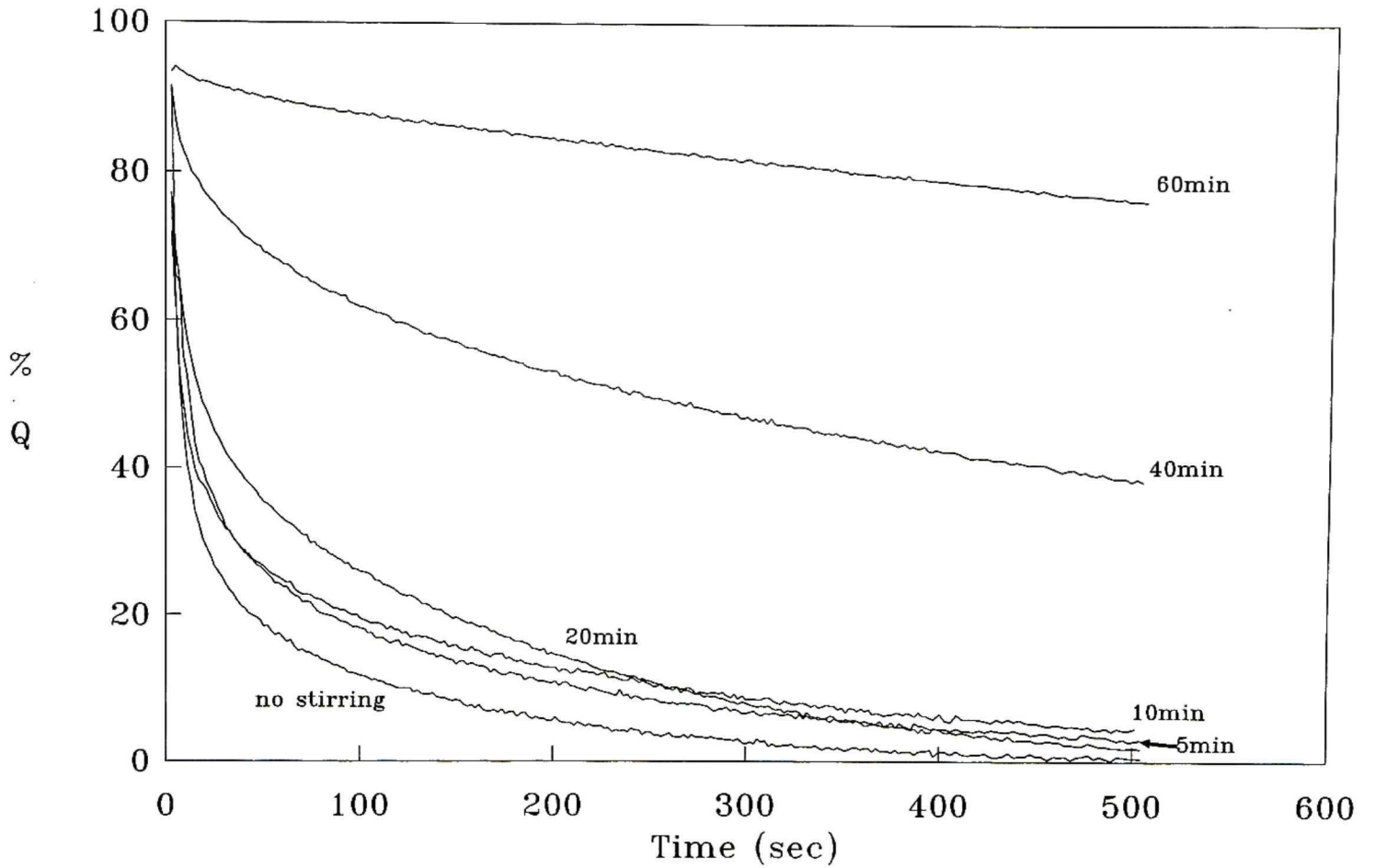

% Q = (1 - (F/Fmax)) x 100

rinsing the cuvette. Second, fresh buffer and MGN2a were placed in the cuvette and stirred for 1 hour. Finally, dye release was initiated by addition of loaded vesicles to the cuvette containing MGN2a in buffer A (Figure 21).

The results of these studies showed that the biphasic release of 6CF induced by MGN2a does not result from aggregates of MGN2a interacting with the lipid bilayer.

c. Possibility of Irreversible MGN2a Inactivation

Another possible explanation for the biphasic release kinetics is that MGN2a rapidly and irreversibly loses most of its lytic activity after it has interacted with lipid vesicles. (Since MGN2a is in a dynamic equilibrium between vesicle-bound and unbound states, one would have to assume that dissociation of inactivated MGN2a from a vesicle does not lead to reactivation of the peptide. If reactivation occurred, only fast-phase release kinetics would be observed.)

To test this hypothesis, MGN2a was preincubated for 100 sec with 5uM unloaded SUVs followed by addition of 25uM 6CF-loaded SUVs, and the kinetics of dye release was compared to a control in which the peptide was added to a mixture containing 5uM unloaded and 25uM loaded vesicles. The results, shown in Figures 22 and 23, indicate that preincubation may reduce the magnitude of the fast phase by

Figure 21

Determination of the interaction of MGN2a with the walls of the cuvette. MGN2a (3.7uM) was placed in 2 ml of buffer A in a cuvette and stirred for 1 hour. This solution of MGN2a and buffer was discarded without rinsing the cuvette, and the same cuvette was refilled with 2 ml of buffer A and MGN2a (3.7uM) and the solution was stirred for 1 hour. PS concentration was 26uM.

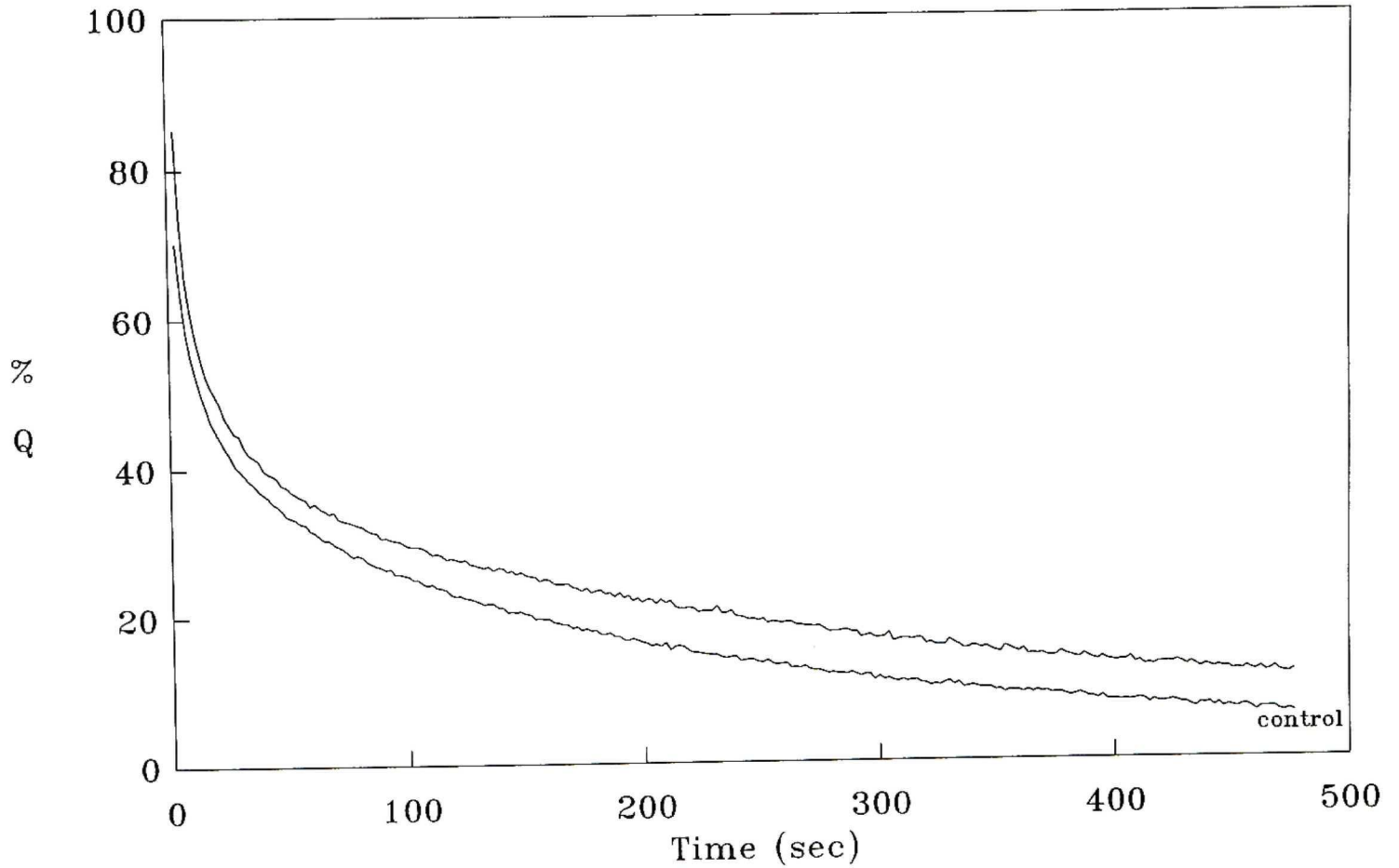

% Q = (1 − (F/Fmax)) x 100

Figure 22

Effect on functional activity of MGN2a interaction with unloaded vesicles prior to addition of loaded vesicles. MGN2a, in the amounts indicated in the figure, was added to unloaded vesicles at a concentration of 5uM PS and allowed to interact for 100 seconds prior to addition of loaded vesicles at a concentration of 25uM PS.

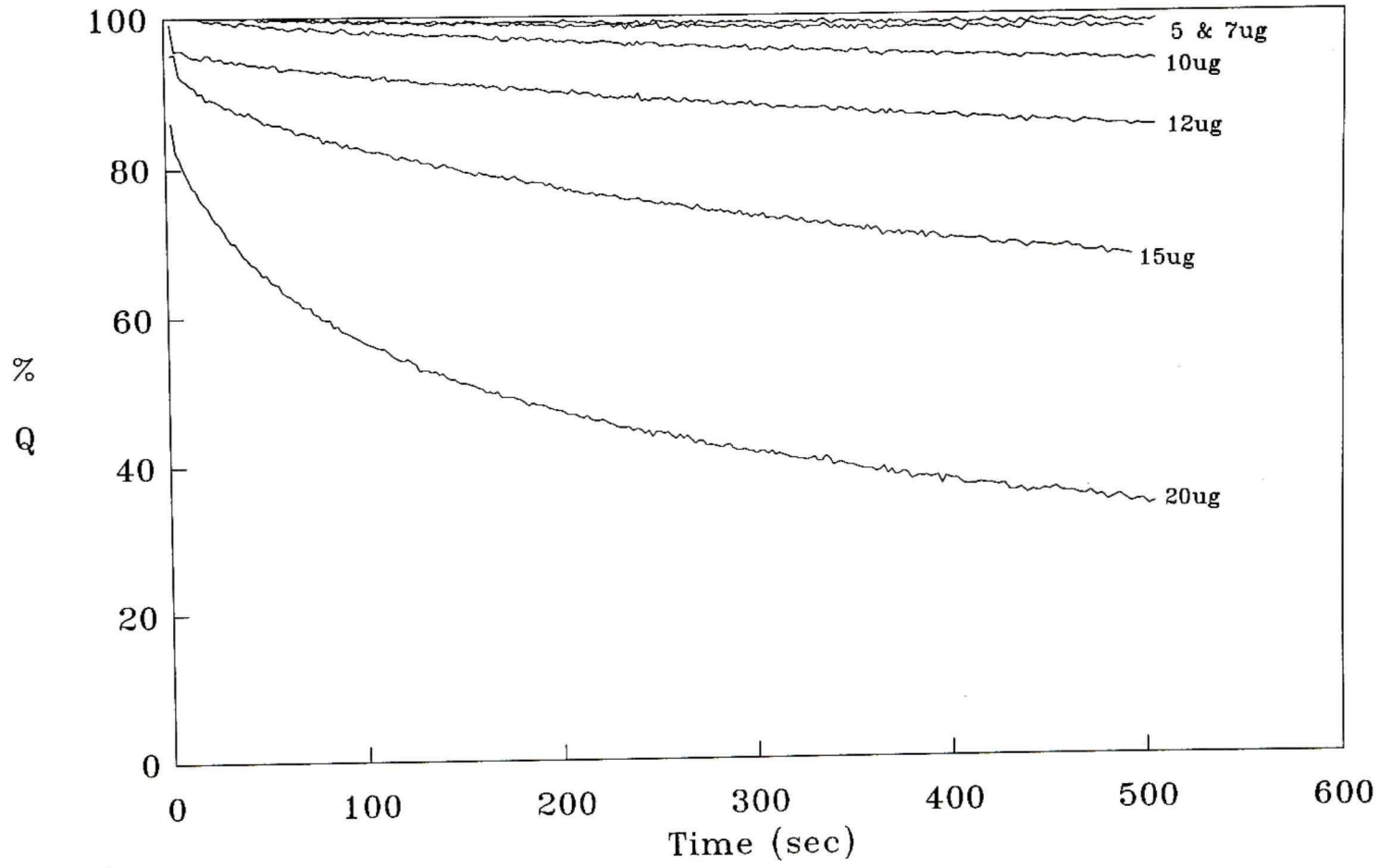

% Q = (1 - (F/Fmax)) x 100

Figure 23

Addition of MGN2a to a mixture of loaded and unloaded vesicles. MGN2a, in the amounts indicated in the figure, was added to a mixture that contained unloaded vesicles at a concentration of 5uM PS, and loaded vesicles at a concentration of 25uM PS.

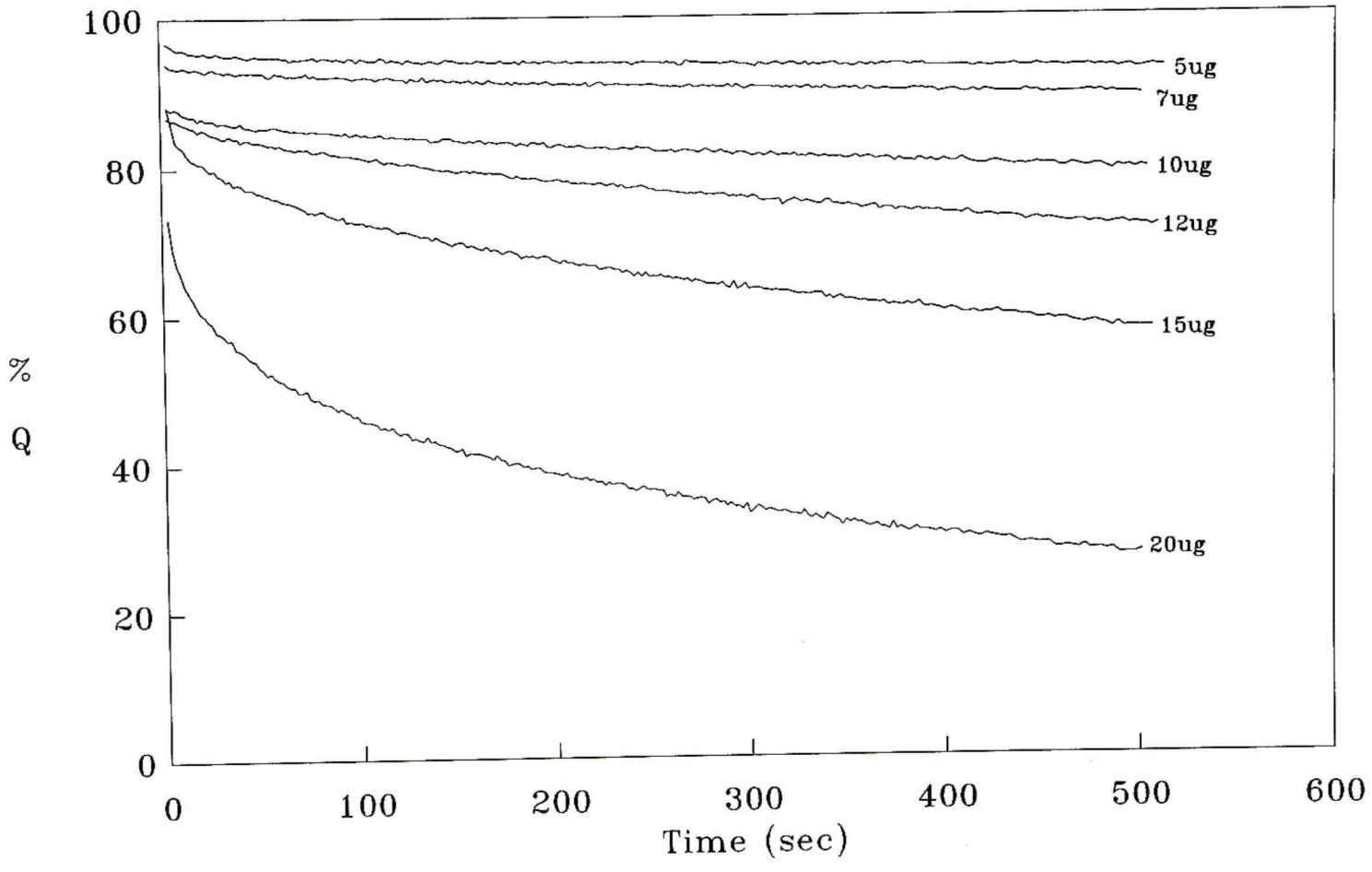

% Q = (1 – (F/Fmax)) x 100

Figure 24

Addition of a mixture of loaded and unloaded vesicles to MGN2a in buffer A. A mixture that contained unloaded vesicles at a concentration of 5uM PS, and loaded vesicles at a concentration of 25uM PS was added to the indicated amounts of MGN2a in 2 ml of buffer A.

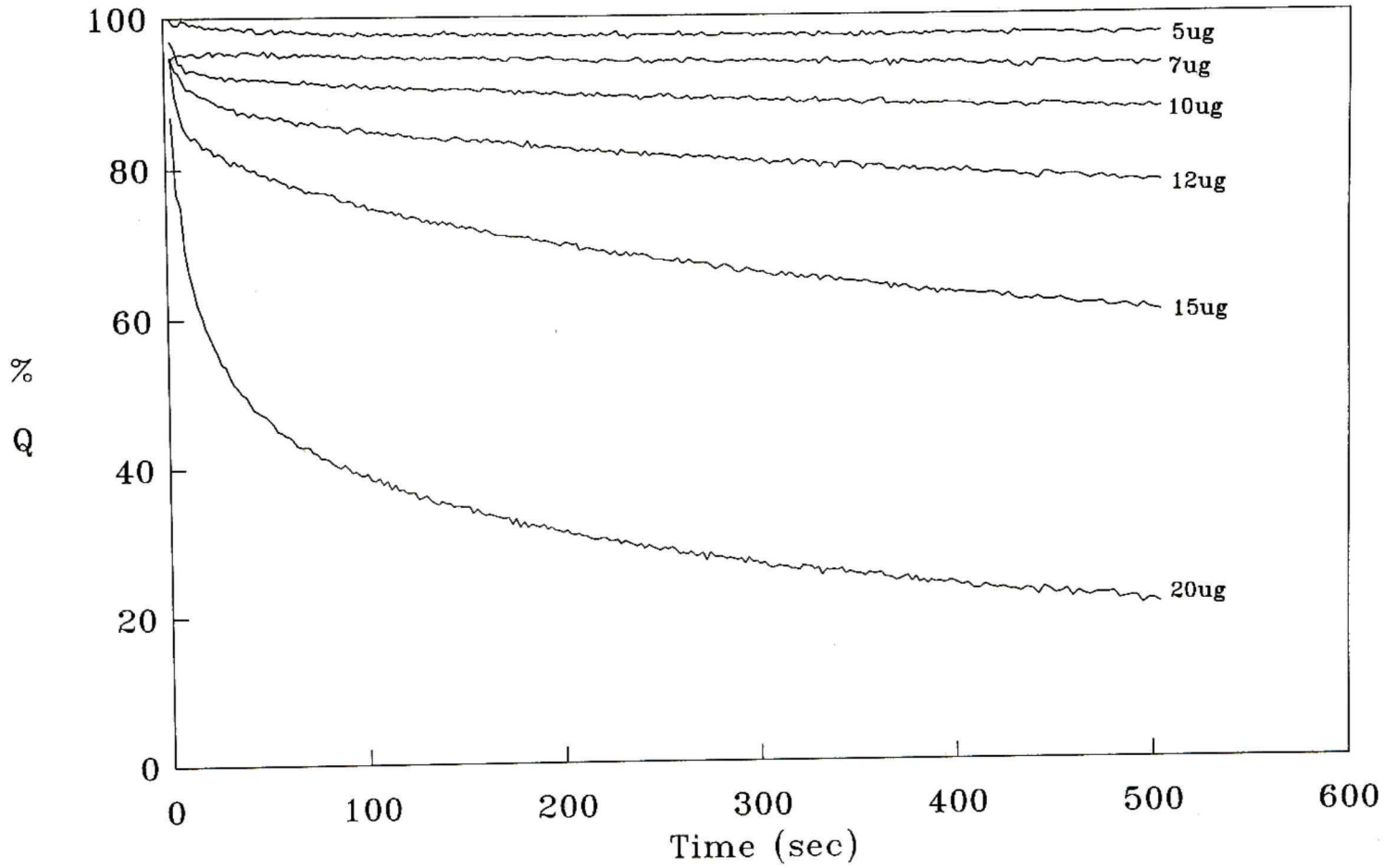

% Q = (1 – (F/Fmax)) x 100

10-25% but biphasic release kinetics are still observed (Figure 25). If the inactivation hypothesis is correct, preincubation should have eliminated the fast phase completely. Therefore, it seems unlikely that the biphasic kinetics results from vesicle-induced, irreversible inactivation of the MGN2a.

Determination of the Mode of Dye Release from SUVs

To characterize MGN2a-induced dye release it is necessary to determine whether MGN2a-treated vesicles release dye in a graded or all-or-none manner. PS SUVs were prepared as described in Materials and Methods and 0.9 - 3.7uM MGN2a (5 - 20ug) was added to 25-30uM PS containing vesicles loaded with either 30mM or 100mM 6CF. After monitoring dye release on a fluorometer for either 100 sec (fast phase) or 500 sec, unloaded vesicles were added to arrest dye release as described in Materials and Methods and demonstrated in Figures 26 and 27. Vesicles were then separated from released 6CF by rapid passage over a 5ml Sephadex G-25 column, and the vesicle fractions were analyzed for residual 6CF, in the absence and presence of Triton X-100 (i.e., the %Q was determined). As shown in Tables III-V, the %Q values are consistent only with an all-or-none release mechanism.

In similar studies, the mode of dye release was also assessed for SUVs treated with melittin, Triton X-100, and

Figure 25

A semilog plot of the effect of MGN2a interaction with unloaded vesicles. These curves are replots of the results shown in Figure 22.

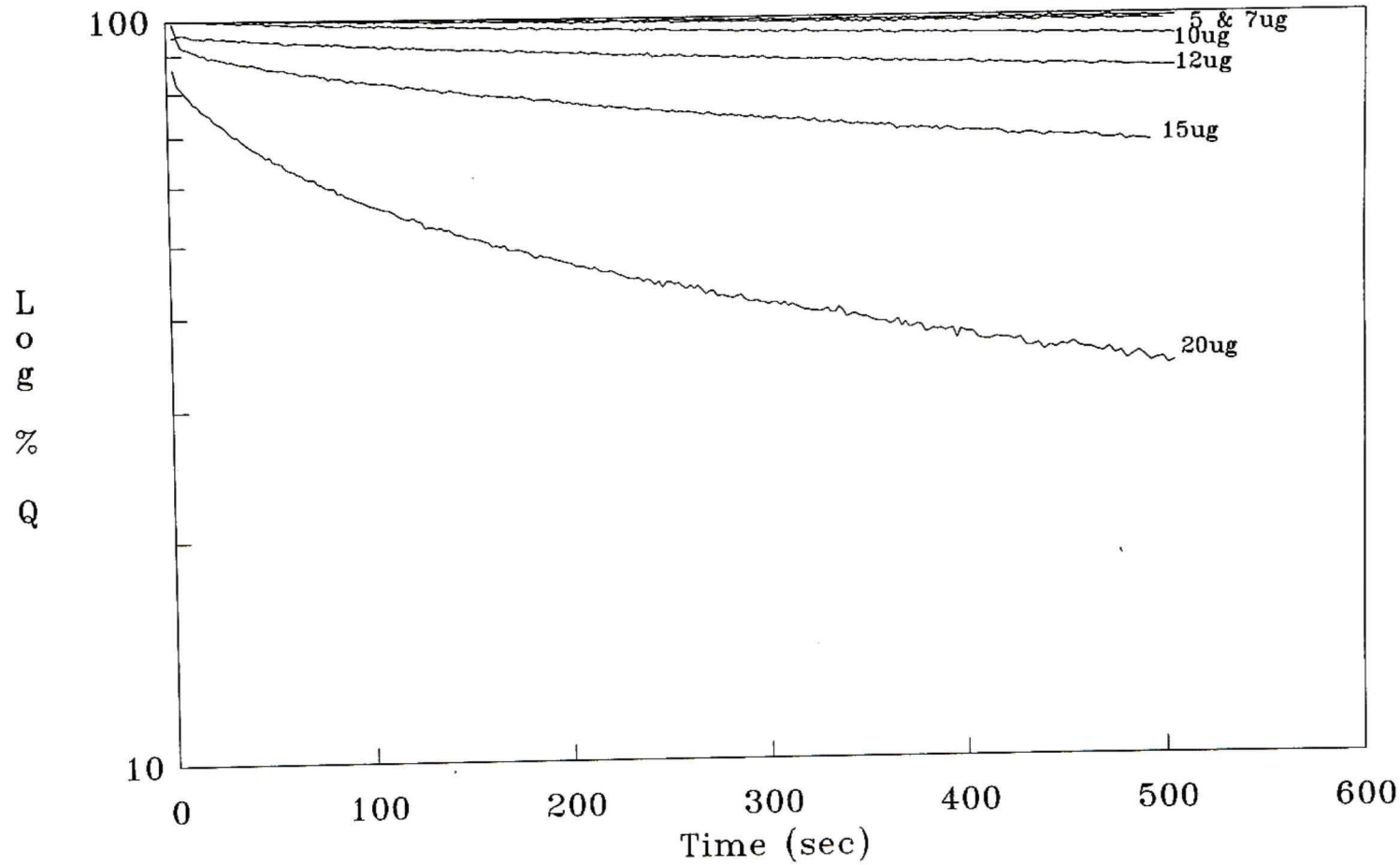

% Q = (1 - (F/Fmax)) x 100

Figure 26

Interaction of MGN2a with a mixture of loaded and unloaded vesicles of approximately equal PS concentration. MGN2a (10ug/ml, 3.7uM) was added to loaded SUVs (PS concentration = 30 uM) and unloaded SUVs (PS concentration = 29uM).

Control = MGN2a (3.7uM) added to unloaded vesicles only.

UL + MGN + L = MGN2a (3.7uM) added to unloaded vesicles prior to addition of loaded vesicles.

MGN + UL + L = MGN2a pre-equilibrated in buffer prior to addition of a mixture of loaded and unloaded vesicles.

UL + L + MGN = Mixture of loaded and unloaded vesicles pre-equilibrated in buffer prior to addition of MGN2a.

Where, MGN = MGN2a, UL = unloaded vesicles and L = loaded vesicles.

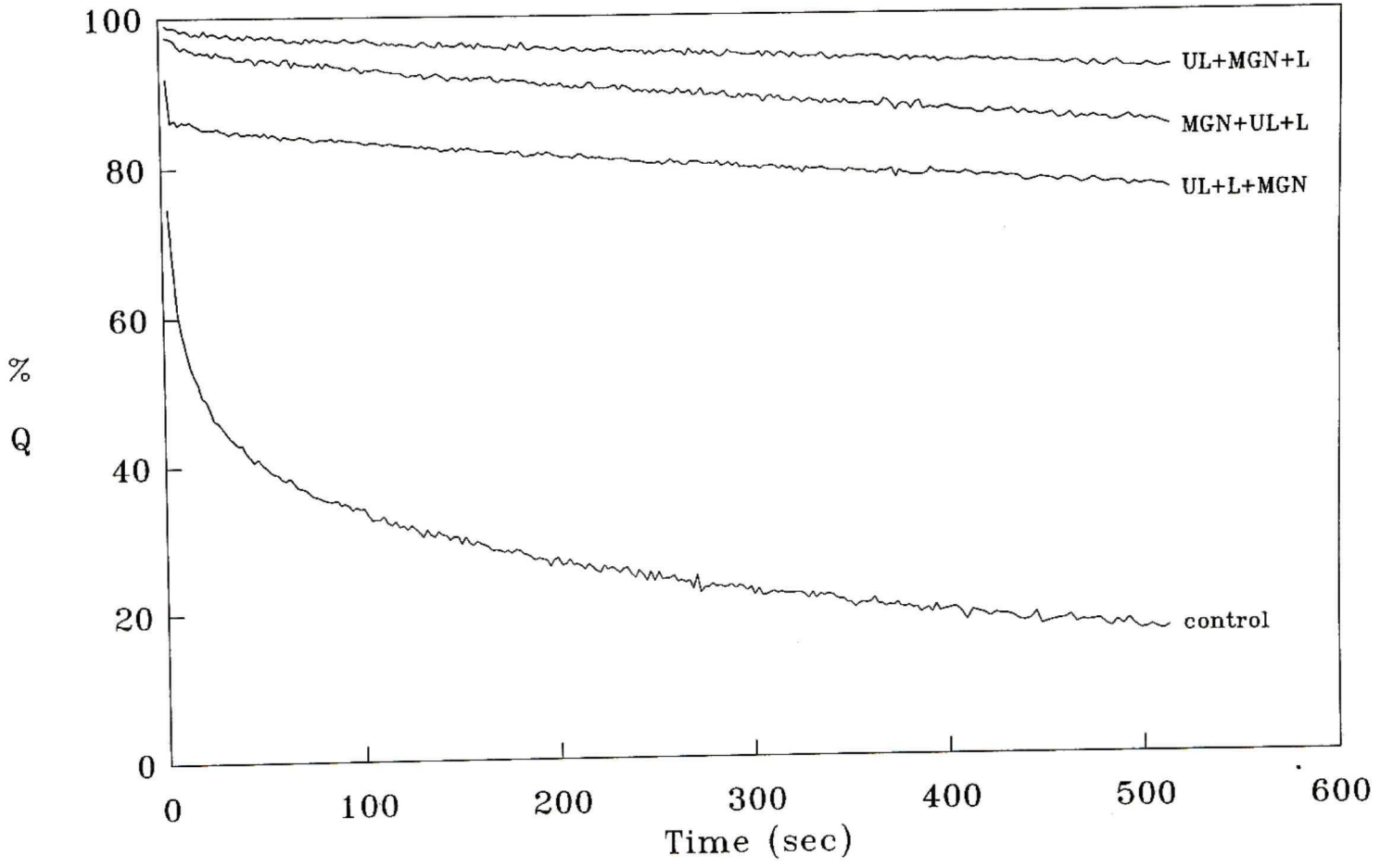

% Q = (1 - (F/Fmax)) x 100

Figure 27

Addition of unloaded vesicles to a mixture of MGN2a and loaded vesicles. MGN2a (3.7uM,10ug/ml) was added to loaded vesicles at a PS concentration of 30uM followed by addition of unloaded PS vesicles (PS concentration = 29uM) at the times indicated in the figure.

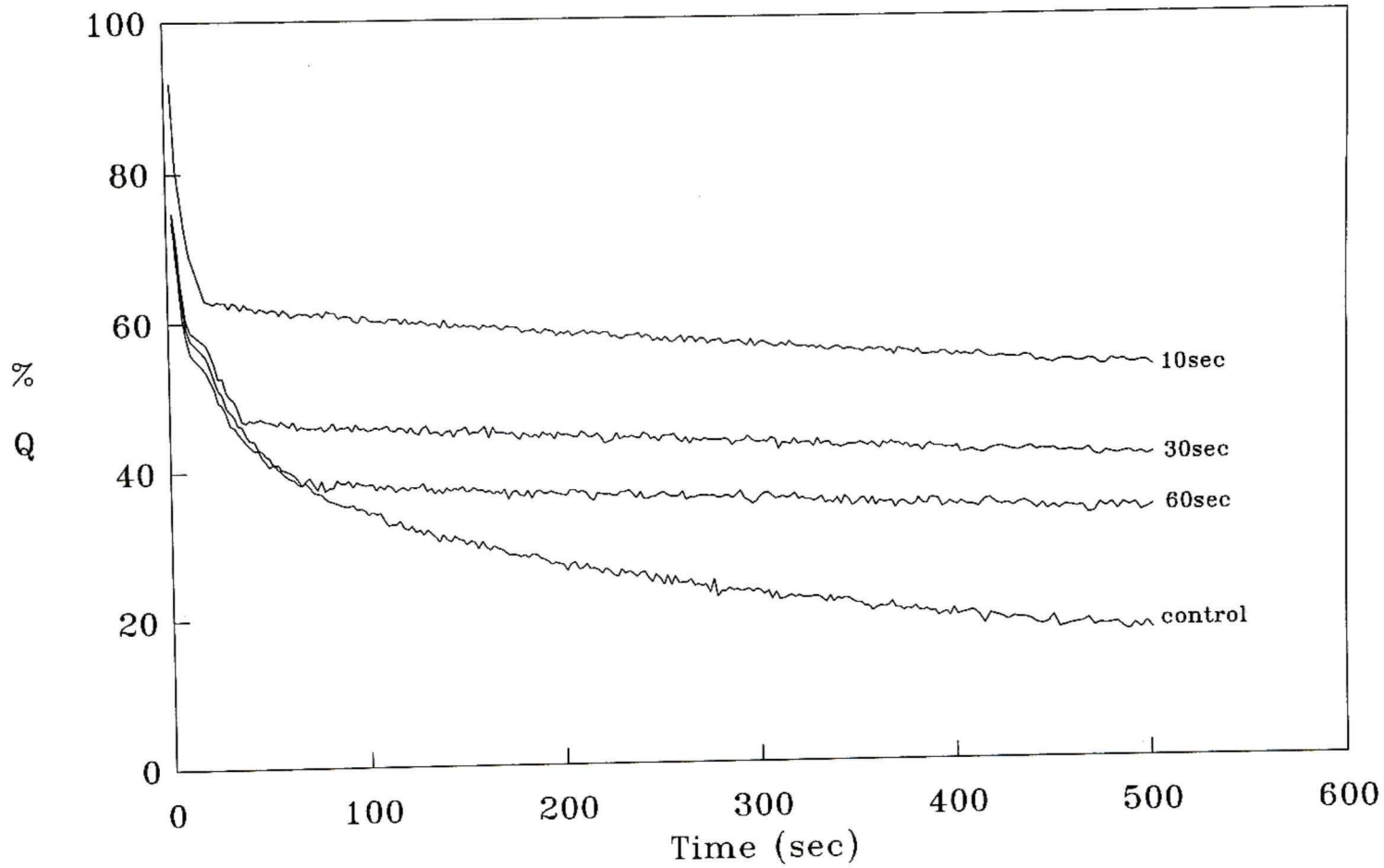

% Q = (1 - (F/Fmax)) x 100

Table III. Internal Fluorescence After MGN2a-induced 6CF Release From SUVs

Sample[a]	% 6CF Release[b]	Predicted %Q for all-or-none[c]	Predicted %Q for Graded Release[d]	Measured %Q[e,f]
control	0	---	---	98
10ug MGN	22	98	94	97
12ug MGN	38	98	92	96
15ug MGN	58	98	85	98
20ug MGN	89	98	56	95

a. 10 to 20ul of 0.37mM MGN2a was added to SUVs (PS concentration = 25-30uM) loaded with 100mM 6CF as described in Materials and Methods.

b. Determined by following 6CF release for 500 sec with a spectrofluorometer. 100% release of 6CF was determined by addition of 10% Triton X-100.

c. Assumes some vesicles released all their dye; others released none.

d. Predicted on the basis of a quenching curve determined by the method of Weinstein et.al. ((1984) In Liposome Technology Vol. III, ed. Gregoriades, G. 183-204. Boca Raton, FL: CRC Press). See Figure 4.

e. Determined following the removal of released 6CF with a Sephadex G-25 column.

f. The estimated uncertainty in the measured %Q is ± 1.5%.

Table IV. Internal Fluorescence After MGN2a-induced 6CF Release From SUVs

Sample[a]	% 6CF Release[b]	Predicted %Q for all-or-none[c]	Predicted %Q for Graded Release[d]	Measured %Q[e,f]
control	0	---	---	80
10ug MGN	13	80	78	82
12ug MGN	17	80	77	80
15ug MGN	28	80	74	80
20ug MGN	64	80	56	79

a. 10 to 20ul of 0.37mM MGN2a was added to SUVs (PS concentration = 25-30uM) loaded with 30mM 6CF as described in Materials and Methods.

b. Determined by following 6CF release for 100 sec with a spectrofluorometer. 100% release of 6CF was determined by addition of 10% Triton X-100.

c. Assumes some vesicles released all their dye; others released none.

d. Predicted on the basis of a quenching curve determined by the method of Weinstein et.al. ((1984) In Liposome Technology Vol. III, ed. Gregoriades, G. 183-204. Boca Raton, FL: CRC Press). See Figure 4.

e. Determined following the removal of released 6CF with a Sephadex G-25 column.

f. The estimated uncertainty in the measured %Q is ± 1.5%.

Table V. Internal Fluorescence After MGN2a-induced 6CF Release From SUVs

Sample[a]	% 6CF Release[b]	Predicted %Q for all-or-none[c]	Predicted %Q for Graded Release[d]	Measured %Q[e,f]
control	0	---	---	80
10ug MGN	18	80	77	80
12ug MGN	30	80	73	80
15ug MGN	50	80	67	79
20ug MGN	82	80	36	76

a. 10 to 20ul of 0.37mM MGN2a was added to SUVs (PS concentration = 25-30uM) loaded with 30mM 6CF as described in Materials and Methods.

b. Determined by following 6CF release for 500 sec with a spectrofluorometer. 100% release of 6CF was determined by addition of 10% Triton X-100.

c. Assumes some vesicles released all their dye; others released none.

d. Predicted on the basis of a quenching curve determined by the method of Weinstein et.al. ((1984) In Liposome Technology Vol. III, ed. Gregoriades, G. 183-204. Boca Raton, FL: CRC Press). See Figure 4.

e. Determined following the removal of released 6CF with a Sephadex G-25 column.

f. The estimated uncertainty in the measured %Q is ± 1.5%.

octylglucoside. Melittin interacted with PS SUVs to cause release of 6CF (Figures 28 and 29) and this release of 6CF appears to be biphasic, similar to that seen with MGN2a (Figures 30 and 31). Table VI shows that the %Q values do not correspond clearly with either the all-or-none or graded release modes although the %Q values are closer to all-or-none. This might suggest that in adding melittin directly to the vesicles from the stock solution, a combination of aggregates and monomers of melittin are interacting with the lipid bilayer to cause predominantly all-or-none release with some graded release of dye. Indeed, Table VII does show that when melittin is allowed to pre-equilibrate in buffer A for 5 min prior to vesicle addition the %Q values are closer to a graded mode of release although a mixed release process is still evident.

Triton X-100 was added to vesicles (or vice versa) which resulted in the release of dye from the vesicles over time (Figures 32-34). Semilog plots of the data suggest that as Triton X-100 is allowed to pre-equilibrate in buffer for various times before adding vesicles the kinetics of dye release appear to be at least bi-exponential (Figures 35-37). Triton X-100 was allowed to pre-equilibrate in buffer A for 24 hours at room temperature in order to disassociate any detergent micelles in equilibrium with monomers. Tables VIII-X show that the measured %Q values are not clearly all-or-none nor graded release, although after 24 hours of pre-

Figure 28

Melittin-induced release of 6CF from PS SUVs. 1 to 12ul of 0.35mM Melittin (1mg/ml, in buffer B) was added to 2ml of buffer A containing PS SUVs (PS concentration = 30uM).

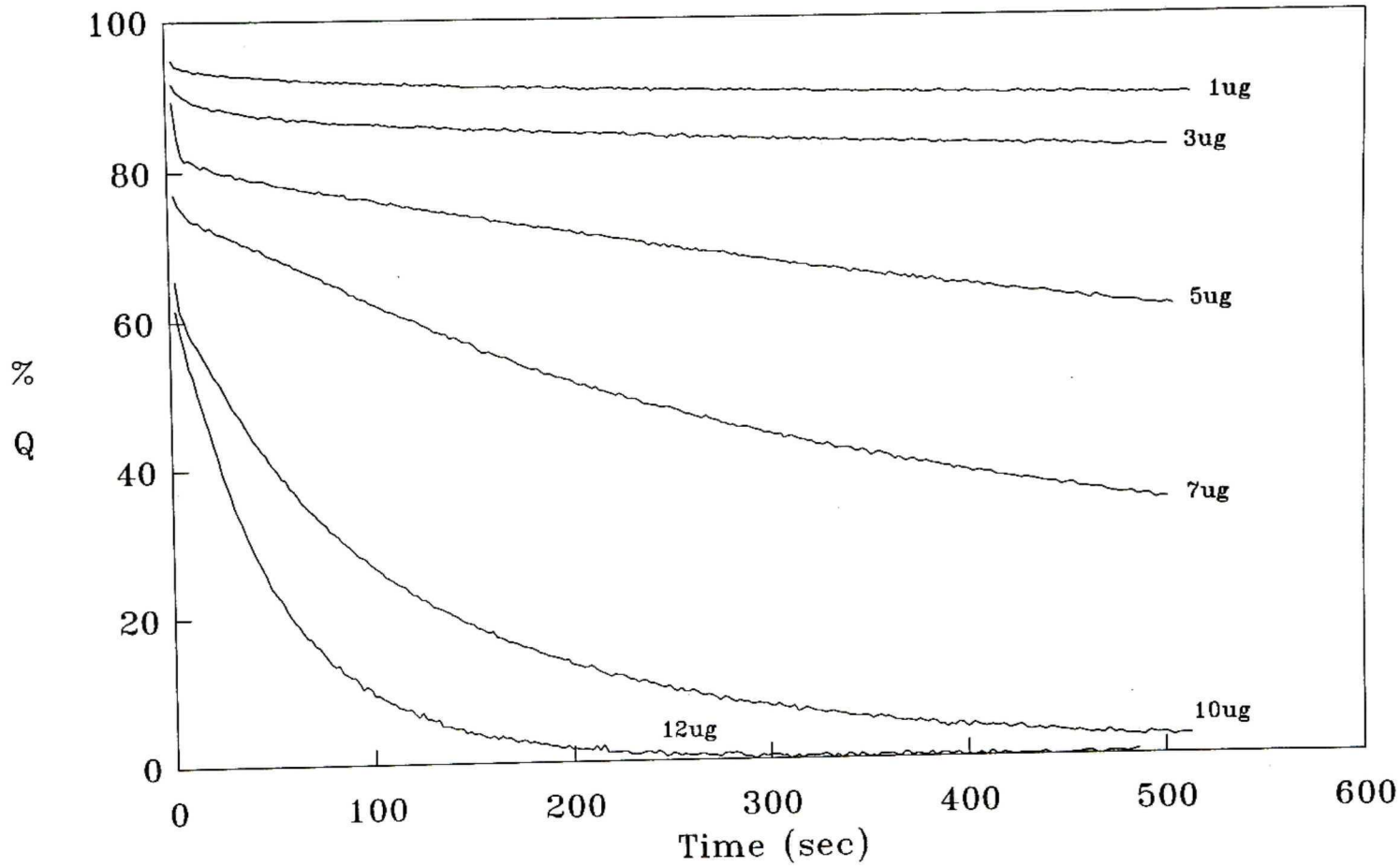

% Q = (1 - F/Fmax) x 100

Figure 29

Effect on functional activity of pre-equilibrating melittin in buffer A. 3 to 10ul of 0.35mM melittin (1 mg/ml, in buffer B) was allowed to pre-equilibrate in 2ml of buffer A for 5 minutes prior to addition of loaded PS SUVs (PS concentration = 27uM).

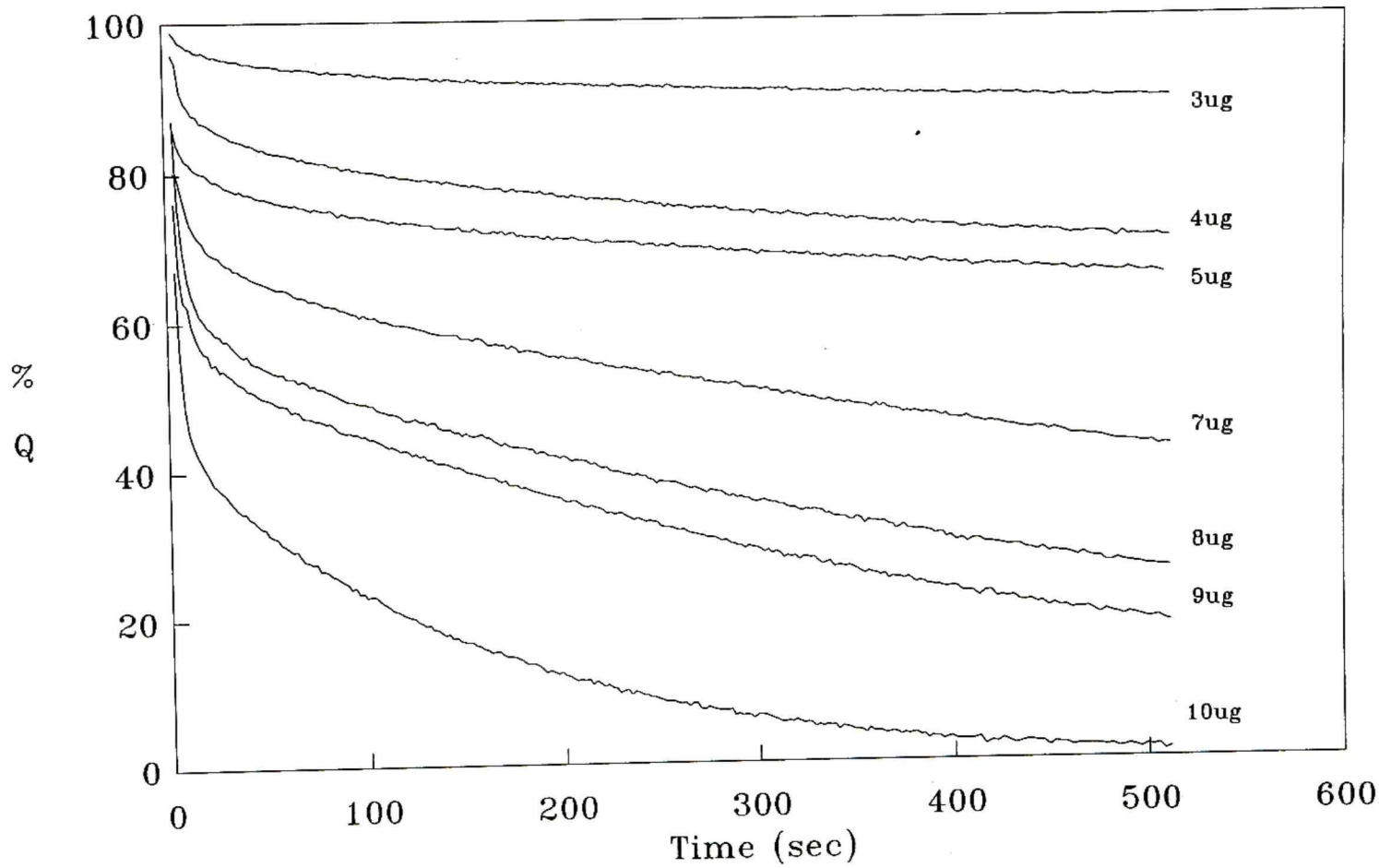

% Q = (1 - (F/Fmax)) x 100

Figure 30

Semilog Plot of melittin-induced release of 6CF from PS SUVs. These curves are replots of the results shown in Figure 28.

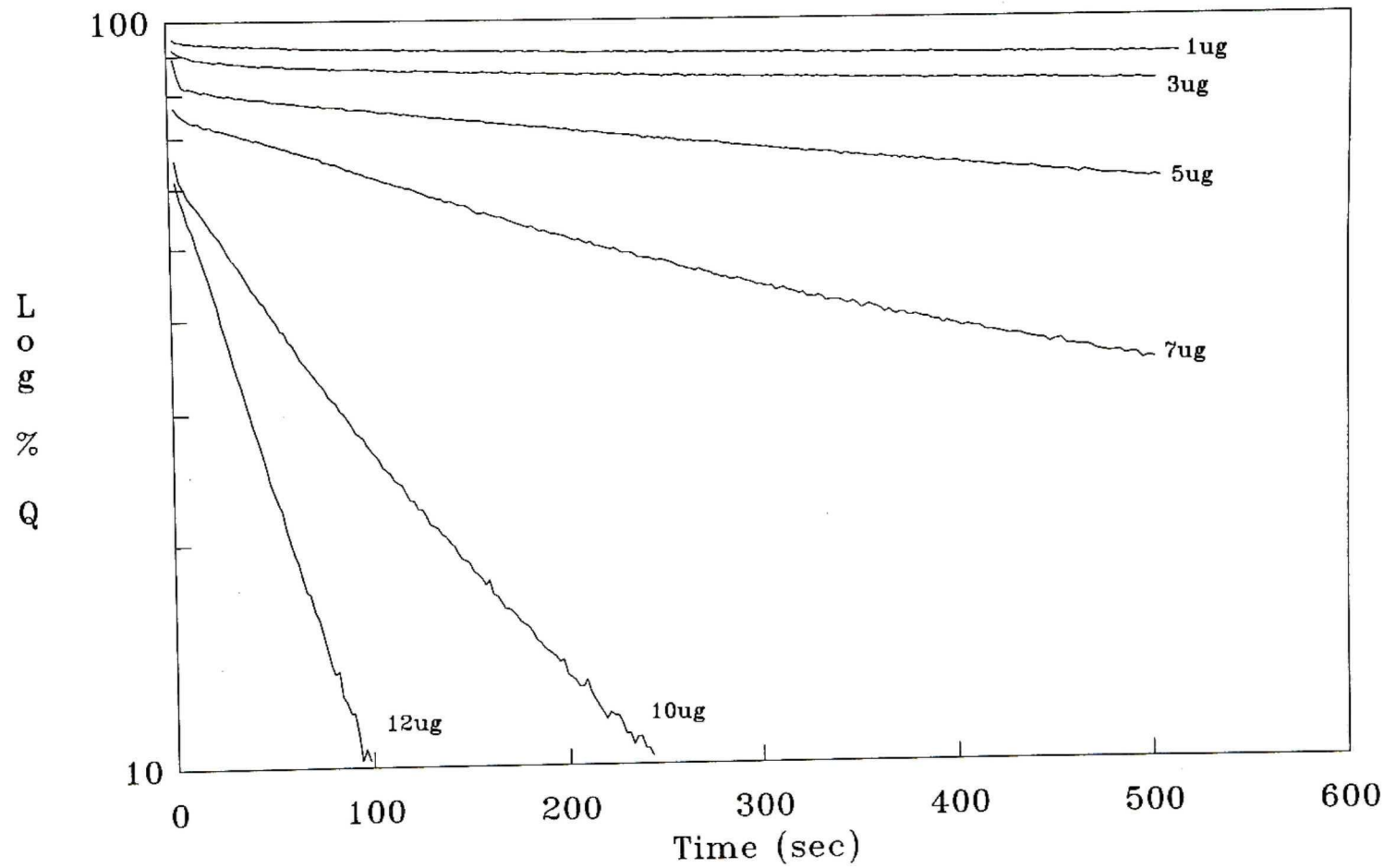

% Q = (1 − F/Fmax) x 100

Figure 31

Semilog Plot of 6CF release from SUVs added to melittin pre-equilibrated in buffer A for 5 minutes. These curves are replots of the results shown in Figure 29.

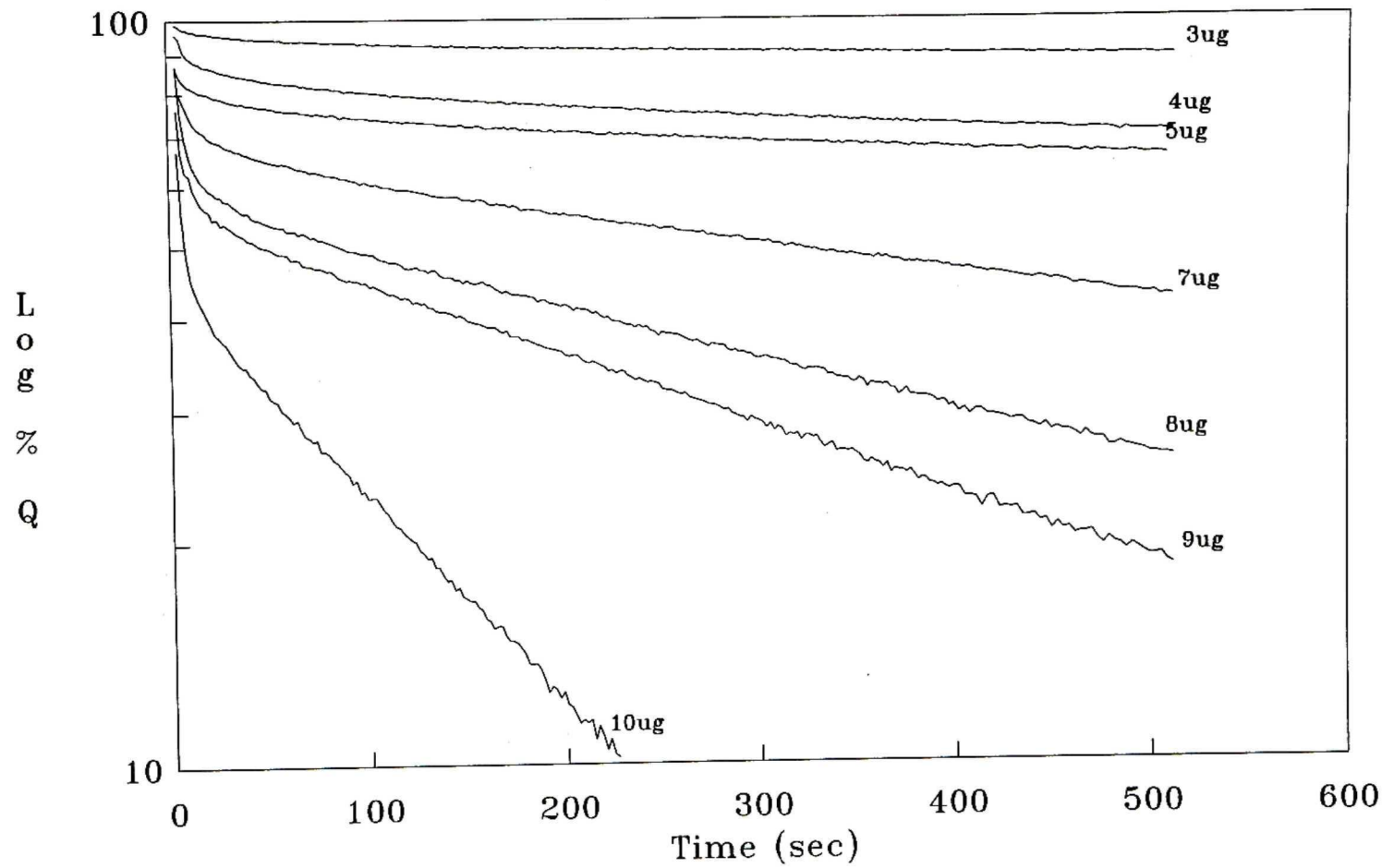

% Q = (1 - (F/Fmax)) x 100

Table VI. Internal Fluorescence After Melittin-induced 6CF Release From SUVs (no pre-equilibration)

Sample[a]	% 6CF Release[b]	Predicted %Q for all-or-none[c]	Predicted %Q for Graded Release[d]	Measured %Q[e,f]
control	0	---	---	97
3ug Melittin	25	97	93	95
5ug Melittin	53	97	88	90
7ug Melittin	83	97	70	84
8ug Melittin	91	97	52	82

a. 3 to 8ul of 0.35mM Melittin in buffer B was added to 2ml of buffer A and SUVs (PS concentration = 25-30uM) loaded with 100mM 6CF as described in Materials and Methods.

b. Determined by following 6CF release for 500 sec with a spectrofluorometer. 100% release of 6CF was determined by addition of 10% Triton X-100.

c. Assumes some vesicles released all their dye; others released none.

d. Predicted on the basis of a quenching curve determined by the method of Weinstein et.al. ((1984) In Liposome Technology Vol. III, ed. Gregoriades, G. 183-204. Boca Raton, FL: CRC Press). See Figure 4.

e. Determined following the removal of released 6CF with a Sephadex G-25 column.

f. The estimated uncertainty in the measured %Q is ± 1.5%.

Table VII. Internal Fluorescence After Melittin-induced 6CF Release From SUVs (5 min pre-equilibration)

Sample[a]	% 6CF Release[b]	Predicted %Q for all-or-none[c]	Predicted %Q for Graded Release[d]	Measured %Q[e,f]
control	0	---	---	95
3ug Melittin	9	95	94	96
4ug Melittin	28	95	92	91
5ug Melittin	32	95	91	90
7ug Melittin	57	95	87	90
8ug Melittin	74	95	79	86
9ug Melittin	80	95	72	75

a. 3 to 9ul of 0.35mM Melittin was allowed to pre-equilibrate in buffer A (2ml) for 5 min prior to addition of SUVs (PS concentration = 25-30uM) loaded with 100mM 6CF as described in Materials and Methods.

b. Determined by following 6CF release for 500 sec with a spectrofluorometer. 100% release of 6CF was determined by addition of 10% Triton X-100.

c. Assumes some vesicles released all their dye; others released none.

d. Predicted on the basis of a quenching curve determined by the method of Weinstein et.al. ((1984) In Liposome Technology Vol. III, ed. Gregoriades, G. 183-204. Boca Raton, FL: CRC Press). See Figure 4.

e. Determined following the removal of released 6CF with a Sephadex G-25 column.

f. The estimated uncertainty in the measured %Q is ± 1.5%.

Figure 32

Triton X-100-induced release of 6CF from PS SUVs. 15 to 110 ul of 0.1% Triton X-100 in buffer B was added to loaded vesicles (PS concentration = 30uM) in buffer A. The ug of added Triton X-100 are indicated in the figure.

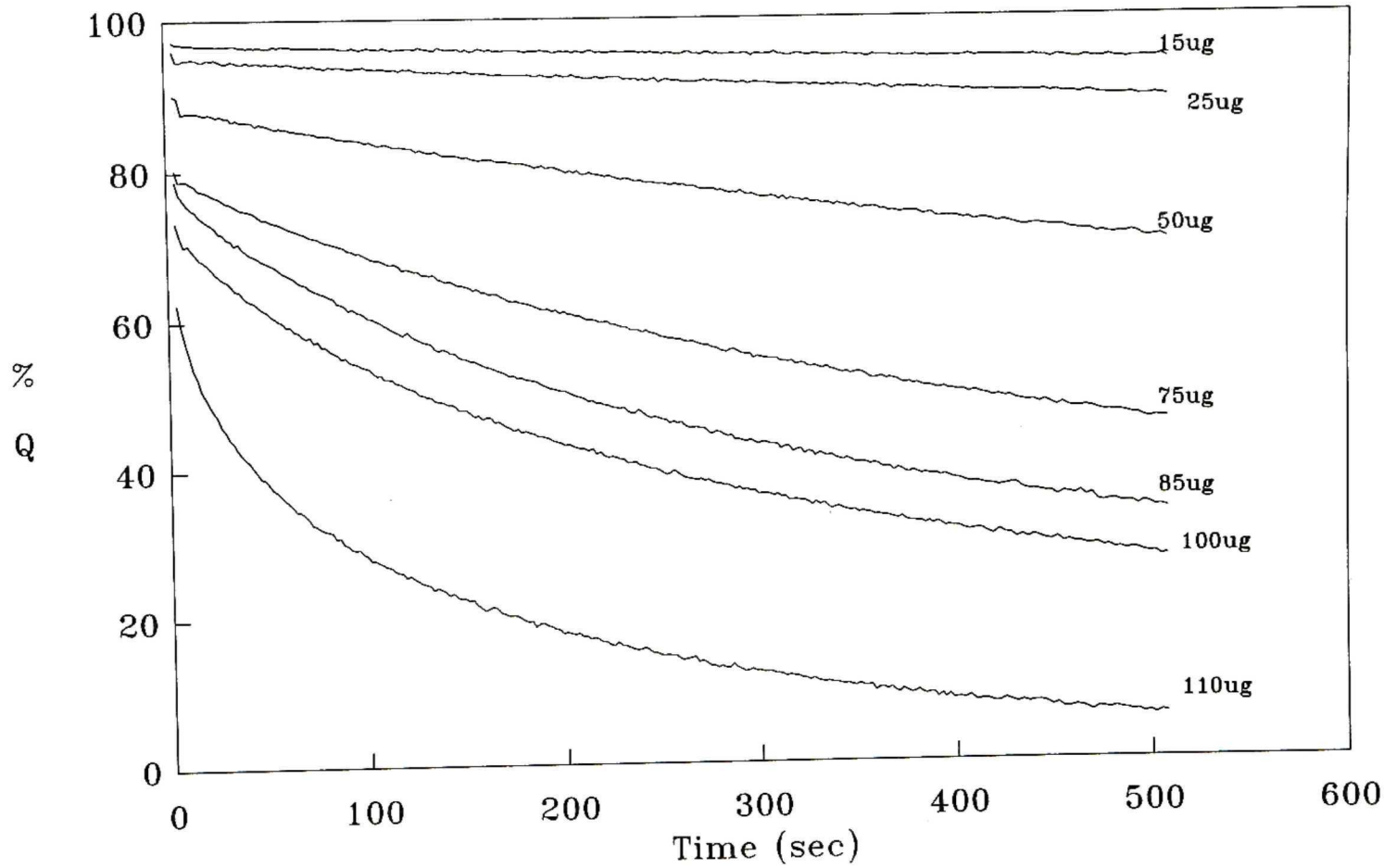

% Q = (1 - (F/Fmax)) x 100

Figure 33

Triton X-100-induced release of 6CF from SUVs. 25 to 110 ul of 0.1% Triton X-100 in buffer B was allowed to pre-equilibrate in 2ml of buffer A for 5 minutes prior to addition of loaded vesicles (PS concentration of 30uM). The ug of Triton X-100 utilized are indicated in the figure.

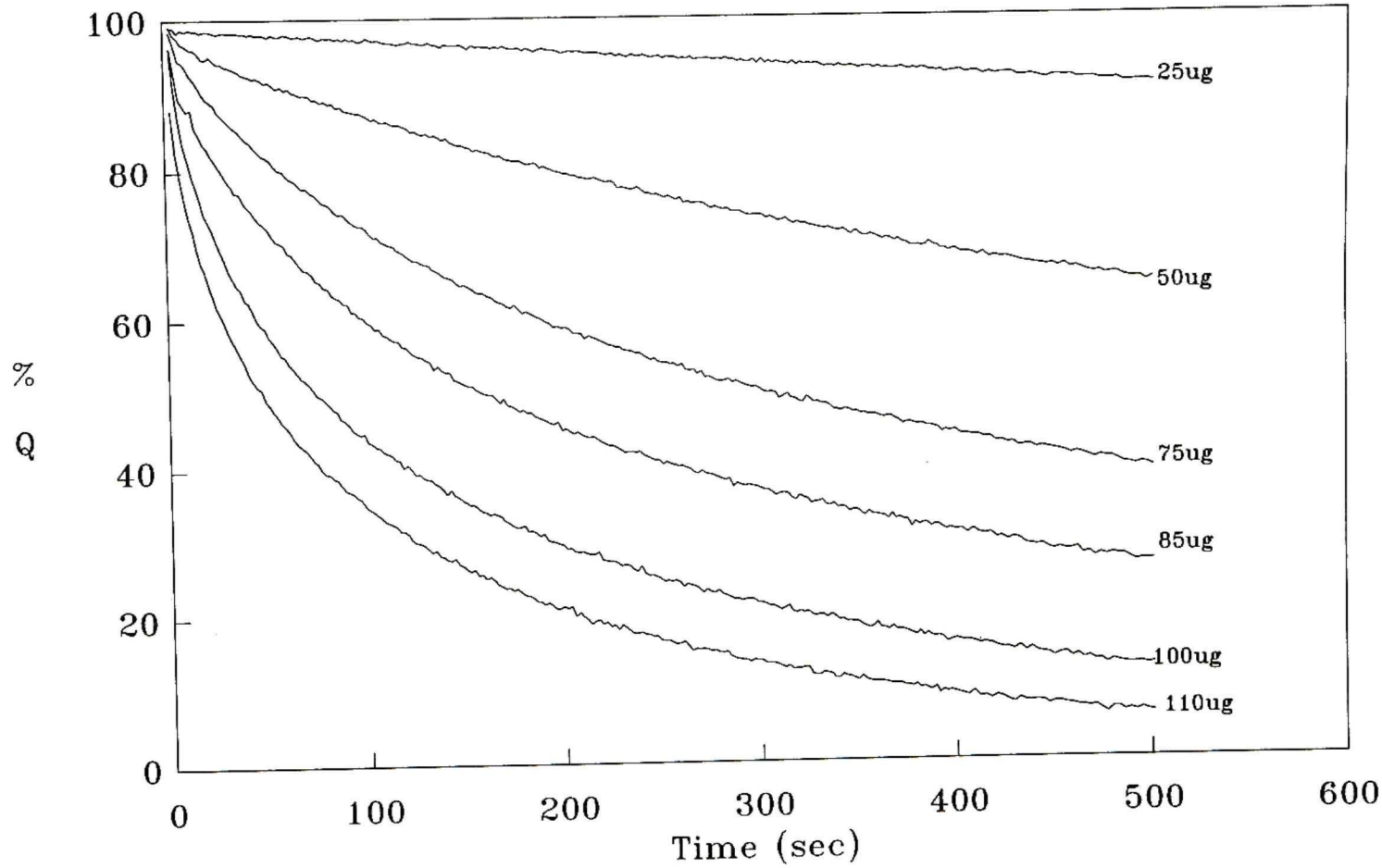

% Q = (1 - (F/Fmax)) x 100

Figure 34

Triton X-100-induced release of 6CF from SUVs. 25 to 110ul of 0.1% Triton X-100 in buffer B was allowed to pre-equilibrate in 2ml of buffer A for 24 hours at room temperature prior to addition of loaded vesicles (Final PS concentration = 30uM).

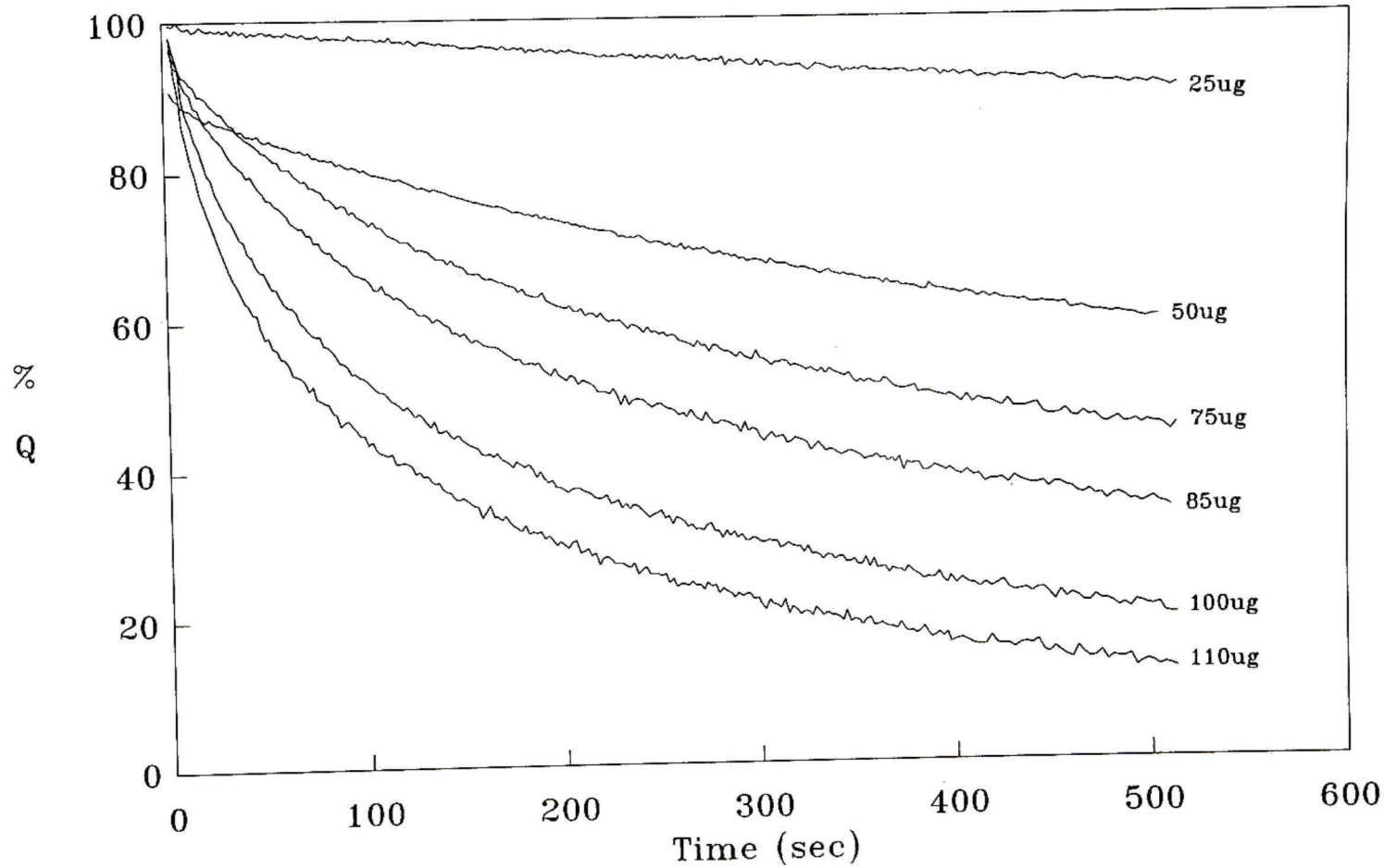

% Q = (1 - (F/Fmax)) x 100

Figure 35

Semilog plot of Triton X-100 induced release of 6CF from PS SUVs. These curves are replots of the results shown in Figure 32.

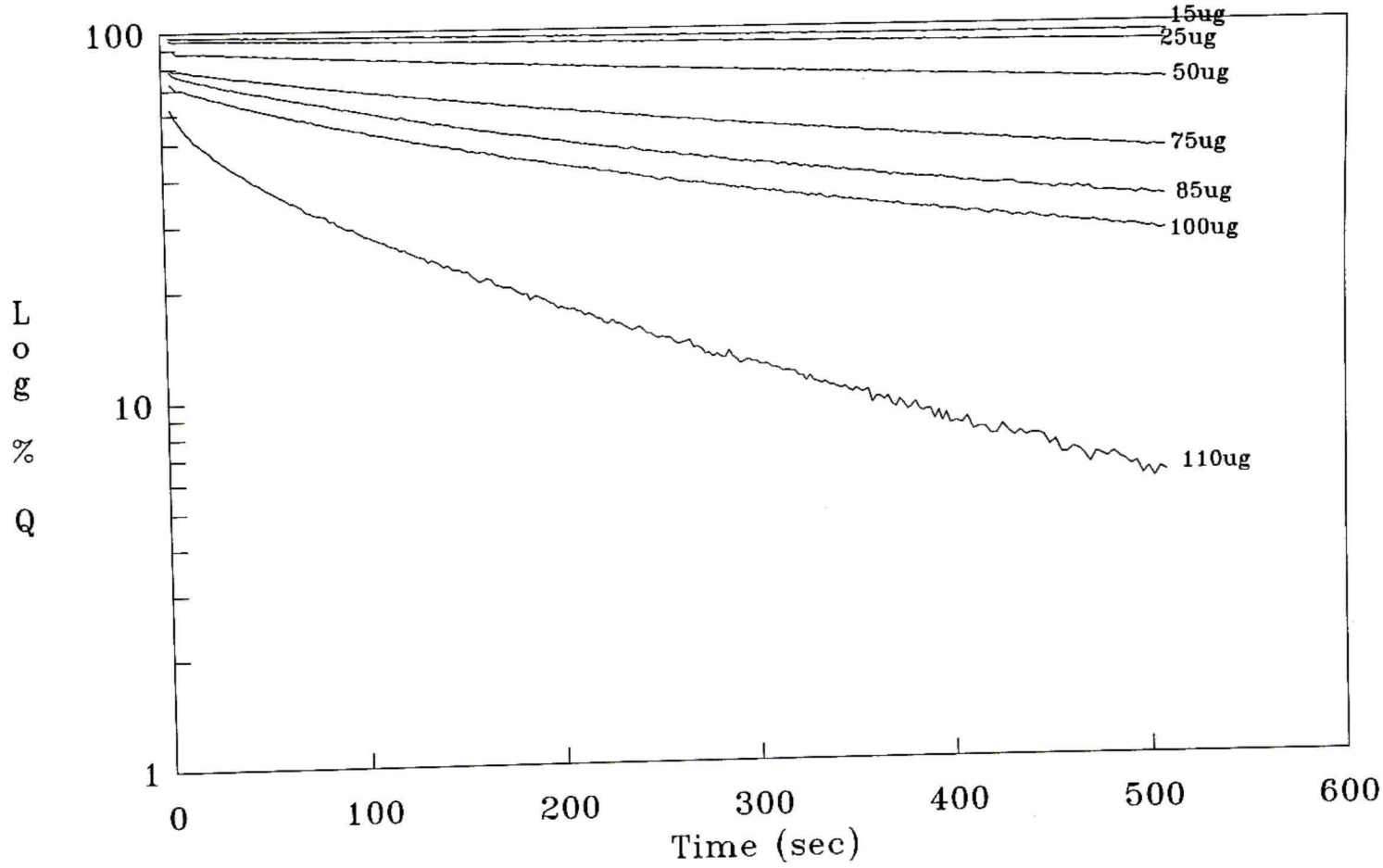

% Q = (1 - (F/Fmax)) x 100

Figure 36

Semilog plot of Triton X-100 induced release of 6CF from PS SUVs. These curves are replots of the results shown in Figure 33.

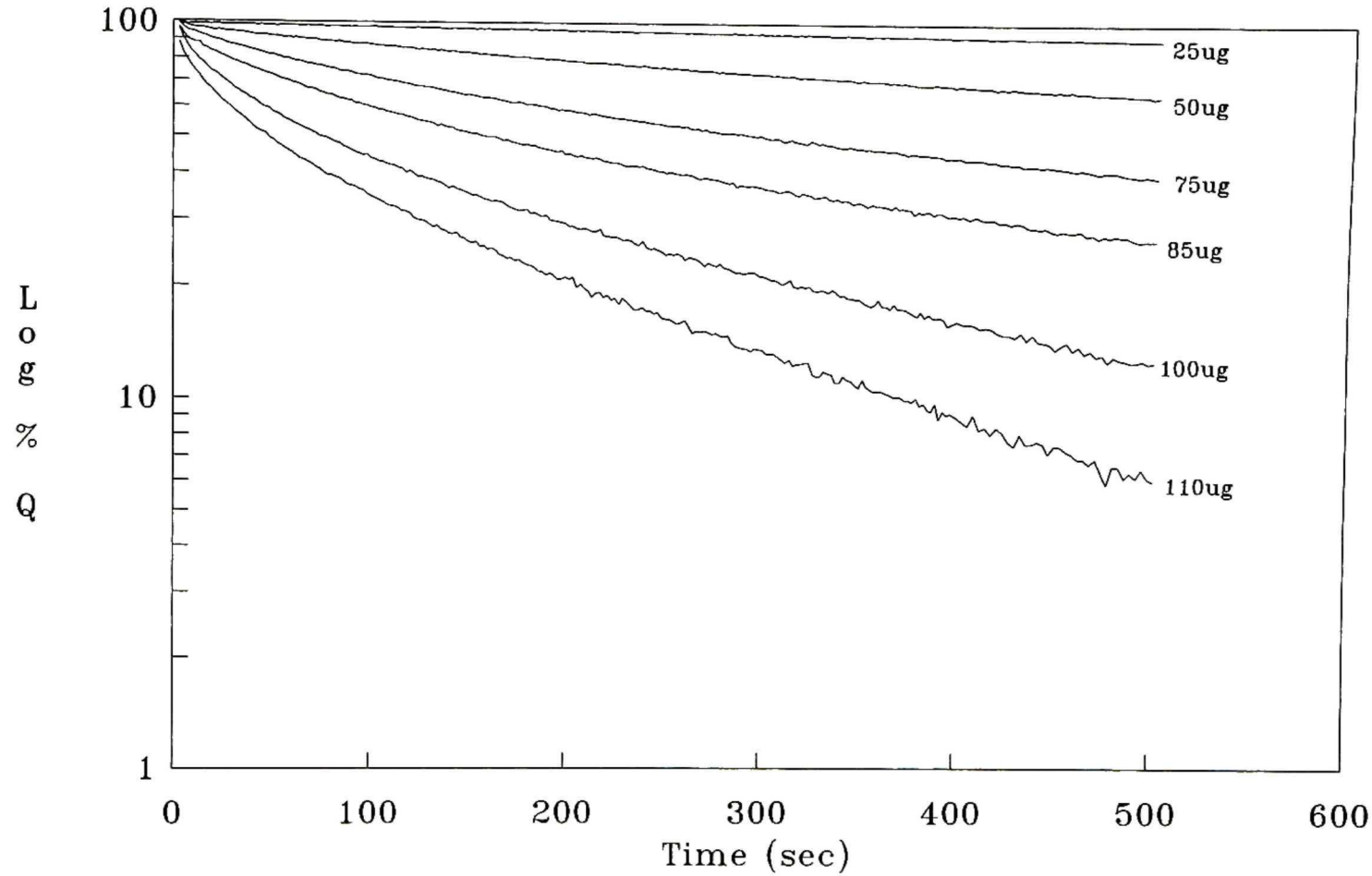

% Q = (1 − (F/Fmax)) x 100

Figure 37

Semilog plot of Triton X-100-induced release of 6CF from PS SUVs. These curves are replots of the results shown in Figure 34.

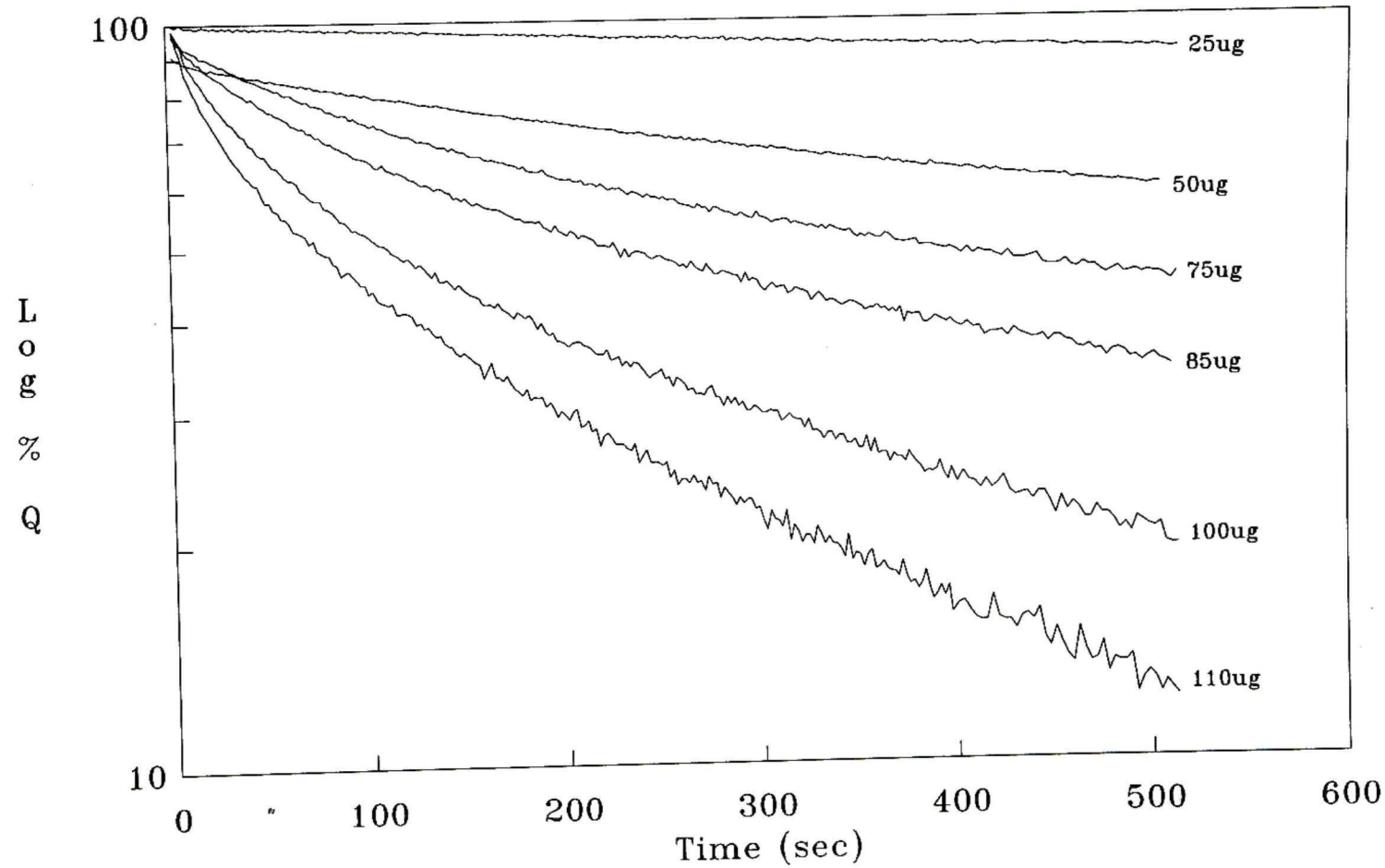

% Q = (1 - (F/Fmax)) x 100

Table VIII. Internal Fluorescence After Triton X-100-induced 6CF Release From SUVs (no pre-equilibration)

Sample[a]	% 6CF Release[b]	Predicted %Q for all-or-none[c]	Predicted %Q for Graded Release[d]	Measured %Q[e,f]
control	0	---	---	98
25ug Triton	9	98	94	96
50ug Triton	28	98	92	94
75ug Triton	52	98	89	89
85ug Triton	65	98	85	88
100ug Triton	72	98	80	86
110ug Triton	94	98	38	77

a. 25 to 110ul of 0.1% Triton X-100 was added to 2ml of buffer A and SUVs (PS concentration = 25-30uM) loaded with 100mM 6CF as described in Materials and Methods.

b. Determined by following 6CF release for 500 sec with a spectrofluorometer. 100% release of 6CF was determined by addition of 10% Triton X-100.

c. Assumes some vesicles released all their dye; others released none.

d. Predicted on the basis of a quenching curve determined by the method of Weinstein et.al. ((1984) In Liposome Technology Vol. III, ed. Gregoriades, G. 183-204. Boca Raton, FL: CRC Press). See Figure 4.

e. Determined following the removal of released 6CF with a Sephadex G-25 column.

f. The estimated uncertainty in the measured %Q is ± 1.5%.

Table IX. Internal Fluorescence After Triton X-100-induced 6CF Release From SUVs (5 min pre-equilibration)

Sample[a]	% 6CF Release[b]	Predicted %Q for all-or-none[c]	Predicted %Q for Graded Release[d]	Measured %Q[e,f]
control	0	---	---	98
50ug Triton	34	98	91	92
85ug Triton	74	98	79	85
100ug Triton	58	98	57	76
110ug Triton	89	98	38	71

a. 50 to 110ul of 0.1% Triton X-100 was allowed to pre-equilibrate for 5 min in 2ml of buffer A prior to addition of SUVs (PS concentration = 25-30uM) loaded with 100mM 6CF as described in Materials and Methods.

b. Determined by following 6CF release for 500 sec with a spectrofluorometer. 100% release of 6CF was determined by addition of 10% Triton X-100.

c. Assumes some vesicles released all their dye; others released none.

d. Predicted on the basis of a quenching curve determined by the method of Weinstein et.al. ((1984) In Liposome Technology Vol. III, ed. Gregoriades, G. 183-204. Boca Raton, FL: CRC Press). See Figure 4.

e. Determined following the removal of released 6CF with a Sephadex G-25 column.

f. The estimated uncertainty in the measured %Q is ± 1.5%.

Table X. Internal Fluorescence After Triton X-100-induced 6CF Release From SUVs (24 hr pre-equilibration)

Sample[a]	% 6CF Release[b]	Predicted %Q for all-or-none[c]	Predicted %Q for Graded Release[d]	Measured %Q[e,f]
control	0	---	---	97
50ug Triton	40	97	91	92
75ug Triton	55	97	88	88
85ug Triton	66	97	85	86
100ug Triton	81	97	71	81
110ug Triton	88	97	57	71

a. 50 to 110ul of 0.1% Triton X-100 was allowed to pre-equilibrate for 24 hours in 2ml of buffer A prior to addition of SUVs (PS concentration = 25-30uM) loaded with 100mM 6CF as described in Materials and Methods.

b. Determined by following 6CF release for 500 sec with a spectrofluorometer. 100% release of 6CF was determined by addition of 10% Triton X-100.

c. Assumes some vesicles released all their dye; others released none.

d. Predicted on the basis of a quenching curve determined by the method of Weinstein et.al. ((1984) In Liposome Technology Vol. III, ed. Gregoriades, G. 183-204. Boca Raton, FL: CRC Press). See Figure 4.

e. Determined following the removal of released 6CF with a Sephadex G-25 column.

f. The estimated uncertainty in the measured %Q is ± 1.5%.

equilibration, the %Q values tend to suggest a more graded mode of release. However, these %Q values are not conclusive enough to indicate a strictly graded mode of release. However, they do suggest that some detergents may cause modes of release that indicate both all-or-none and graded release processes are occurring simultaneously.

Octylglucoside, a nonionic detergent, interacted with vesicles to cause release of dye (Figure 38) and the release of dye appears to follow first order kinetics when OG is allowed to pre-equilibrate for 5 min before adding vesicles (Figure 39). Shown in Tables XI and XII are the %Q values that suggest that OG causes graded release of dye from PS sonicated vesicles with or without pre-equilibration. This observation is in line with the intuitive notion of how detergents affect the permeability barrier of the lipid bilayer before membrane solubilization. However, as demonstrated with Triton X-100, also a nonionic detergent, the mode of release may not always be completely all-or-none or graded. It is also interesting to note that detergents cause all-or-none release effects in yeast cells (Borst-Pauwels, 1981).

These data show that the peptides MGN2a and melittin display all-or-none and mixed modes of release respectively. OG causes graded release of dye and Triton X-100 shows a mixed mode of release. The mixed modes of release suggest that the kinetics of release are not single exponential and

Figure 38

OG-induced release of 6CF from PS SUVs. 25 to 70ul of 10% OG in buffer B was allowed to pre-equilibrate in 2ml of buffer A for 5 min at room temperature prior to addition of loaded vesicles (Final PS concentration = 28uM). The mg of added OG are indicated in the figure.

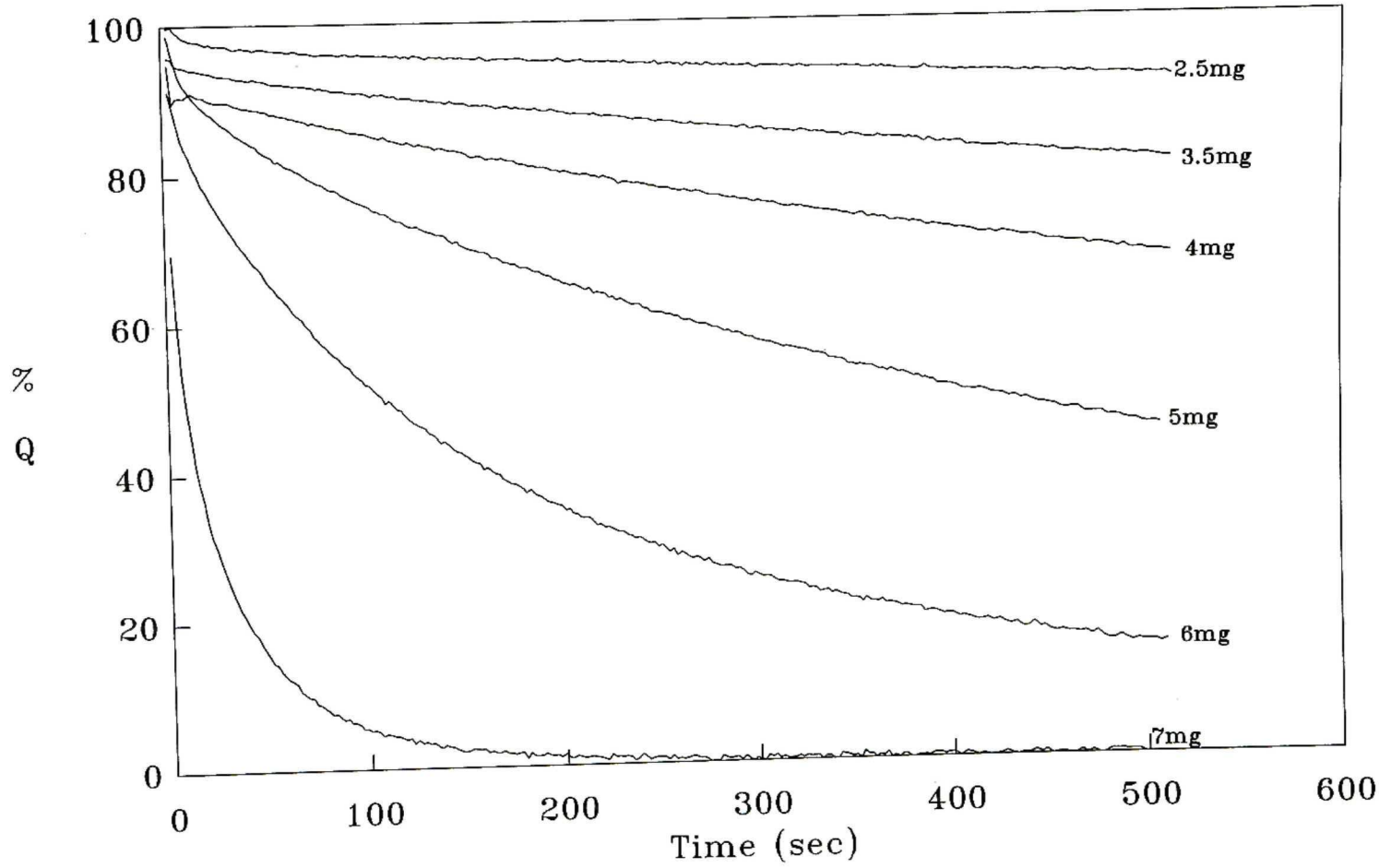

% Q = (1 – (F/Fmax)) x 100

Figure 39

Semilog plot of OG-induced release of 6CF from PS SUVs. These curves are replots of the results shown in Figure 38.

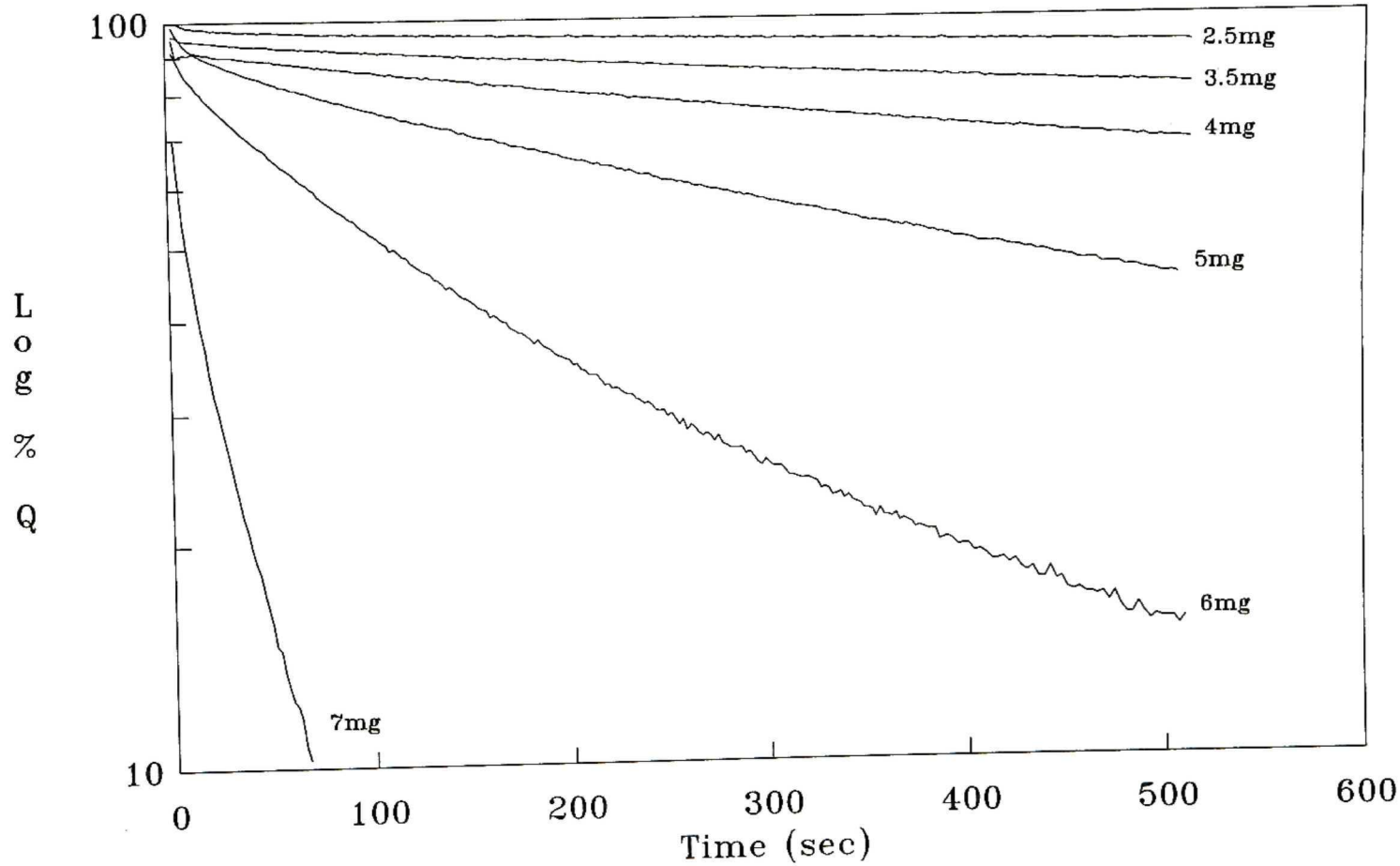

% Q = (1 – (F/Fmax)) x 100

Table XI. Internal Fluorescence After Octylglucoside-induced 6CF Release From SUVs (no pre-equilibration)

Sample[a]	% 6CF Release[b]	Predicted %Q for all-or-none[c]	Predicted %Q for Graded Release[d]	Measured %Q[e,f]
control	0	---	---	97
2.5mg OG	26	97	93	96
3.5mg OG	42	97	91	93
5mg OG	74	97	79	79
6mg OG	88	97	57	59

a. 25 to 60ul of 10% OG was added to 2ml of buffer A and SUVs (PS concentration = 25-30uM) loaded with 100mM 6CF as described in Materials and Methods.

b. Determined by following 6CF release for 500 sec with a spectrofluorometer. 100% release of 6CF was determined by addition of 10% Triton X-100.

c. Assumes some vesicles released all their dye; others released none.

d. Predicted on the basis of a quenching curve determined by the method of Weinstein et.al. ((1984) In Liposome Technology Vol. III, ed. Gregoriades, G. 183-204. Boca Raton, FL: CRC Press). See Figure 4.

e. Determined following the removal of released 6CF with a Sephadex G-25 column.

f. The estimated uncertainty in the measured %Q is ± 1.5%.

Table XII. Internal Fluorescence After OG-induced 6CF Release From SUVs (5 min pre-equilibration)

Sample[a]	% 6CF Release[b]	Predicted %Q for all-or-none[c]	Predicted %Q for Graded Release[d]	Measured %Q[e,f]
control	0	---	---	98
2.5mg OG	17	98	94	95
3.5mg OG	31	98	92	95
5mg OG	54	98	88	90
6mg OG	85	98	63	69

a. 25 to 60ul of 10% OG was allowed to pre-equilibrate in 2ml of buffer A for 5 min prior to addition of SUVs (PS concentration = 25-30uM) loaded with 100mM 6CF as described in Materials and Methods.

b. Determined by following 6CF release for 500 sec with a spectrofluorometer. 100% release of 6CF was determined by addition of 10% Triton X-100.

c. Assumes some vesicles released all their dye; others released none.

d. Predicted on the basis of a quenching curve determined by the method of Weinstein et.al. ((1984) In Liposome Technology Vol. III, ed. Gregoriades, G. 183-204. Boca Raton, FL: CRC Press). See Figure 4.

e. Determined following the removal of released 6CF with a Sephadex G-25 column.

f. The estimated uncertainty in the measured %Q is ± 1.5%.

thus the measured %Q values do not reflect a single process (i.e. all-or-none or graded release) but most probably a combination of all-or-none and graded release. Therefore, these findings would suggest that although MGN2a displays an all-or-none mode of release, which is generally attributed to channel/pore formation, MGN2a may still have detergent-like properties when interacting with the lipid bilayer.

DISCUSSION

We have examined the effects of MGN2a on the lipid bilayer permeability by using fluorescent dye-loaded PS vesicles. MGN2a-induced leakage of 6CF from PS SUVs is characterized by biphasic kinetics; dye release is initially fast followed by a slow release phase. This biphasic mode of release is not limited to SUVs but is also observed in LUVs.

Several plausible explanations for biphasic release were examined. First, the lipid packing and/or size of the PS SUVs was considered because of their highly constrained lipid bilayer. PS LUVs were utilized to determine whether the unique size of SUVs was a contributing factor of the observed MGN2a-induced kinetics of release. However, biphasic release was still observed. We also entertained the possibility that SUVs, which are prepared by sonication, are trapped during preparation in a metastable state in which the monolayer mass ratio of lipids deviates from the ratio required for maximum vesicle stability. If this is the case, the fast release phase could result from MGN2a-induced flip-flop of the lipids, accompanied by 6CF leakage. Flip-flop and fast leakage would cease when the optimal monolayer mass ratio had been attained. To test this possibility, small amounts of MGN2a were added sequentially at 100 sec intervals to the SUVs, and the kinetics of dye release was

monitored after each addition. If the metastable vesicle hypothesis is correct, one would expect that the first addition of peptide would enable the vesicle to relax to a more stable state, so that subsequent additions of peptide should not show biphasic kinetics. The fact that biphasic kinetics were observed with each addition of peptide argues against the metastable vesicle hypothesis. Second, we considered the possibility that aggregates of MGN2a, arising from the concentrated stock solution, could be destabilizing the lipid bilayer, leading to fast phase release. However, we found that preincubation of MGN2a in buffer A for up to 24 hr prior to addition of 6CF loaded vesicles did not significantly alter the release kinetics. Third, we considered the possibility that MGN2a is rapidly and irreversibly inactivated after initial interaction with the PS SUVs. To test this, MGN2a was allowed to interact with vesicles containing no 6CF prior to addition of 6CF loaded vesicles. If vesicle interaction inactivates the peptide, then the fast release phase should not be observed. However, the data suggests that this too is an unlikely possibility because biphasic kinetics were still observed. Finally, it was also demonstrated by light scattering measurements that aggregation and/or fusion of vesicles was not apparent and therefore was not a significant factor in the action of MGN2a.

Having ruled out several mechanisms for MGN2a-induced dye release, we are left with two mechanisms for

consideration. The first is that MGN2a forms multimeric channels in the bilayer, and the second is that it acts as a bilayer destabilizer, similar to a detergent.

There are three lines of evidence against channel formation. First, our binding isotherm shows that interaction of MGN2a with the vesicles is best accounted for by simple partitioning, which argues against significant aggregation of MGN2a in the bilayer. This is further supported by the observation that the fractional leakage rate is linearly dependent on r (the ratio of bound peptide per lipid molecule). If the functional lesion resulted from a small fraction of the peptide forming multimers within the bilayer, the fractional leakage rate would increase exponentially with r.

Second, Williams et al. (1990) have shown that in membrane mimetic solvents or when associated with bilayers, MGN2a does not form helices long enough to span the membrane. (Of course, this cannot rule out the possibility that a small fraction of the peptide forms sufficiently long helices.)

Third, channel activity in planar bilayers is seen with magainins only when high voltages are applied. In our system, there is no transmembrane potential to drive such channel formation.

There are two lines of evidence that appear to favor channel formation. The first is that a critical number of

peptide molecules must interact with the bilayer before leakage occurs (suggesting that a complete dose response curve is sigmoidal). Although this dose response behavior has been interpreted by some as evidence for the cooperative formation of peptide multimers, we point out that the same behavior has been observed with detergents. Indeed, the critical number for MGN2a is in the same range as is found for detergents (Matsuzaki et al., 1989a). Therefore, we discount this piece of evidence for channels.

The second piece of experimental data that appears to strongly support channel formation is the mode-of-release studies showing that release of 6CF is all-or-none rather than graded. It is generally believed that detergents cause leakage exclusively by a graded mechanism whereas only channels can cause release by the all-or-none mechanism. However, we found that Triton X-100 shows some all-or-none release behavior, and it has been shown that both cationic and anionic detergents display an all-or-none mechanism in yeast (Borst-Pauwels, 1981). Therefore, we do not believe that the mode-of-release studies can be used at this time to distinguish between channel-like and detergent-like behavior. Clearly, more work with detergents is required to resolve the mechanism of detergent-induced leakage.

The weight of evidence, in our view, supports a mechanism in which MGN2a acts as a bilayer destabilizer rather than as a discrete channel or pore. To explain the

biphasic release kinetics , we propose that the initial interaction of MGN2a with the vesicles creates a packing imbalance across the bilayer, forming an unstable complex that we shall call PV^*. PV^* then relaxes to a more stable structure via flip-flop of the lipids, as has been seen by Greenhut and Roseman (1985) in a study of cytochrome b_5 interaction with vesicles. During the relaxation process, defects or "holes" are formed in the bilayer, having a statistical range of sizes. At a given peptide to lipid ratio, a small fraction of the holes will be large enough to allow rapid release of 6CF. If the lifetime of PV^* is short, and the probability of forming large holes is low, we can account for the observation that a fraction of the vesicles show all-or-none release during the fast phase.

Once the vesicles relax to a new equilibrium state, subsequent release of 6CF from the vesicles is slow. The slow release could be caused by MGN2a acting as a detergent, although it is possible that slow release takes place via the formation of channels so long as channel formation is very inefficient; by inefficient we mean that channels are produced with low frequency and involve only a small fraction of the bound peptide. This stipulation is required to account for the slow rate of dye release and the linearity of the binding isotherm.

The model can be summarized in the following scheme:

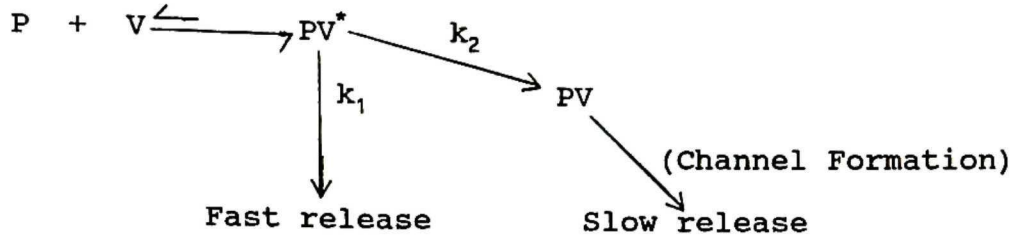

(PV^* represents a lipid packing imbalance)

Both fates of the complex results in all-or-none release of the dye and the proportion of vesicles undergoing total disruption during the fast phase is greater as the concentration of peptide increases. In the sequential addition study, where equal aliquots of MGN2a were added to PS SUVs (Figure 15), this model would suggest that upon each addition of peptide the vesicles rearrange to accommodate the added peptide with total disruption of some vesicles. Each subsequent addition of peptide creates further lipid packing imbalances resulting in rearrangement to accept the added peptide thus displaying biphasic release of 6CF.

This model combines the present data with current reported data on MGN2a's interaction with the lipid bilayer in order to present a viable model to explain the action of MGN2a on this model membrane system. This model based on the PS membrane system could provide valuable insights about the action of MGN2a on its target membrane. However, there are still other areas that will require further investigation to include characterization of the effective size of the membrane lesion, permeability effect of the magainins on vesicles of various lipid compositions, and more insight

about the nature of the initial membrane destabilization by various perturbants (i.e. peptides and detergents) before a more detailed mechanism can be proposed for the overall action of magainins.

REFERENCES

Arbuthnott, J.P., Freer, J.H., and Bernheimer, A.W. (1967) Journal of Bacteriology, 94, 1170-1177.

Barenholz, Y., Gibbes, D., Litman, B.J., Goll, J., Thompson, T.E. and Carlson, F.D. (1977) Biochemistry, 16, 2806-2810.

Bartlett, G.R. (1959) Journal of Biological Chemistry, 234, 466-468.

Bernheimer, A.W., Kim, K.S., Remsen, C.C., Antanavage, J., and Watson, S.W. (1972) Infection and Immunity, 6, 636-642.

Blumenthal, R., Millard, P.J., Henkart, M.P., Reynolds, C.W. and Henkart, P.A. (1984) Proceedings of National Academy of Sciences, USA, 81, 5551-5555.

Borst-Pauwels, G.W.F.H. (1981) Biochimica et Biophysica Acta, 650, 88-127.

Cassidy, P., Six, H.R., and Harshman, S. (1974) Biochimica et Biophysica Acta, 332, 413-423.

Chen, H.-C., Brown, J.H., Morell, J.L., and Huang, C.M. (1988) FEBS Letters, 236, 462-466.

Cruciani, R.A., Stanley, E.F., Zasloff, M., Lewis, D.L., and Barker, J.L. (1988) Biophysical Journal, 53, 9a.

Cuervo, J.H., Rodriguez, B., and Houghten, R.A. (1988) Peptide Research, 1, 81-86.

Dawson, C.R., Drake, A.F., Helliwell, J. and Hider, R.C. (1978) Biochimica et Biophysica Acta, 510, 75-86.

DeBony, J., Dufourcq, J. and Clin, B. (1979) Biochimica et Biophysica Acta, 552, 531-534.

DeGrado, W.F., Kezdy, F.J., and Kaiser, E.T. (1981) Journal of American Chemical Society, 103, 679-681.

DeGrado, W.F., Musso, G.F., Lieber, M., Kaiser, E.T. and Kezdy, F.J. (1982) Biophysical Journal, 37, 329-338.

Drake, A.F. and Hider, R.C. (1979) Biochimica et Biophysica Acta, 555, 371-373.

Duclohier, H., Molle, G., and Spach, G. (1989) Biophysical

Journal, 56, 1017-1021.

Duzgunes, N., Wilschut, J., Hong, K., Fraley, R., Perry, C., Friend, D., James, T.L. and Papahadjopoulos, D. (1983) Biochimica et Biophysica Acta, 732, 289-299.

Erspamer, V. and Melchiorri, P. (1980) Trends in Pharmacological Sciences, 1, 391-395.

Freer, J.H., Arbuthnott, J.P., and Bernheimer, A.W. (1968) Journal of Bacteriology, 95, 1153-1168.

Freer, J.H., Arbuthnott, J.P., and Billcliffe, B. (1973) Journal of Genetics and Microbiology, 75, 321-332.

Fujita, T., Takaishi, Y., Matsuura, K., Takeda, Y., Yoshioka, Y., and Bruckner, H. (1984a) Chemical and Pharmaceutical Bulletin, 32, 2870-2873.

Fujita, T., Takaishi, Y., Moritoki, H., Ogawa, T., and Tokimoto, K. (1984b) Chemical and Pharmaceutical Bulletin, 32, 1822-1828.

Fussle, R., Bhakdi, S., Sziegoleit, A., Tranumjensen, J., Kranz, T., and Wellensiek, H.-J. (1981) Journal of Cell Biology, 91, 83-94.

Georghiou, S., Thompson, M. and Mukhopadhyay, A.K. (1982) Biochimica et Biophysica Acta, 688, 441-452.

Gibson, B.W., Poulter, L., Williams, D.H., and Maggio, J.E. (1986) Journal of Biological Chemistry, 261, 5341-5349.

Giovannini, M.G., Poulter, L., Gibson, B.W., and Williams, D.H. (1987) Biochemistry Journal, 243, 113-120.

Green, F.R., Lynch, B., and Kaiser, E.T. (1987) Proceedings of the National Academy of Sciences, USA, 84, 8340-8344.

Greenhut, S.F. and Roseman, M.A. (1985) Biochemistry, 24, 1255-1260.

Guy, H.R. and Raghunathan, G. (1988) Jerusalem Symposium of Quantum Chemistry and Biochemistry, 21, 369-379.

Habermann, E. (1972) Science, 177, 314-322.

Juretic, D., Hendler, R.W., Zasloff, M., and Westerhoff, H.V. (1989a) Biophysical Journal, 55, 572a.

Juretic, D., Chen, H.-C., Brown, J.H., Morell, J.L., Hendler, R.W., and Westerhoff, H.V. (1989b) FEBS Letters, 249,

219-223.

Kempf, C., Klausner, R.D., Weinstein, J.N., Renswoude, J.V., Pincus, M. and Blumenthal, R. (1982) Journal of Biological Chemistry, 257, 2469-2476.

Kini, R.M. and Evans, H.J. (1989) International Journal of Peptide and Protein Research, 34, 277-286.

Lavialle, F., Adams, R.G. and Levin, I.W. (1982) Biochemistry, 21, 2305-2312.Lelkes, P.I. (1984) In Liposome Technology Vol. III, ed. Gregoriades, G. 226-234. Boca Raton, FL: CRC Press.

Loh, Y.P., Parish, D.C., and Tuteja, R. (1985) Journal of Biological Chemistry, 260, 7194-7205.

Marion, D., Zasloff, M. and Bax, A. (1988) FEBS Letters, 227, 21-26.

Matsuzaki, K., Handa, T., Miyajima, K. Mikura, Y., Shimiza, H. and Toguchi, H. (1988) Chemical & Pharmaceutical Bulletin, 36, 4253-4260.

Matsuzaki, K., Harada, M., Handa, T., Funakoshi, S., Fujii, N., Yajima, H., and Miyajima, K. (1989a) Biochimica et Biophysica Acta, 981, 130-134.

Matsuzaki, K., Nakai, S., Handa, T., Takaishi, Y., Fujita, T., and Miyajima, K. (1989b) Biochemistry, 28, 9392-9398.

Nakajima, T. (1981) Trends in Pharmacological Sciences, 2, 202-205.

Olsen, F.C., Munjal, D., and Malviya, A.N. (1974) Toxicon, 12, 419-425.

Rana, F. and Blazyk, J. (1989) Biological and Synthetic Membranes, Alan R. Liss, Inc., 77-85.

Roseman, M.A., Holloway, P.W., Calabro, M.A. and Thompson, T.E. (1977) Journal of Biological Chemistry, 252, 4842-4849.

Roseman, M.A. (1988) Journal of Molecular Biology, 201, 621-623.

Sessa, G., Freer, J.H., Colacicco, G., and Weissmann, G. (1969) Journal of Biology Chemistry, 244, 3575-3582.

Soravia, E., Giuseppe, M. and Zasloff, M. (1988) FEBS Letters, 228, 337-340.

Terry, A.S., Poulter, L., Williams, D.H., Nutkins, J.C., Giovannini, M.G., Moore, C.H., and Gibson, B.W. (1988) Journal of Biological Chemistry, 263, 5745-5751.

Terwilliger, T.C., Weissman, L., and Eisenberg, D. (1982) Biophysical Journal, 37, 353-361.

Thelestam, M., Jolivet-Reynaud, C., and Alouf, J.E. (1983) Biochemical and Biophysical Research Communications, 111, 444-449.

Thron, C.D. (1964) Journal of Pharmacology and Experimental Therapeutics, 145, 194-201.

Tosteson, M.T., Alvarez, O. and Tosteson, D.C. (1985a) Regulatory Peptides, 13 (Suppl. 4), 39-45.

Tosteson, M.T., Holmes, S.J., Razin, M. and Tosteson, D.C. (1985b) Journal of Membrane Biology, 87, 33-44.

Urrutia, R., Cruciani, R.A., Barker, J.L., and Kachar, B. (1989) FEBS Letters, 247, 17-21.

Weinstein, J.W., Ralston, E., Leserman, L.D., Klausner, R.D., Dragsten, P., Henkart, P. and Blumenthal, R. (1984) In Liposome Technology Vol. III, ed. Gregoriades, G. 183-204. Boca Raton, FL: CRC Press.

Weissmann, G., Hirshhorn, R., and Krakavier, K. (1969) Biochemical Pharmacology, 18, 1771-1775.

Westerhoff, H.V., Juretic, D., Hendler, R.W., and Zasloff, M. (1989a) Proceedings of the National Academy of Sciences, USA, 86, 6597-6601.

Westerhoff, H.V., Hendler, R.W., Zasloff, M., and Juretic, D. (1989b) Biochimica et Biophysica Acta, 975, 361-369.

Williams, R.W., Starman, R., Taylor, K.M.P., Gable, K., Beeler, T., Zasloff, M., and Covell, D. (1990) Biochemistry, 29, 4490-4496.

Zasloff, M. (1987) Proceedings of the National Academy of Sciences, USA, 84, 5449-5453.

Zasloff, M., Martin, B., and Chen, H. (1988) Proceedings of the National Academy of Sciences, USA, 85, 910-913.